SYNTHESIS AND CHARACTERIZATION OF METAL FUNCTIONAL POLYBENZOXAZINES

A THESIS SUBMITTED TO
THE GRADUATE SCHOOL OF NATURAL AND APPLIED SCIENCES
OF
MIDDLE EAST TECHNICAL UNIVERSITY

BY

TUĞBA ORHAN LEKESİZ

IN PARTIAL FULFILLMENT OF THE REQUIREMENTS
FOR
THE DEGREE OF DOCTOR OF PHILOSOPHY
IN
CHEMISTRY

SEPTEMBER 2014

Approval of the thesis:

SYNTHESIS AND CHARACTERIZATION OF METAL FUNCTIONAL POLYBENZOXAZINES

submitted by **TUĞBA ORHAN LEKESİZ** in partial fulfillment of the requirements for the degree of **Doctor of Phİlosophy in Chemistry Department**, **Middle East Technical University** by,

Prof. Dr. Canan Özgen _____
Dean, Graduate School of **Natural and Applied Sciences**

Prof. Dr. İlker Özkan _____
Head of Department, **Chemistry**

Prof. Dr. Jale Hacaloğlu _____
Supervisor, **Chemistry Dept., METU**

Prof. Dr. H. Ceyhan Kayran _____
Co-Supervisor, **Chemistry Dept., METU**

Examining Committee Members:

Prof. Dr. Yusuf Yağcı _____
Chemistry Dept., ITU

Prof. Dr. Jale Hacaloğlu _____
Chemistry Dept., METU

Prof. Dr. Teoman Tinçer _____
Chemistry Dept., METU

Prof. Dr. Erdal Bayramlı _____
Chemistry Dept., METU

Assoc. Prof. Tamer Uyar _____
UNAM

Date: 26/09/2014

I hereby declare that all information in this document has been obtained and presented in accordance with academic rules and ethical conduct. I also declare that, as required by these rules and conduct, I have fully cited and referenced all material and results that are not original to this work.

Name, Last name: Tuğba Orhan LEKESİZ

Signature:

ABSTRACT

SYNTHESIS AND CHARACTERIZATION OF METAL FUNCTIONAL POLYBENZOXAZINES

Orhan Lekesiz, Tuğba
Ph.D., Department of Chemistry
Supervisor: Prof. Dr. Jale Hacaloğlu
Co-Supervisor: Prof. Dr. H. Ceyhan Kayran
September 2014, 185 pages

Polybenzoxazines possessing excellent mechanical and physical properties has been developed to overcome the shortcomings associated with the use of traditional phenolics. Various approaches for performance improvement of polybenzoxazine were examined. These approaches include alloying with other high performance polymers, hybridization with inorganics, and designing of novel monomers as well as high molecular weight polymeric precursors.

In the first part of this work, benzoxazines based on phenol and aniline or aniline derivatives namely aminopyridine, aminobenzonitrile and nitroaniline are synthesized and polymerized by curing the monomers systematically. In the second part of the work metal or metal ions are incorporated to benzoxazine monomers based on aminopyridine, aminobenzonitrile and nitroaniline. The structural and thermal characteristics of the polybenzoxazines and metal or metal ion functional polybenzoxazines are analyzed via FTIR, NMR, DSC, TGA and DP-MS techniques. The effects of curing program used and incorporation of metal and/or metal ion on structural and thermal characteristics of the polybenzoxazines are investigated.

In general, the benzoxazines based on aniline or aniline derivatives are polymerized via ring opening of oxazine ring followed by attack of NCH_2 groups to mainly para positions of phenol and aniline ring. The char yield and presence of chains that can only decompose at elevated temperatures mainly depend on extent of crosslinking and

unsaturated linkages. Coordination of metal and/or metal ion to pyridine in case of aminopyridine based benzoxazine, to CN groups in case of aminobenzonitrile and finally to NO_2 groups in case of nitroaniline cause drastic changes in structural and thermal characteristics of the polybenzoxazines produced. The coordination of metal or metal ion to the aromatic ring of the benzoxazine monomer promotes the evolution of amine or substituted amine groups which in turn causes an increase in the formation of unsaturated linkages but a decrease in the extent of crosslinking.

Keywords: polybenzoxazine, thermal characterization, DP-MS, metal coordination

ÖZ

METAL FONKSİYONLU POLİBENZOKSAZİNLERİN SENTEZİ VE KARAKTERİZASYONU

Orhan Lekesiz, Tuğba
Doktora, Kimya Bölümü
Tez Yöneticisi: Prof. Dr. Jale Hacaloğlu
Ortak Tez Yöneticisi: Prof. Dr. H. Ceyhan Kayran
Eylül 2014, 185 sayfa

Polybenzoksazinler geleneksel fenoliklerin eksikliklerini kapatmak için geliştirilmiştir. Polibenzoksazinlerin performansını artırmak için bir çok uygulama denenmiştir. Yüksek performanslı polimerlerle alaşımlama, anorganik maddelerle hibrit oluşumu ya da yüksek moleküler ağırlıklı polimer başlatıcıların yanında yeni monomer dizaynı kullanılan yöntemlerden birkaçıdır.

Bu çalışmanın birinci kısmında fenol ve anilin yada anilin türevleri olarak aminopiridin, aminobenzonitril ve nitroanilin esaslı benzoksazinler sentezlenmiş ve sistematik kürleme programı kullanılarak polimerleştirilmiştir. Çalışmanın ikinci kısmında metal ve/veya metal iyonlarının aminopiridin, aminobenzonitril ve nitroaniline esaslı benzoksazin monomerlere inkorporasyonu gerçekleştirilmiştir. Polibenzoksazinlerin yapısal ve ısıl karakteristikleri FTIR, NMR, DSC, TGA ve DP-MS teknikleri kullanılarak analiz edilmiştir. Kürleme programı ve metal ve/veya metal iyon inkorporasyonunun polibenzoksazinlerin yapısal ve ısıl karakteristiklerine etkisi araştırılmıştır.

Genelde, anilin ve anilin türevleri esaslı benzoksazinler oksazin halkasının açılmasını takiben NCH_2 grubunun fenol ve anilin halkasına saldırısı ile polimerleşmektedir. Kömür verimi ve sadece yüksek sıcaklıklarda bozunan zincirlerin oluşumu çapraz

bağlanma derecesi ve doymamış polimer zincirlerine bağlıdır. Aminopiridin esaslı benzoksazinlerde piridin halkasına, aminobenzonitril esaslı benzoksazinlerde nitril grubuna ve son olarak nitroanilin esaslı benzoksazinlerde nitro grubuna metal ve/veya metal iyon koordinasyonu polibenzoksazinlerin yapısal ve ısıl karakterisklirinde şiddetli değişikliklere sebep olmuştur. Metal ve/veya metal iyonunun benzoksazin monomerinin aromatik halkasına koordinasyonu amin ve amin substitütif gruplarının evolüsyonununda artışa fakat çapraz bağlanma derecesinde azalmaya sebep olmuştur.

Anahtar kelimeler: polibenzoksazin, ısıl karakterizasyon, DP-MS, metal koordinasyonu

to my dear husband and precious family..

ACKNOWLEDGEMENTS

The preparation of this important document would not have been possible without the support, hard work and endless efforts of a large number of individuals.

I would like to express my deep and sincere gratitude to my advisor Prof. Dr. Jale Hacaloğlu. Her wide knowledge and logical way of thinking have been of great value for me. Her understanding, encouraging and personal guidance have provided a good basis not for the present thesis but also for my life.

I am deeply grateful to my co-advisor Prof. Dr. Ceyhan Kayran for her important support throughout this work.

I wish to thank to Prof. Dr. Yusuf Yağcı and Prof. Dr. Teoman Tinçer for their guidance.

I also wish to thank to Assoc. Prof. Tamer Uyar for his help at the beginning of this work.

I truly thank to Esra Özdemir for her endless support and friendship. She is always ready to give a hand whenever I needed.

I owe many thanks to my dear friends Pınar Akay Mercan, Derya Çelik Özhava and Emrah Yıldırım who were with me in this sometimes challenging process to share their valuable opinions and comments.

I am forever grateful to my husband Ömer Lekesiz for his patience, support and belief in me. It makes me feel an extraordinarily lucky person to know that he was, is and will be there for me whenever I call for help.

Lastly, my deepest gratitude goes to my beloved parents who always supported me and believed in me. Without their, especially my father's encouragement and immeasurable sacrifice, I could never finish this journey.

Table of Contents

LIST OF TABLES

LIST OF FIGURES

LIST OF SCHEMES

CHAPTER 1

INTRODUCTION

Traditional phenolic resins are widely used in electronics, aerospace and other industries due to their good heat resistance, low flammability, electrical insulation and dimensional stability. Among these attractive properties, they have a number of shortcomings such as brittleness, necessity of use of acid or base catalysts and generation of by-products during curing causing some environmental problems. Polybenzoxazines are a class of thermosetting phenolic resins that are connected by a Mannich bridge ($-CH_2-N(R)-CH_2-$) instead of methylene ($-CH_2-$) bridge associated with the traditional phenolics. Polybenzoxazines have been developed to overcome the shortcomings of traditional phenolic resins such as releasing condensation by-products and using acid or base catalysts for polymerization. The polybenzoxazine monomer can easily be obtained from the reaction of a phenol, an amine and formaldehyde or paraformaldehyde and variations of the raw materials provide wide molecular design flexibility. Polymerization is achieved simply curing the monomer and proceeds through ring opening of the cyclic monomer. They provide additional characteristics that are not found in traditional phenolics such as; excellent dimensional stability, low water absorption and stable dielectric properties. Nevertheless, polybenzoxazines are also brittle as all thermosets and are cured at relatively high temperature for the ring-opening polymerization. Various approaches for performance improvement of polybenzoxazine were examined. These approaches include alloying with other high performance polymers, hybridization with inorganics, and designing of novel monomers as well as high molecular weight polymeric precursors. By these approaches, lowering of the cure temperature, improvement of toughness, and enhancement of thermal and mechanical properties were achieved. Incorporation of metal/metal ion into polymers is also used to improve the thermal stability of polymers.

1.1. Benzoxazine Chemistry in Solution and Melt

Benzoxazine is a molecule involving an oxazine ring (a heterocyclic six-membered ring with oxygen and nitrogen atom). Benzoxazine monomers are usually prepared through the Mannich reaction between a phenol (RC_6H_4OH), an amine (RNH_2) and formaldehyde or paraformaldehyde either in solution or melt state.

Synthesis of benzoxazine in solution system has some disadvantages such as slow reaction rate, large amount of solvent required and poor solubility of the precursors. The use of organic solvent increases the cost and causes environmental problems and solvent residue leads to problems during processing. Hopefully, Ishida [1] proposed the solventless synthesis in the melt state to overcome these disadvantages.

The choice of the phenol and amine partners permits the design of monomers exhibiting flexibility and tailoring of the polymer properties. The quantity of oligomers mainly depends on the basicity of the oxygen and nitrogen atoms on the oxazine ring, which influences the possibility of ring opening and, thus, the formation of oligomers[2,3]. Several studies were focused on the choice of phenols, amines and reactive functional groups to improve thermal stability and char yield [4–10].

1.1.1. Monofunctional benzoxazine monomers

In 1944, Holly and Cope synthesized the first aromatic oxazine in a solution as a two-step synthesis as shown in Fig. 1.1[11]. In 1950s, Burke found that condensation reaction of phenol with formaldehyde and methylamine in a mole ratio of 1:2:1 resulted in high yield and more rapid polymerization. This study also reported that phenolic compound reacts prudentially with the free ortho and para-positions of the phenolic compound.

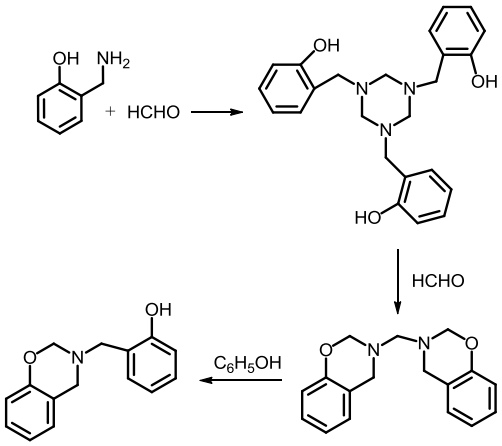

Figure 1.1 The synthetic method of benzoxazines adopted by Holy and Cope.

A series of monofunctional benzoxazine resins were developed as shown in Fig. 1.2 by using unsubstituted phenol, formaldehyde and primary aromatic amines as starting materials and polymerization behavior of these resins were also studied[12]. The objective of this study was to develop monofunctional benzoxazine resins that were liquid at room temperature. The low viscosity benzoxazines can potentially be developed into high-performance polybenzoxazines that were of interest for some applications and the polymerization of liquid benzoxazines can possibly be faster than their solid counterparts. It was reported that the aliphatic amine-based benzoxazines showed lower viscosities than the aromatic amine-based counterparts and in the aliphatic or aromatic category; the viscosity of the benzoxazine monomer was increased with the increase in the size of the amine moiety.

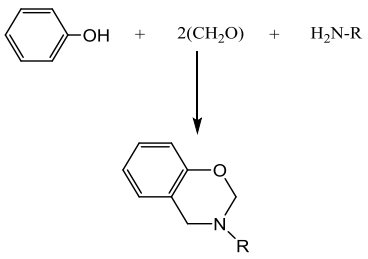

Figure 1.2 Monomer synthesis based on various amines.

It has been showed that the reaction site of the ring opening polymerization in monofunctional aromatic amine-based benzoxazines is the *ortho* position to the hydroxyl group. High temperature and/or long cure times are needed for the reaction at *meta* position of the aromatic ring. The regioselectivity of various arylamines reacted with formaldehyde and various secondary aliphatic amines are also studied The Mannich reaction took place at the *para* position when N,N-dimethyl aniline was used . It has been determined that when there is a labile hydrogen on the nitrogen, reaction at the nitrogen is preferred under weakly acidic conditions while the reaction at para position dominates under strongly acidic conditions.

The effect of addition of a weakly activating group on the regioselectivity was examined for various secondary and tertiary toluidines. The aminoalkylation at the ring position took place under much less acidic conditions when the ring was activated through electrophilic aromatic substitution by the presence of additional methyl substituent.

The regioselectivity of Mannich reaction was studied for various benzoxazines having both phenolic and arylamine ring sites available. For this purpose, different types of alkylated phenols and aryl amines were selected as shown in Fig. 1.3. The results showed that electron-donating alkyl substituent groups at one or both *meta* positions on the arylamine ring facilitate ring opening/degradation at lower temperatures.

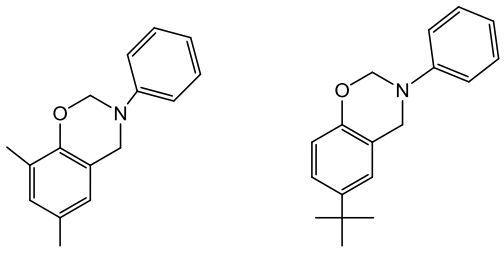

24DMP-a 4TBUPH-a

Figure 1.3 Nomenclature of benzoxazine compounds

1.1.2. Difunctional and multifunctional benzoxazine monomers

Despite their high performance, the crosslinking densities of benzoxazine-based resins are lower than those of traditional thermosetting resins[13]. Studies showed that introducing bifunctional or multifunctional benzoxazine precursors can increase the crosslinked network structures. This approach also eliminated the release of condensation of by-products and prevented the use of toxic phenols [1]. Additionally, curing of monofunctinal benzoxazine monomers yielded only oligomeric phenolic structures with average molecular weight around 1000 Da. Thus, high molecular weight linear structures cannot be obtained as the thermo-dissociation of the monomer competed with the chain propagation reaction. In 1994, Ning and Ishida reported the first study on bisphenol-A based polybenzoxazines and concluded that benzoxazine ring structures were obtained at both ends of bisphenol-A producing crosslinked structures upon curing [14].

The polyfunctionality required to form an infinite network structure upon polymerization may be achieved by using a multifunctional phenolic resin with a monoamine or with a multifunctional amine with a mono-phenol. Rigid bisphenol backbone upon which polymerization took place results in a brittle nature that limits the potential applications. A series of linear aliphatic diamine-based benzoxazines was developed to improve the inherent flexibility as shown in Fig. 1.4. Investigation of the kinetics of polymerization by infrared spectroscopy revealed that the polymerization rate increases with decrease in aliphatic diamine chain length. The aliphatic-diamine based polybenzoxazines have high glass transition temperatures. Melting points of these benzoxazines increase as a function of diamine chain length [15].

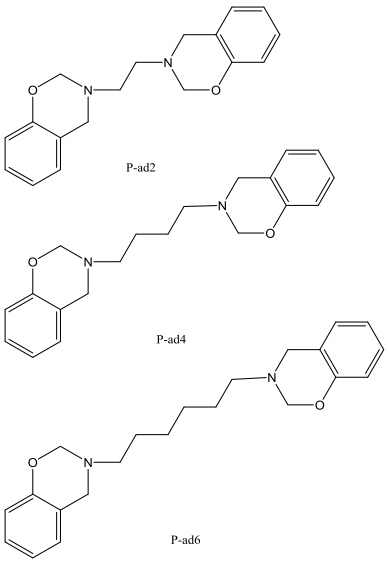

Figure 1.4 Structures of linear aliphatic diamine-based benzoxazine monomers.

It was determined that the polymerization rate of a series of aliphatic diamine-based benzoxazines with different phenolic substitution, decreased with the phenol substitution. The highest rate was recorded for unsubstituted benzoxazines, followed by *para* substitution and slowest for *ortho* substitution [16].

1.1.3. Reactive functional benzoxazine monomers

The amine substituent in the benzoxazine monomer exists as a dangling group and this dangling group is easily evaporated upon thermal cleavage and decrease the thermal stability of polybenzoxazines[17]. Further improvement of thermal properties of polybenzoxazines can be achieved by using reactive functional groups in the monomer synthesis which polymerizes into three dimensional void-free networks with increased cross-linked density and high solvent resistance and moisture resistance [18]. The char yield can also be improved if the evaporation of these groups is delayed.

1.1.3.1. Allyl functional benzoxazine monomers

Allyl group is an effective crosslinkable site for benzoxazines. The allyl-containing monomers from monofunctional (P-ala) and bifunctional phenol (B-ala) were prepared. (Fig. 1.5). Two separate exotherms were present in the DSC thermogram of P-ala corresponding to the polymerization of allyl group and ring opening polymerization of benzoxazine monomer[19]. The thermosets obtained exhibited higher thermal stability and mechanical property with constant storage moduli up to high temperatures.

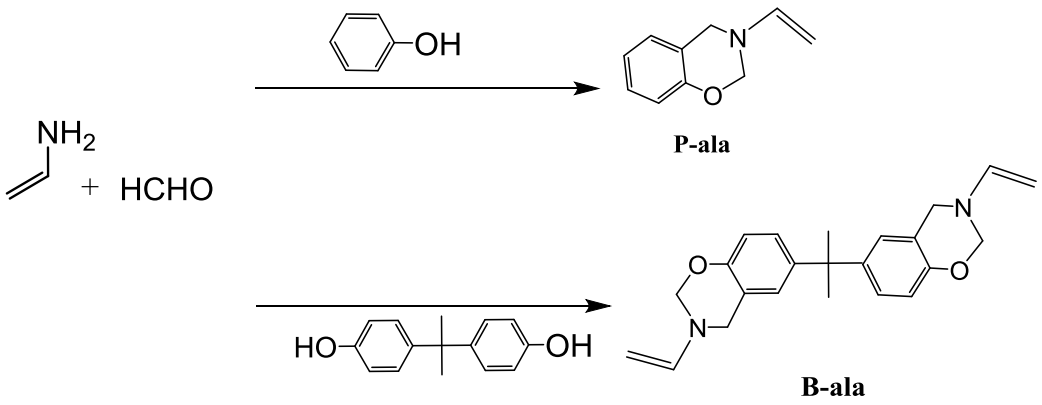

Figure 1.5 Preparation of P-ala and B-ala

1.1.3.2. Acetylene functional monomers

Acetylene functional benzoxazine monomers were synthesized from 3-aminophenylacetylene and various phenolic derivatives such as bisphenol-A, 2,2'-biphenol, hydroquinone and 4,4'-dihydroxybenzophenone (Fig. 1.6). The effect of reactive amine groups on the degradation of different types of phenolic polybenzoxazines was investigated. It was found that the type of the phenolic compound had no effect on the thermal stability, as the char yield of the polybenzoxazines with different phenolic moieties were almost identical.

Additionally, the initial thermal degradation of polybenzoxazines was improved significantly when compared with nonreactive amine-based polybenzoxazines[17].

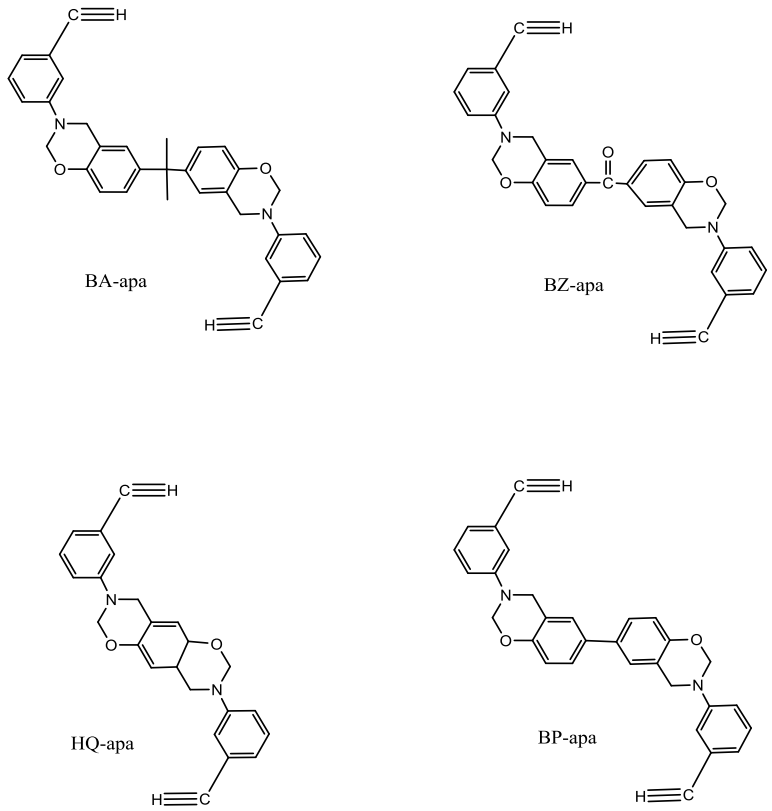

Figure 1.6 Structures of 3-Aminophenylacetylene-based benzoxazine monomers

1.1.3.3. Propargyl functional monomers

The propargyl group was also used to improve thermal and mechanical properties of polybenzoxazines as it is a possible crosslink site for benzoxazine [20]. Polybenzoxazines were obtained from novel monomers such as propargyl ether-based monofunctional (P-appe) and bifunctional benzoxazine (B-appe) as shown in Fig. 1.7. In addition to improvement of thermal properties such as higher Tg, higher 5% and 10% weight loss temperature and high char yield, storage modulus was also maintained constant up to 300℃.

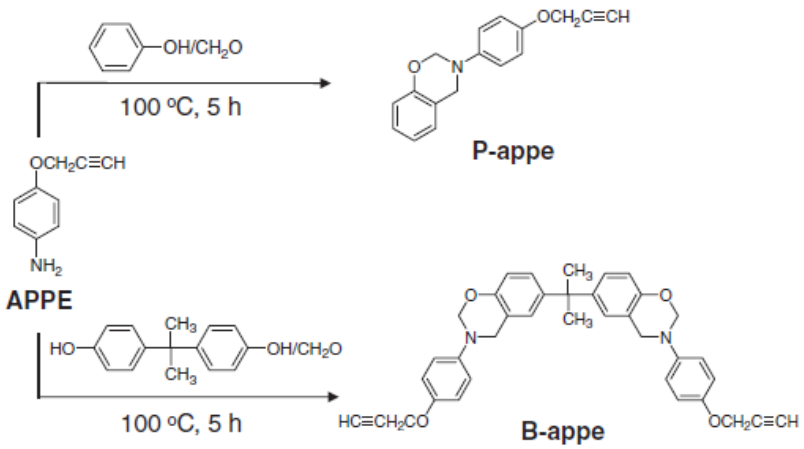

Figure 1.7 Preparation of P-appe and B-appe

1.1.3.4. Nitrile functional monomers

Phenylnitrile and phththalonitrile functional polybenzoxazines are another type of reactive benzoxazine monomers developed for higher thermal stability. Two types of phenylnitrile functional benzoxazines were synthesized by using aniline ad 4,4'-diamino diphenylether and 4-cyanophenol as shown in Fig. 1.8. FTIR and DSC results revealed that the cure temperatures of phenylnitrile benzoxazines were lower and the polybenzoxazines derived from phenylnitrile functional monomers had higher Tg, higher thermal stability and better mechanical properties[18].

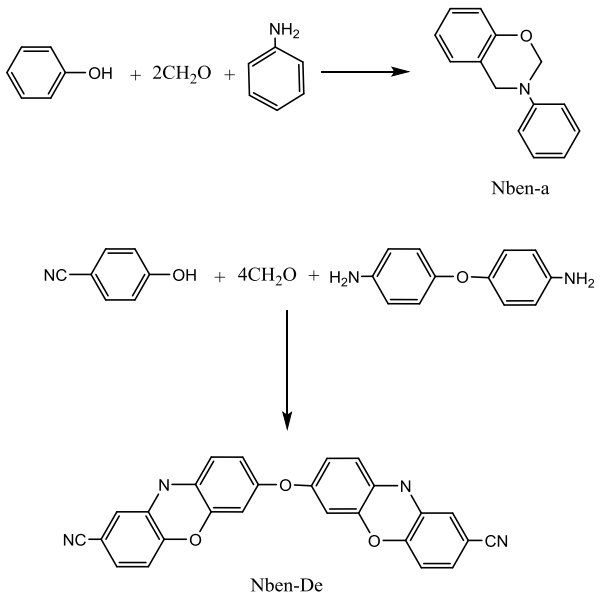

Figure 1.8 Preparation of phenylnitrile benzoxazines

In general, processibility of phenylnitrile-functional benzoxazines are easy due to their low melt viscosity, but their thermal stability need to be enhanced. Brunovska and Ishida [5], studied the copolymers of phenylnitrile and phthalonitrile functional polybenzoxazines to combine the high thermal stability of phthalonitrile and easy processibility of phenylnitrile groups (Fig.1.9). The copolymers prepared by using various mole percentages exhibited the best performance among phenylnitrile functional polybenzoxazines with high Tg, low melt viscosity and high char yield.

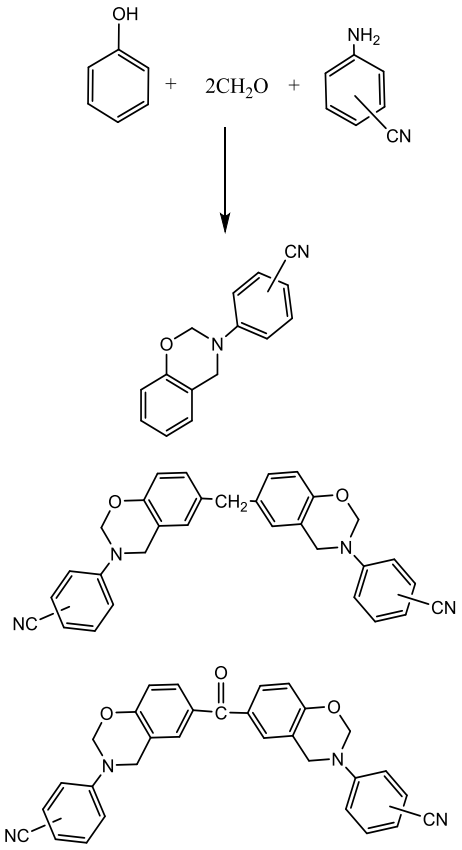

Figure 1.9 Synthesized benzoxazine monomers

1.1.3.5. Methylol functional monomers

Traditional phenolic resins exhibit an additional condensation reaction and methylol functional benzoxazines can be considered as the combination of traditional phenolics and benzoxazines which may provide higher crosslinking density. The methylol functional benzoxazine prevents the condensation byproducts and void formation. Methylol-functional phenols and aromatic amines including methylenedianiline (4,4'-diaminodiphenylmethane) and oxydianiline (4,4'-diaminodiphenyl ether) were used to synthesize the benzoxazine monomers and the effect of position of metylene group was also studied.

In oxydianiline (ODA) series, the ring-opening temperature was lower for para position, whereas meta position had the lower temperature in methylenedianiline(DDM). Furthermore, the polybenzoxazines with higher thermal properties were developed as a consequence of the higher degree of crosslinking by the presence of the methylol functional group[21].

1.1.3.6. Maleimide and norbornene functional monomers

Imide functionality was also used for the synthesis of benzoxazines to improve thermal properties. Monofunctional polybenzoxazines with maleimide and norbornene functionality exhibited a high char yield and Tg without increasing the viscosity of the monomer[22].

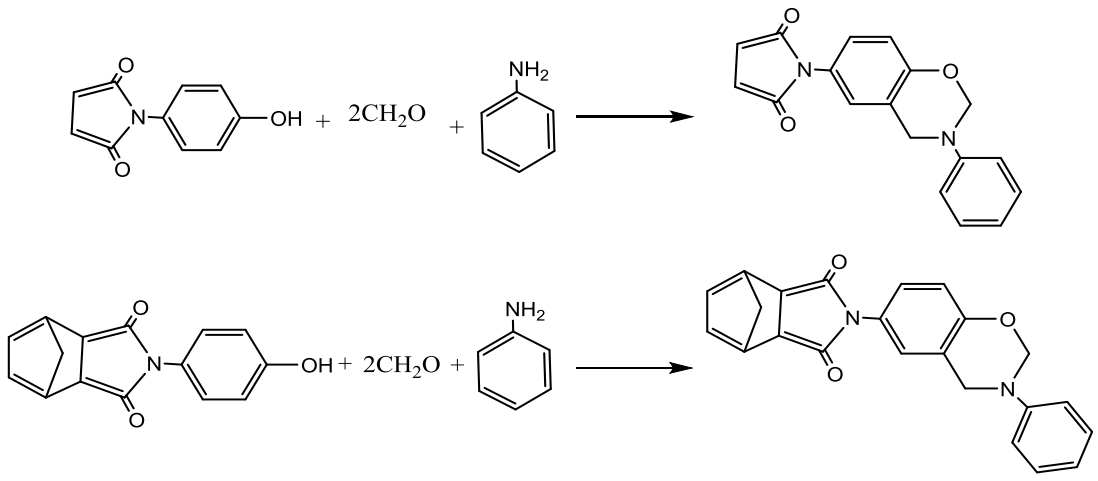

Figure 1.10 Synthesis of MIB and NOB benzoxazine monomers

Nitrile functionality was also added to the maleimide functional benzoxazine monomers to achieve a higher thermal stability and good processibility. For this purpose, a maleimide and 2-aminobenzonitrile (MIan) based benzoxazine was prepared and the crosslinking density of polymer was increased as the maleimide and nitrile groups were also polymerized. The resulting polybenzoxazine provided good

processibility with an increased shear viscosity in addition to excellent mechanical and thermal properties [23].

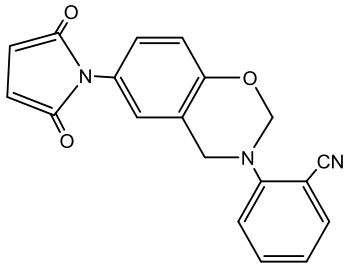

Figure 1.11 Structure of maleimide and 2-aminobenzobitrile functionalized benzoxazine

1.2. Polybenzoxazine Composites, Hybrid materials and Nanocomposites

1.2.1. Polybenzoxazine/Fiber Composites

Carbon Fiber (CF)-reinforced phenolic composites provide excellent mechanical property, ablation resistance, good flame retardancy and low smoke generation. Fiber diameter, fiber length, volume fraction of fibers and orientation of fibers are main variables that affect the properties of the fibrous composites. The effect of variation of fiber length was studied and results showed that flexural strength increased with increasing fiber length and optimized at about 17 mm fiber length as the fiber length is directly proportional to the contact area of a given fiber with the matrix[24]. The result of this study revealed that composites of PBz with good strength, ductility and modulus could be successfully developed using CFs of appropriate length and composition.

1.2.2. Polybenzoxazine/Clay Nanocomposites

Polymer-clay nanocomposite, prepared through the dispersion of clay as layered silicates at nanometer scale in polymer matrix, is a new class of composite material. Montmorillonite, MMT, has a hydrophilic character and surface modification is required to increase the diffusion of a nonpolar monomer or polymer into clay galleries and to achieve nano-size dispersion of clay into a polymer matrix. Three types of nanocomposites can be prepared depending on the interaction between the clay and the polymer such as immiscible, intercalated or exfoliated.

Due to the nanoscale dispersion in the polymer matrix, a small amount of well-dispersed clay layers can improve the mechanical and thermal properties of the polymer. Solution mixing and melt blending are two common methods to prepare polymer-clay nanocomposites.

Agag et al. reported the first polybenzoxazine-MMT nanocomposites by melt blending method for bisphenol A/aniline type benzoxazine monomer (BA-a)[25]. The exothermic polymerization peak was shifted to lower temperatures for various types of organically modified montmorillonites, OMMT's, indicating the catalyst effect on ring-opening polymerization.

1.2.3. Polybenzoxazine/CNT Nanocomposites

Carbon nanotubes (CNTs) have attracted great attention for the preparation of high performance materials through formation of polymer-CNT nanocomposites. However, the preparation of polybenzoxazine/CNT composites is limited due to the poor dispersion of CNTs in polybenzoxazine matrix. The key point for the high performance PBz/CNT nanocomposites is to enhance the dispersion and control the de-aggregation of CNTs in the matrix. Therefore, the most effective approach to overcome the dispersion problem is the functionalization of CNTs with benzoxazine moieties. Wang et. al. studied for the first time preparation of Bz-functionalized multi-

walled CNTs (MWCNTs) nanohybrids and their applications in generation of high performance PBz/CNT nanocomposites. Benzoxazine functionalized MWCNTs have multiple Bz groups that can copolymerize with benzoxazine monomer and effectively enhance the adhesion between PBz matrix and MWCNTs and the dispersion in the polymer matrix. The polybenzoxazine/CNT nanocomposites showed a great electrical conductivity and provide the opportunity to improve electrical and mechanical property of polybenzoxazines[26].

1.2.4. Polybenzoxazine/POSS Nanocomposites

Polyhedral oligomeric silsesquioxane, POSS, is an inorganic core and up to eight functional groups can be added that are polimerizable and crosslinkable. Even distributions of these inorganic POSS particles in the polymer matrix at nanometer scale provide a significant improvement in thermal and mechanical properties of the polymers[27–32]. Inorganic POSS particles offer the advantages such as monodispersity, low density, stability at high temperatures, lack of trace metal and interfacial interaction between composite and polymer segments. The POSS can be introduced into the matrix with polimerizable groups.

Incorporation of monofunctional benzoxazine-substituted POSS (MBz-POSS) into polybenzoxazine matrix by ring-opening polymerization improved the thermal properties relative to those of neat polybenzoxazine[33]. Later, eight benzoxazine groups were introduced into the POSS and multifunctional POSS was copolymerized with other benzoxazine monomers based on phenol and bisphenol-A. The dispersion at a nanometer scale was obtained for low POSS content and higher MBz-POSS content improved the glass transition temperature and thermal decomposition temperatures[34].

1.2.5. Polybenzoxazine/Magnetic Nanocomposites

Magnetic nanocomposites have attracted great interest due to their potential use in electronic devices, magnetic data storage, biotechnology/biomedicine, rechargeable batteries, etc. [35] Magnetite (Fe_3O_4) nanoparticles can be well dispersed into the polymer matrix by using functional groups such as carboxylic acids, phosphates and sulfates that can bind to the surface of nanomagnetite.

Kiskan et. al. reported the synthesis of carboxylic acid functional benzoxazine that can be easily coated on the magnetite and polybenzoxazine-nanomagnetite nanocomposites were successfully prepared[23]

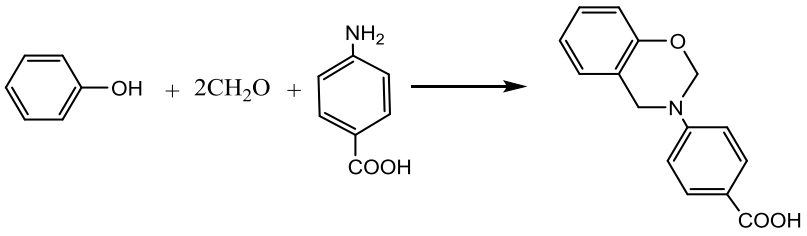

Figure 1.14 Synthesis of benzoxazine-benzoic acid (Pa-t)

The nanocomposites maintained their magnetic character after curing and the thermal stability of polybenzoxazine-magnetite nanocomposites increased with increasing nanomagnetite content.

1.2.6. Polybenzoxazine/Metal or Metal oxide Hybrid system

Low and co-workers[36] studied the effects of metal salts on the thermal stability of polybenzoxazines. It is shown that the transition metal salts initiate the ring opening but do not catalyze the polymerization of benzoxazines. Furthermore, metal salts were found to promote the formation of carbonyl groups during the polymerization of benzoxazines. It is proposed that the flammability of polybenzoxazines is reduced by

the presence of metal salts as a higher concentration of CO_2 is observed upon thermal degradation. It is also shown that the mechanism of degradation is not significantly affected by the presence of metals, except that the rate of weight loss is lower.

Moreover, Chirachanchai et.al focuses on an investigation of ortho-substituted group in phenol unit belonging to HBA in macrocyclization. N,N-bis(2-hydroxyalkylbenzyl)alkylamine (HBA) is a derivative obtained from a single time ring opening of benzoxazines. A series of HBA were chosen with and without methyl group at ortho position and the inclusion phenomena of these macrocycles with alkali ions.as representative compounds. The results showed that all macrocycles derived from HBA showed the inclusion phenomena with alkali ions[37].

1.3. Polymerization Mechanisms

The basic method of obtaining polybenzoxazines is to polymerize the monomers at elevated temperatures without catalysts. However, studies on catalyst-assisted benzoxazine curing showed that the curing time can be reduced and polymerization rate can be increased by adding addition of a catalyst.

The benzoxazine ring is a six-membered heterocyclic ring consisting N and O on the oxazine ring. The ring strain due to this molecular conformation makes this molecule undergo ring-opening polymerization under certain conditions via a cationic mechanism. Possible polymerization initiation site in benzoxazine molecule can be N or O due to their high basicity by Lewis definition. It has been proposed that oxygen on the oxazine ring will act as the initiation site due to its high negative charge distribution. When the polymerization starts from oxygen site, upon attack of a cationic initiator, a cyclic tertiary oxonium ion is formed which further react with additional monomers to yield a Mannich base phenoxy-type (Type I) polybenzoxazine structure [38].

Scheme 1.1 Polymerization mechanism A

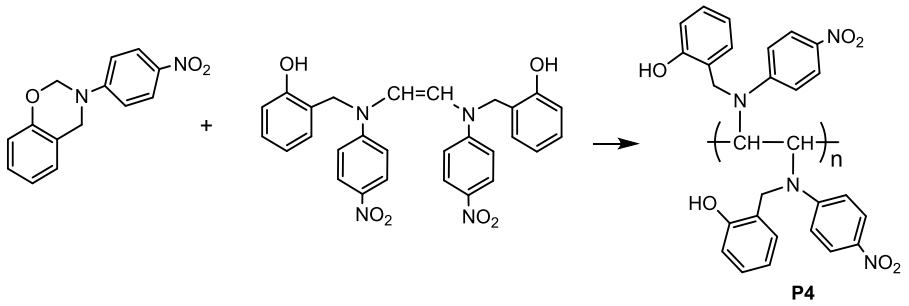

An alternative polymerization route is similar to this mechanism but the initiation and propagation site is nitrogen which can also lead to the formation of a Mannich base phenoxy-type (Type I) polybenzoxazine structure.

Scheme 1.2 Alternative of polymerization mechanism A

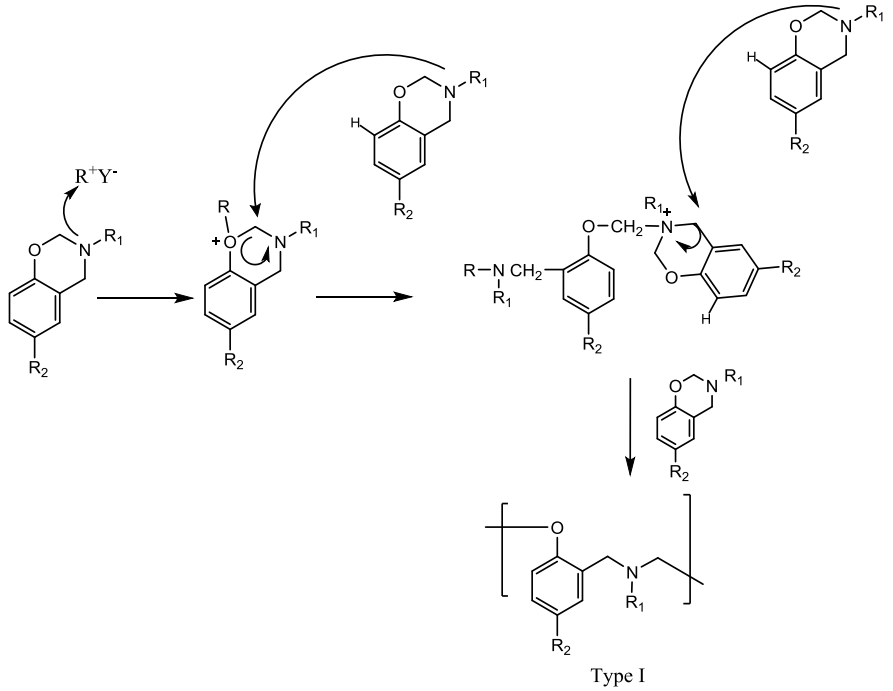

In addition to electron-rich oxygen and nitrogen, the benzene ring in the benzoxazine molecule has high reactivity toward thermal polymerization with or without catalyst. Therefore, the propagation can also proceed through the attack to the benzene ring upon initiation by a cationic initiator, producing a Mannich base phenolic-type (Type II) polymer. In this case, the propagation will occur via more stable carbocations, stabilized by intramolecular hydrogen bonding leading to high molecular weight polymer.

Scheme 1.3 Polymerization mechanism B

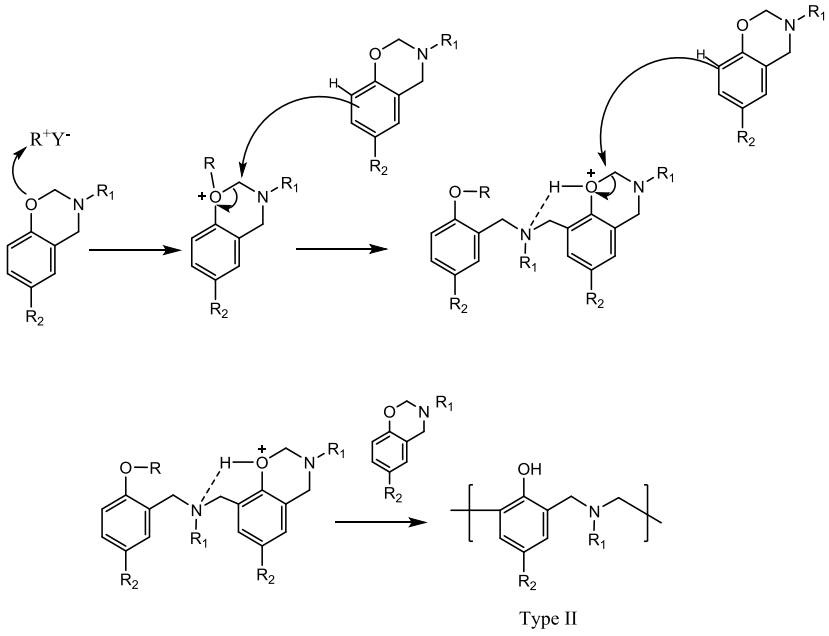

Burke et. al. reported that benzoxazine rings prefentially react with the ortho position to the hydroxyl group of free phenolic compound[39]. McDonagh and Smith reported the ring/chain tautomerism of benzoxazine molecule when protonated by migration of proton to the nitrogen atom, yielding iminium ions in the chain form. Riess et. al. showed the high reactivity of the ortho position and suggested that protonation at the oxygen atom of the ozaxine ring should occur at the initial step of polymerization to

form an iminium ion and then electrophilic aromatic substitution, as shown in Scheme 1.4.

Scheme 1.4 Formation of iminium ion

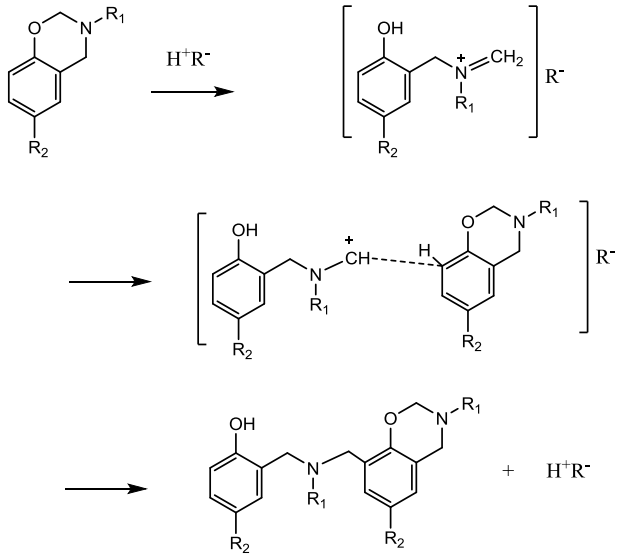

The structure of the resulting reactive intermediate is controlled by the pKa of the acid and in 1999, Dunkers and Ishida studied the effect of acidity on the polymerization of benzoxazine and concluded that as pKa value was increased, the formation of iminium ion was reduced. Trifluoro- and trichloroacetic acid provided a stable counter ion for the iminium ion. When p-cresol was used as a catalyst, the benzoxazine ring consumption was fast and complete but the benzene ring conversion was lower than the benzoxazine catalyzed with a strong acid[40].

Another type of linkage, *N,O*-acetal type, formed under limited conditions was reported. Polymerization of benzoxazine having two or three methyl groups yielded the *N,O*-aetal-type structure as the *ortho* position of the benzene ring is blocked or sterically hindered to prevent Mannich bridge formation[38].

Scheme 1.5 Formation of *N,O*-acetal-type structure

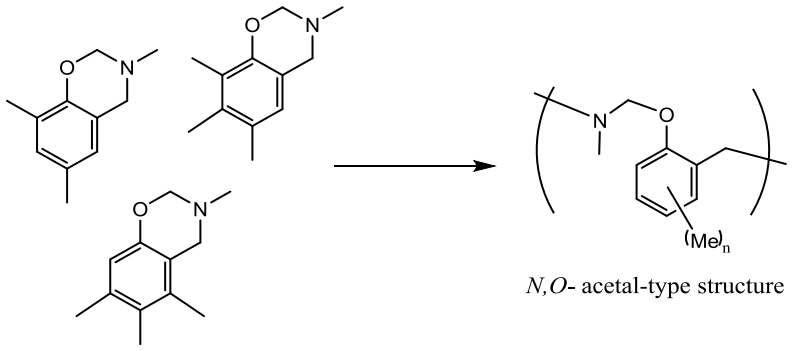

The formation of *N,O*-acetal type linkages in addition to Mannich-type structures has been reported using PCl_5 at low temperatures for the cationic polymerization of benzoxazine monomer.

Scheme 1.6 Cationic polymerization of benzoxazine monomer

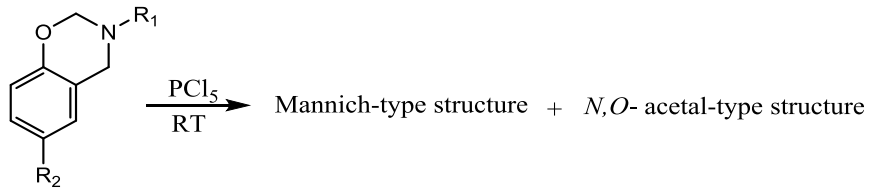

In a recent study, the catalytic activities of various catalyst and their effects on the structure of the final product were established. It is well-known that polymerization of benzoxazine includes three main ring-opening patterns, as *o*-attack, *N*-attack and *aryl*-attack, resulting in various phenoxy CH_2 and phenolic CH_2 units. Phenoxy CH_2 units finally rearrange into relatively stable phenolic CH_2 units. The ring-opening and electrophilic reactions are fast, while the rearrangement proceeds in a relatively slow rate [41].

The results showed that no ring-opening was observed without catalyst and the catalytic activity of lithium cation was affected by the anion partner. The polymerization was improved with high nucleophilicity and good leaving group ability of the anion and the trend was decreased in the order $I^- > Br^- > Cl^-$. The structure of the catalyst is also important; the relatively free lithium cation showed higher activity as observed for $LiClO_4$. Basic catalysts were also tested and no efficiency was seen for the polymerization of benzoxazine.

The effect of catalyst on the final structure of polybenzoxazine was also studied and p-toluenesulfonic acid, PTS, showed high percentage of true phenolic CH_2 structure. 2-athyl-4-methylimidazole, EMI yielded a more complex polymer including a significant amount of phenoxy CH_2 units due to the lower activity in the rearrangement step. LiI showed very high activity in the rearrangement step and produced almost only phenolic CH_2 units. These results showed that the structure of the final polymer can be specified by using appropriate catalyst to obtain the desired properties.

Recently, the polymerization mechanism of polybenzoxazines was studied in our group by Direct Pyrolysis Mass Spectrometry (DP-MS) technique in detail and results showed that polymerization of benzoxazine monomer may proceed through various reaction paths; the heterocyclic ring opening may be followed by attack of $-NCH_2$ groups to ortho and para positions of phenol and pyridine rings as shown in Scheme 2, generating **P1** and **P2** respectively [42,43]. In addition, the dimer generated by the coupling of $-NCH_2$ groups may polymerize via attack of $-NCH_2$ groups to phenol and/or pyridine rings or through vinyl polymerization yielding **P31**, **P32** and **P4** as presented in Scheme 3. As a consequence of these competing reaction pathways, generation of a cross-linked structure is expected. Thus, the trends in TGA and TIC curves, and the very high char yield are in accordance with the expectations confirming the heterogeneous and cross-linked polymer structures[42,43].

Scheme 1.7 Ring-opening polymerization of benzoxazines

a) by attack to phenyl ring

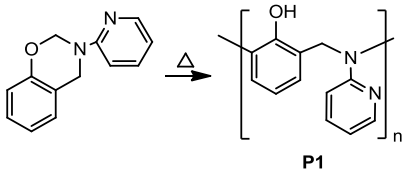

P1

a) by attack to pyridyl ring

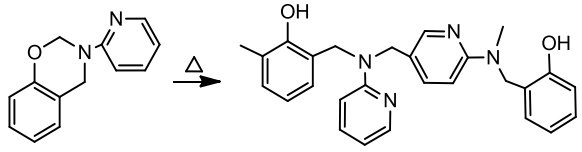

P2

Scheme 1.8. a) Generation of the dimer by coupling of $-NCH_2$ groups

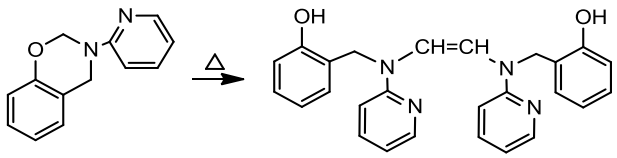

b) polymerization of the dimer

i) by attack of NCH_2 groups

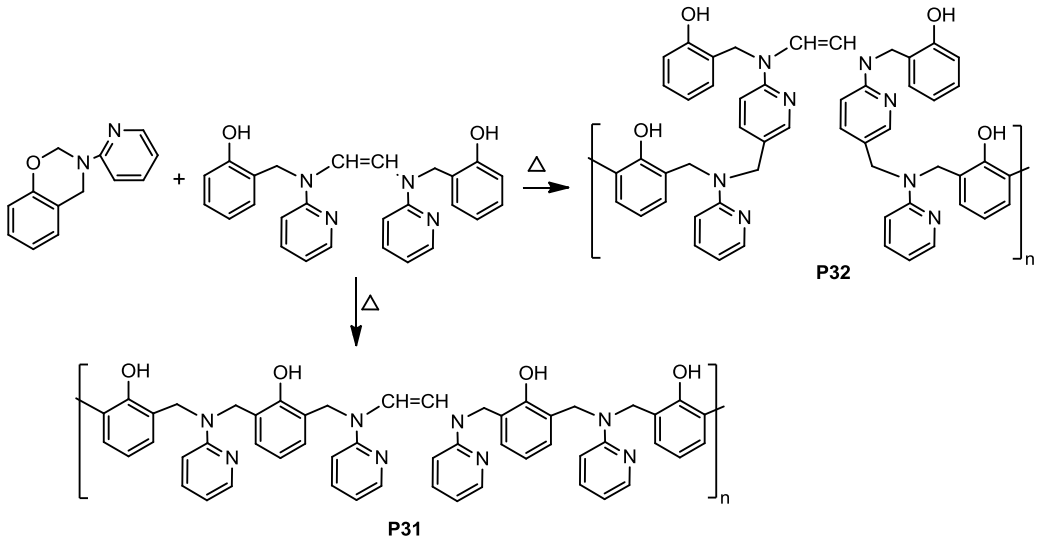

ii) by vinyl polymerization

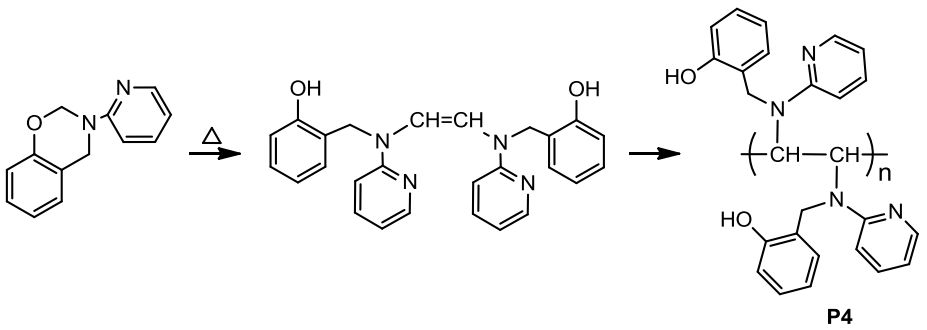

1.4. Unique Properties of Benzoxazines and Polybenzoxazines

Benzoxazines are the precursors for cross-linked polybenzoxazines and these cross-linked polymer exhibits a number of unique properties [44–54].

One of common problem of resins is their relatively high water uptake as much as 3-20% by weight upon saturation. Presence of polar groups in the resin is main reason for this high water absorption. Polybenzoxazines with the polar groups in its chemical structure exhibits low water absorption contrary to the general expectation. For example, a bisphenol-A and aniline based polybenzoxazine has 1.9% water uptake by weight and bisphenol-A and methyl amine based polymer has 1.3% water uptake at saturation[44]. This is an important property in terms of actual applications. Benzoxazines resins have near-zero shrinkage with high mechanical integrity [55] and their volumes change within ±1% upon polymerization. Polybenzoxazines are cross-linked resins and show high glass transition temperatures ranging from 160 to 400℃. The char yield of polybenzoxazines is one of the highest among the other processable polymers. Thermal properties of polybenzoxazines prepared from different benzoxazine monomers are listed below in Table 1.

Table 1.1 Unique properties of benzoxazine monomers

Monomers	T_g (°C)	$T_{5\%}$ (°C)	$T_{10\%}$ (°C)	Char Yield (%)	Reference
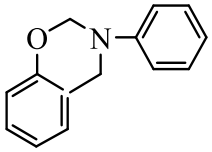	146	342	369	44	[19,44]
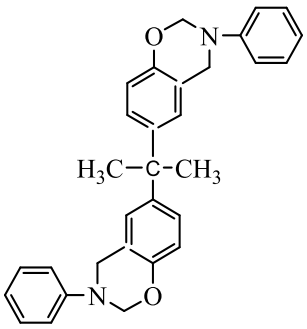	150	310	327	32	[19,44]
Acetylene functional benzoxazine					
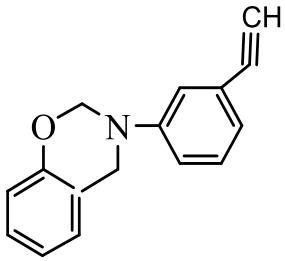	329	491	592	81	[56]
Allyl functional benzoxazine					
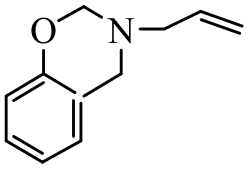	285	348	374	44	[19]

Nitrile functional benzoxazine 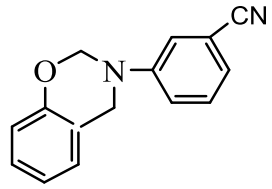	175	332	371	60	[4]
Maleimide functional benzoxazine 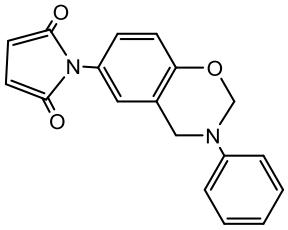	252	375	392	56	[57]

1.5. Characterization of Benzoxazines

There are several characterization techniques used to identify the benzoxazine structure and its open Mannich base.

1.5.1. Nuclear Magnetic Resonance Spectroscopy (NMR)

Nuclear magnetic resonance (NMR) spectroscopy is one of the most common methods to verify the structure of the benzoxazine monomer[58-61].

General frequency ranges for the characteristic ^{1}H resonances of oxazine CH_2 groups, Ph-CH_2-N(R) and O-CH_2-N(R)-, are 3.8-4.8 ppm and 4.7-5.7 ppm with the seperation about 0.8-0.9 ppm. These two resonances are easily recognized and are very useful for the identification of the structure.

The characteristic ^{13}C resonances of oxazine ring are seen in the range of 79-84 ppm for Ph-CH_2-N(R) and 49-59 ppm for O-CH_2-N(R)- groups.

Information on the monomeric (78 ppm) and open Mannich base structure (71 ppm) can be directly obtained from ^{15}N-NMR.

Solid-state NMR is a useful technique for the characterization of the cross-linked polybenzoxazine as the polymer is insoluble in most of the common solvents.

1.5.2. Fourier Transform Infrared Spectroscopy

There are various bands for the benzene ring modes that are associated with the oxazine ring attached to benzene ring. However, these modes are not readily recognized due to heavy overlapping bands. The band assignments for the monomers and dimers have been reported. The band at around 1500 cm^{-1} is characteristic mode of trisubstituted benzene and this band shifts to 1490 cm^{-1} upon benzoxazine polymerization forming tetrasubstituted benzene structure. The band in the range of 960-910 cm^{-1} is attributed to the benzene ring with the ozaxine ring structure and the disappearance of this band is associated with the ring-opening of the oxazine ring. In addition to this band, the decrease in the intensity of bands such as; asymmetric stretching vibration band of C-O-C of oxazine ring at around 1232 cm^{-1}, the symmetric stretching vibration band of C-O-C at around 1028 cm^{-1}, the characteristic bands of benzene ring with an oxazine ring at around 974 and 959 cm^{-1}, symmetric vibration band of C-N-C of the oxazine ring at 823 cm^{-1} and benzoxazine ring breathing band at 750 cm^{-1} are evidences for the ring-opening of the benzoxazine ring.[62-65].

1.5.3. Thermal Characterization

1.5.3.1. Differential Scanning Calorimetry (DSC)

Differential scanning calorimetry (DSC) is used to determine the ring-opening polymerization exotherms of the benzoxazines. Benzoxazines show a symmetric exotherms in the range of 200-250℃ if the sample is pure. This exotherms shifts to the lower temperatures with an asymmetric shape in the presence of impurities, such as phenolic compound and amines used as raw materials for the synthesis of the monomer, acting as initiators and/or catalysts.

1.5.3.2.Thermogravimetric Analysis (TGA)

Thermal stability and degradation mechanism of the polybenzoxazines is widely studied by thermogravimetry analysis (TGA) technique as the rate of degradation, degradation process and char yield can be determined. Char yield of the polybenzoxazines is in the range of 35% and 80% and three stages of decomposition are seen at 300, 400 and 500℃, attributed to the decomposition of the chain ends, evolution of amine and decomposition of the phenolic component, respectively.

1.5.3.3.Mass Spectrometry

Among several thermal analysis methods, thermal gravimetry-FTIR (TG-FTIR), thermal gravimetry-mass spectrometry (TG-MS) and pyrolysis mass spectrometry (py-MS) are the ones that give information not only on thermal stability but also on thermal degradation products that can be used to investigate thermal degradation mechanism.

Pyrolysis is thermal degradation of materials by cleavage at their weakest point to produce smaller volatile fragments in an inert atmosphere or vacuum. Pyrolysis is widely applied to investigate thermal characteristics of a compound such as, thermal stability, degradation products and decomposition mechanism. It is also used as a pre-

processing step to convert large molecules into lower mass molecules that are easily detectable. For instance, when polymers are pyrolyzed, smaller fragments, oligomers, are produced and analysis of these fragments aids in the identification of the polymers.

Pyrolysis technique can be coupled with FT-IR, GC (Py-GC), GC/MS (Py-GC/MS) or MS (DP-MS). Among these various analytical pyrolysis techniques, pyrolysis gas chromatography mass spectrometry, Py-GC-MS and direct pyrolysis mass spectrometry, DP-MS, have several advantages such as sensitivity, reproducibility, minimal sample preparation and consumption and speed of analysis [66-69].

Although py-GC-MS technique is significantly sensitive, only stable thermal degradation products can be detected with the use of this technique. On the other hand, DP-MS technique offers several advantages. The high vacuum inside the mass spectrometer favors vaporization and thus, allows the analysis of higher molar mass pyrolyzates. As the high vacuum system rapidly removes the degradation products from the heating zone, secondary reactions and condensation reactions are almost totally avoided. Furthermore, because of the rapid detection system of the mass spectrometers, unstable thermal degradation products can also be detected.

1.6. Thermal Degradation of Polybenzoxazines

Few studies on thermal degradation products of polybenzoxazines involved pyrolysis GC-MS, TGA-FTIR and DP-MS analyses. Yet, with the use of GC-MS and TGA-FTIR techniques secondary reactions during heating cannot be eliminated and only stable degradation products can be detected. Thus, the data obtained cannot be used to investigate thermal degradation mechanism [70-73].

Direct pyrolysis mass spectrometry analyses [42,43] revealed that thermal degradation of polybenzoxazines starts by the loss of alkyl amines and diamines in the case of polybenzoxazine based on phenol and methyl amine, poly(Ph-m) and bisphenol A and methylamine, poly(BA-m) and by the evolution of aniline in the case of polybenzoxazine based on phenol and aniline, poly(Ph-a) at around 280 °C.

Evolutions profiles of fragments involving aromatic units showed several peaks and shoulders revealing the presence of units with different thermal stabilities and hence, presence of linkages with different structures along the polymer chains.

1.7. Aim of the study

The aim of this study is to investigate the thermal and structural characteristics of polybenzoxazines based on various amines namely, aniline, aminopyridine, aminobenzonitrile and nitroaniline. In the first part of this work, benzoxazines based on phenol and aniline or aniline derivatives namely aminopyridine, aminobenzonitrile and nitroaniline are synthesized and polymerized by curing the monomers systematically to investigate the effect of curing conditions on polymerization and thermal degradation of polybenzoxazines. In the second part of the work metal or metal ions are incorporated to benzoxazine monomers based on aminopyridine, aminobenzonitrile and nitroaniline. The structural and thermal characteristics of the polybenzoxazines and metal or metal ion functional polybenzoxazines are analyzed via FTIR, NMR, DSC, TGA and DP-MS techniques. The effects of curing program used and incorporation of metal and/or metal ion on structural and thermal characteristics of the polybenzoxazines are investigated.

CHAPTER 2

EXPERIMENTAL

2.1. Materials

Phenol (99.5%), paraformaldehyde, anhydrous cobalt(II) chloride, sodium hydroxide and chloroform were purchased from Sigma Aldrich Co. 2-aminopyridine (99.5%) $Cr(CO)_6$ and $CrCl_3$, aniline, nitroaniline, aminobenzonitrile, hexane, ethyl acetate, MgSO4 were supplied by Merck. All chemicals were used as received without further purification.

2.2. Characterization Techniques

2.2.1. Nuclear magnetic resonance spectroscopy (NMR)

Proton NMR spectra were acquired with a Bruker AC250 (250.133 MHz) spectrometer using $CDCl_3$ as the solvent and tetramethylsilane (TMS) as the internal standard.

2.2.2. Infrared spectrophotometer (ATR-FT-IR)

ATR-FT-IR analysis of the samples was performed by directly insertion of solid sample using Bruker Vertex 70 Spectrophotometer with 0.4 cm^{-1} resolution.

2.2.3. Scanning Electron Microscope (SEM)

SEM studies of the samples in powder form, fixed on an aluminum stab using carbon tape, were conducted using a scanning electron microscope Quanta 400 F Field Emission SEM instrument.

2.2.4. Thermogravimetry (TGA) and Differential Scanning Calorimetry (DSC)

TGA and DSC analyses were performed on a Perkin Elmer Instrument STA6000 under nitrogen atmosphere at a flow rate of 20 mL/min and a heating rate of 10 ℃/min.

2.2.5. Direct pyrolysis mass spectrometry (DP-MS)

Direct pyrolysis mass spectrometry (DP-MS) analyses of the samples (0.010 mg) in flared quartz sample vials were performed on a Waters Micromass Quattro Micro GC Mass Spectrometer with a mass range of 15-1500 Da coupled to a direct insertion probe. The samples were heated to 650 ℃ at a rate of 10 ℃/min while recording 70 eV EI mass spectra, at a rate of 1 scan/s. The step-wise curing of the monomers and the pyrolysis of the polymers, if generated any, during the curing process were also utilized inside the mass spectrometer while recording the mass spectra continuously at a rate of 1 scan/s. All the analyses were repeated at least twice to ensure reproducibility.

Collision induced dissociation experiments were conducted using argon as the collision gas and 40, 30 and 20 eV EI ionization. The daughter spectra of the precursor ions were recorded at the temperatures at which the yield of the selected precursor ion was maximized. Interpretation of the pyrolysis mass spectra was achieved by analyses of the trends in single ion evolution profiles and precursor-ion spectra.

2.3. Synthesis

2.3.1. Synthesis of benzoxazine based on aniline, Ph-a

Synthesis of benzoxazine monomer, Ph-a

Benzoxazine monomer was prepared according to the literature methods. The mixture of phenol (5 mmol), aniline (5 mmol), and paraformaldehyde (10 mmol) was stirred

at 110℃ for 60 min. Subsequently, the viscous liquid was cooled to about 50℃, and about 30 mL chloroform was gradually introduced into the flask. Then, the chloroform solution was poured into a separatory funnel and washed several times with NaOH aqueous solution (3 mol/L) and deionized water, respectively. The chloroform solution was dried over anhydrous $MgSO_4$ and the solvent was removed under reduced pressure. The residue was fractionated by silica gel column chromatography using hexane/ethyl acetate mixture as an eluent to obtain crude benzoxazine as a yellow solid.

Synthesis of benzoxazine polymer, PPh-a

Benzoxazine monomers based on phenol and aniline cured step by step systematically.

2.3.2. Synthesis of benzoxazine based on p-nitroaniline, Ph-na

Synthesis of benzoxazine monomer, Ph-na

Benzoxazine monomer was prepared according to the literature methods. The mixture of phenol (5 mmol), p-nitroaniline (5 mmol), and paraformaldehyde (10 mmol) was stirred at 140℃ for 60 min. Subsequently, the viscous liquid was cooled to about 50℃, and about 30 mL chloroform was gradually introduced into the flask. Then, the chloroform solution was poured into a separatory funnel and washed several times with NaOH aqueous solution (3 mol/L) and deionized water, respectively. The chloroform solution was dried over anhydrous $MgSO_4$ and the solvent was removed under reduced pressure. The residue was fractionated by silica gel column chromatography using hexane/ethyl acetate mixture as an eluent to obtain crude benzoxazine as a yellow-orange solid.

Preparation of metal functional benzoxazine monomers M-Ph-na

For the coordination of Co^{2+} or Cr, Ph-na and metal salt, $CoCl_2$ or $Cr(CO)_6$, in 1:1 mole ratio, were mixed in chloroform and refluxed for 6 hours. Evaporation of the solvent yielded metal and/or metal ion functional benzoxazine monomers.

Synthesis of benzoxazine polymer, PPh-na

Benzoxazine monomers based on phenol and p-nitroaniline cured step by step systematically.

Synthesis of metal and/or metal ion functional benzoxazine polymers, M-PPh-na

Polymerizations of the metal and/or metal ion coordinated benzoxazine monomers based on phenol and p-nitroaniline were achieved by stepwise curing of the monomers for 3 hours at 180 and 2 hours at 200°C in an oven.

2.3.3. Synthesis of benzoxazine based on 3-aminobenzonitrile, Ph-abn

Synthesis of benzoxazine monomer, Ph-abn

Benzoxazine monomer was prepared according to the literature methods. The mixture of phenol (5 mmol), 3-aminobenzonitrile (5 mmol), and paraformaldehyde (10 mmol) was stirred at 110℃ for 60 min. Subsequently, the viscous liquid was cooled to about 50℃, and about 30 mL chloroform was gradually introduced into the flask. Then, the chloroform solution was poured into a separatory funnel and washed several times with NaOH aqueous solution (3 mol/L) and deionized water, respectively. The chloroform solution was dried over anhydrous $MgSO_4$ and the solvent was removed under reduced pressure. The residue was fractionated by silica gel column chromatography using hexane/ethyl acetate mixture as an eluent to obtain crude benzoxazine as a light yellow solid.

Preparation of metal functional benzoxazine monomers, M-Ph-abn

For the coordination of Co^{2+} or Cr, Ph-abn and metal salt, $CoCl_2$ or $Cr(CO)_6$, in 1:1 mole ratio, were mixed in chloroform and refluxed for 6 hours. Evaporation of the solvent yielded metal and/or metal ion functional benzoxazine monomers.

Synthesis of benzoxazine polymer, PPh-abn

Benzoxazine monomers based on phenol and 3-aminobenzonitrile cured step by step systematically.

Synthesis of metal and/or metal ion functional benzoxazine polymers, M-PPh-abn

Polymerizations of the metal and/or metal ion coordinated benzoxazine monomers based on phenol and 3-aminobenzonitrile cured step by step systematically.

2.3.4. Synthesis of benzoxazine based on 2-aminopyridine, Ph-ap

Synthesis of benzoxazine monomer, Ph-ap

Benzoxazine monomer was prepared according to the literature methods. The mixture of phenol (5 mmol), 2-aminopyridine (5 mmol), and paraformaldehyde (10 mmol) was stirred at 110℃ for 60 min. Subsequently, the viscous liquid was cooled to about 50℃, and about 30 mL chloroform was gradually introduced into the flask. Then, the chloroform solution was poured into a separatory funnel and washed several times with NaOH aqueous solution (3 mol/L) and deionized water, respectively. The chloroform solution was dried over anhydrous $MgSO_4$ and the solvent was removed under reduced pressure. The residue was fractionated by silica gel column chromatography using hexane/ethyl acetate mixture as an eluent to obtain crude benzoxazine as a yellow solid. Contrary to the general applications, purification of the monomer to separate any side product generated by the condensation reaction of formaldehyde with the aromatic units that would inhibit the coordination of metal ion, was highly curicial.

Preparation of metal functional benzoxazine monomer, M-Ph-ap

For the coordination of Co^{2+} ion, the purified benzoxazine monomer, Ph-ap and metal salt, $CoCl_2$, in 2:1, 1:0.75, 1:1, 1:1.5 and 1:2 mol ratios, were mixed in chloroform and refluxed for 6 h according to the literature methods [23]. Evaporation of the solvent yielded greenish yellow solid.

For the coordination of Cr or Cr^{3+}, Ph-ap and metal salt, $CoCl_2$ or $CrCl_3$, in 1:1 mole ratio, were mixed in chloroform and refluxed for 6 hours. Evaporation of the solvent yielded metal and/or metal ion functional benzoxazine monomers.

Synthesis of the neat and metal and/or metal ion functional benzoxazine polymers, PPh-ap and M-PPh-ap

Polymerizations of the neat and metal and/or metal ion coordinated benzoxazine monomers were achieved by stepwise curing of the monomers at 170 and 200°C for 60 min each and 210 °C for 120 min in an oven. The temperatures at which evaporation and/or degradation of monomer take place were determined by gradual heating of the monomer inside the mass spectrometer. The temperatures of the steps of the curing cycle were selected as few centigrates lower than these values. The curing of the monomers was also performed inside the mass spectrometer while recording mass spectra continuously.

CHAPTER 3

RESULTS AND DISCUSSION

3.1. Polymerization of benzoxazines

Polymerization of benzoxazine monomers based on phenol and aniline and aniline derivatives, namely, nitroaniline, aminobenzonitrile and aminopyridine are achieved by curing the monomers systematically. The effect curring on structural and thermal characteristics are investigated.

3.1.1. Benzoxazine monomer based on aniline

Benzoxazine monomer was synthesized from phenol, 2-aminopyridine and paraformaldehyde via solventless method (Scheme 3.1).

Scheme 3.1 Synthesis of benzoxazine monomer based on aniline and phenol

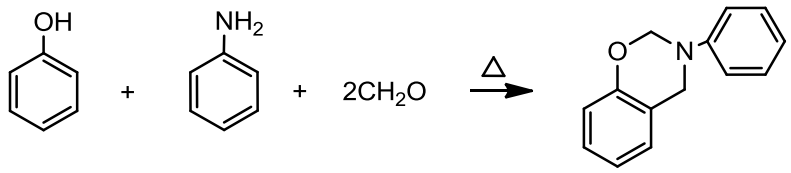

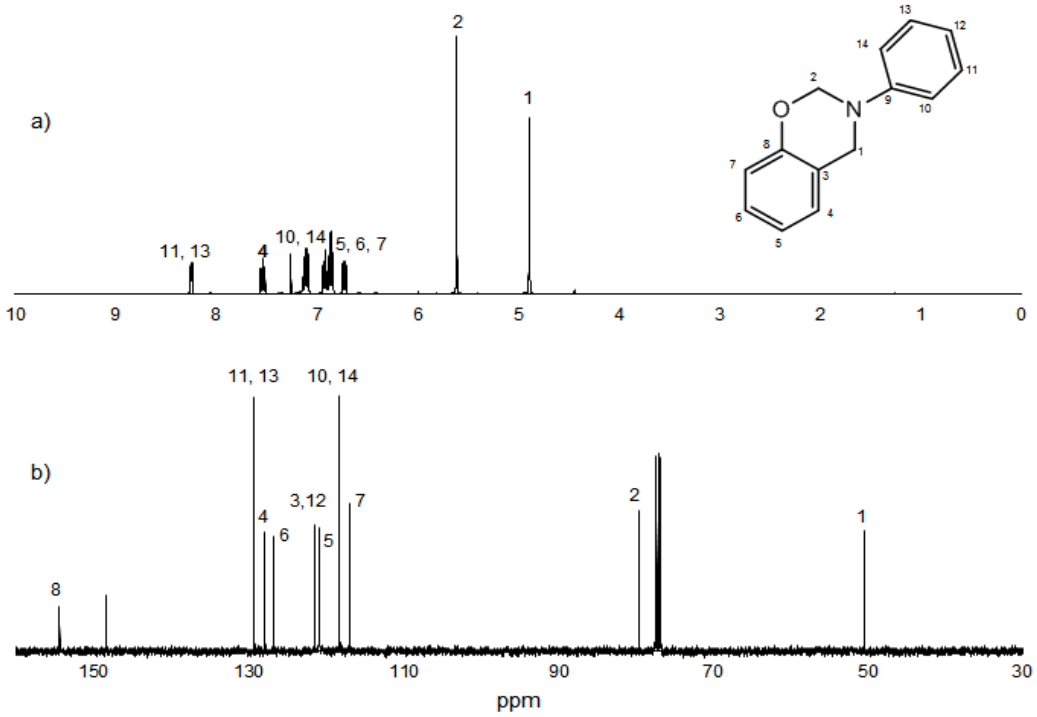

Figure 3.1 a) Proton-NMR and b)13C-NMR spectra of benzoxazine monomer.

The resonances at 4.88 and 5.60 ppm correspond to the methylene protons (H1 and H2) of Ar-CH_2-N and O-CH_2-N of the oxazine ring, respectively. The chemical shifts (ppm) at 6.71 (1H, H12), 6.84 (1H, H6), 6.86 (1H, H7), 6.91 (1H, H5) 7.08 (2H, H10 and H14), 7.52 (1H, H4), and 8.24 (2H, H11 and H13) are assigned to the aromatic protons. The resonances at 50.45 and 79.51 ppm correspond to the methylene carbons (C1 and C2) of Ar-CH_2-N and O-CH_2-N of the oxazine ring, respectively. Other chemical shifts (ppm) are assigned to the resonances of the carbons: 117.08 (C7), 118.31 (C10, C14), 120.85 (C5), 120.95 (C12), 121.48 (C3), 126.78 (C6), 127.91 (C4), 129.36 (C11, C13), 148.45 (C9), 154.45 (C8). Anal. calcd. for C14H13NO: C, 79.62; H, 6.16; N, 6.64; O,7.58%. Found: C, 79.16; H, 6.14; N, 6.71; O,7.99%.

The FTIR spectrum of the benzoxazine monomer is shown in Fig.3.2a. The typical absorption bands for the benzoxazine are observed at 1484, 1374, 1230, 1030 and 948 cm^{-1}, corresponding to the di-substituted benzene rings, CH_2 wagging, Ar-O-C anti-symmetric stretching, C-O-C symmetric stretching of oxazine ring and vibration

modes of benzene ring with an oxazine ring, respectively. The band at 823 cm^{-1} corresponds to the symmetric stretching vibration of C-N-C of the oxazine ring and the C-H out-of-plane bending of the aromatic ring, whereas the band at 750 cm^{-1} is ascribed to the benzoxazine ring breathing.

In general, the peaks in the region 1600-1585 and 1500-1400 cm^{-1} are assigned to C-C stretching vibrations in aromatic compounds. The ring C-C stretching vibrations occur in the region 1600-1350 cm^{-1}. The peaks at 1595, 1576 and 1434 cm^{-1} are related to C-C stretching vibrations. The aromatic C-H in plane bending and out-of-plane deformation modes of benzene and its derivatives are observed in the region 1300-1000 cm^{-1}, and 1000-600 cm^{-1} regions respectively. Thus, several peaks present in these regions are associated with both of the di-substituted benzene rings present in the structure.

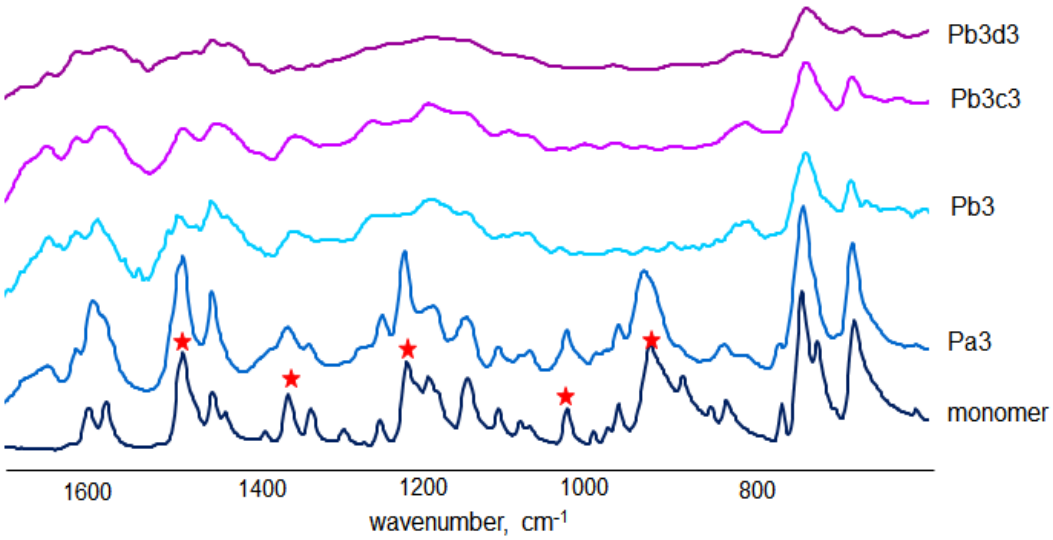

Figure 3.2 FT-IR spectrum of a)Ph-a monomer, b)Pa3, c)Pb3, d)Pb3c3, e)Pb3d3

Polymerization of the aniline based benzoxazine monomer was achieved by applying different curing programs involving systematic changes in the temperature, period and number of steps of curing, in order to determine the effects of these variables on

the structure and thus on thermal characteristics of polybenzoxazines generated. Abbreviations used for the products are given according to DSC results and the temperature and the period applied during the curing process; if DSC data indicated incomplete polymerization, then the samples are symbolized by letter M, if complete polymerization was achieved according to DSC data, then the samples are symbolized by P. The curing temperatures are denoted by letters a, b, c and d for 150, 175, 200 and 225°C respectively, and the duration of the curing in hours are also stated in the symbols. The curing programs applied and the abbreviations used for the products are summarized in Table 3.1.

Table 3.1 The temperature (°C) and period (h) of each step of the curing process and the abbreviations used for the products obtained

one step curing		
T	P	Abr.
150	3	Pa3
	6	Pa6
175	1.5	Pb6
	3	Pb3
200	1.5	Pc1.5
	3	Pc3
225	1.5	Pd1.5
	3	Pd3

two step curing			
T_1	T_2	P	Abr.
175	200	1.5	Pb1.5c1.5
	225		Pb1.5c1.5
	200	3	Pb3c3
	225		Pb3c3
200	225	1.5	Pc1.5d1.5
	225	3	Pc3d3

three step curing				
T_1	T_2	T_3	P	Abr.
175	200	225	1	Pb1c1d1
175	200	225	3	Pb3c3d3

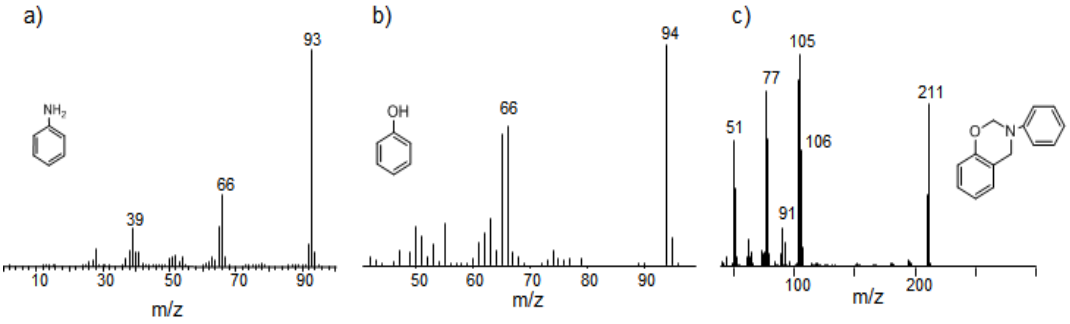

Figure 3.3 The mass spectra for a)aniline, b)phenol and c)benzoxazine monomer based on aniline and phenol

Polymerization of the benzoxazine monomers cured with different curing programs systematically is controlled by DSC analyses. The exothermic ring opening polymerization peak in the temperature range of 220-230°C is observed for the sample Ma3 which was cured at 150℃ for 3 hours, indicating that the polymerization was not completed for these samples (Fig. 3.4). The disappearance of this peak in the DSC curves of the rest of the samples confirms polymerization of the Ph-a monomer by the applied curing programs. As representative examples DSC profiles for Pb1.5, Pc1.5 and Pd1.5 cured at 175, 200 and 225 °C for 1.5 hours, respectively are also depicted in Fig.3.4.

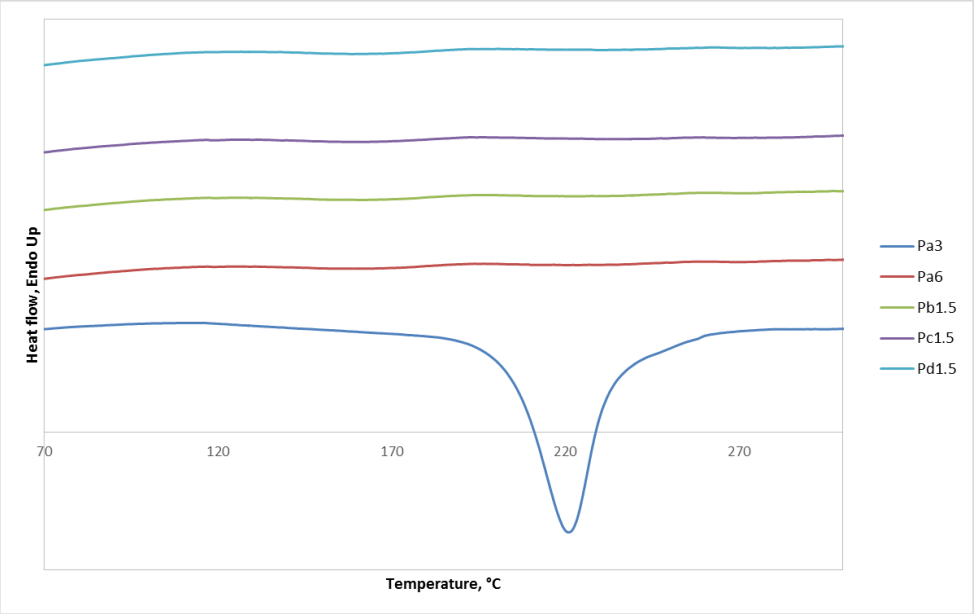

Figure 3.4 DSC profiles of benzoxazines Pa3 and Pa65 cured at 150°C for 3 and 6 h respectively and Pb1.5, Pc1.5 and Pd1 cured at 175, 200 and 225°C for 1.5h.

Polymerization of the monomer is also confirmed by FTIR analyses as shown in Fig.3.2b,c,d and e. The polymer spectrum exhibits disappearance of the characteristic peaks of oxazine and di-substitute benzene rings at 1487, 1366, 1227, 1039 and 959 cm^{-1} indicating complete polymerization via ring opening of oxazine ring. The peaks in the region 1600-1550 and 1500-1400 cm^{-1} assigned to C-C stretching vibrations are also diminished significantly. This behavior may be related to crosslinked structure of the polymer generated. The aromatic C-H in plane bending and out-of-plane deformation modes of aromatic rings are detected again in the range 1250-1050 and 900-700 cm^{-1}.

Thermal degradation of polybenzoxazines

To investigate the thermal characteristics of the polymers generated, the samples for which complete polymerization was indicated by DSC findings, were analyzed by TGA and DP-MS techniques. The TGA curves of these polymers are shown in Fig. 3.5 and the results are tabulated in Table 3.2.

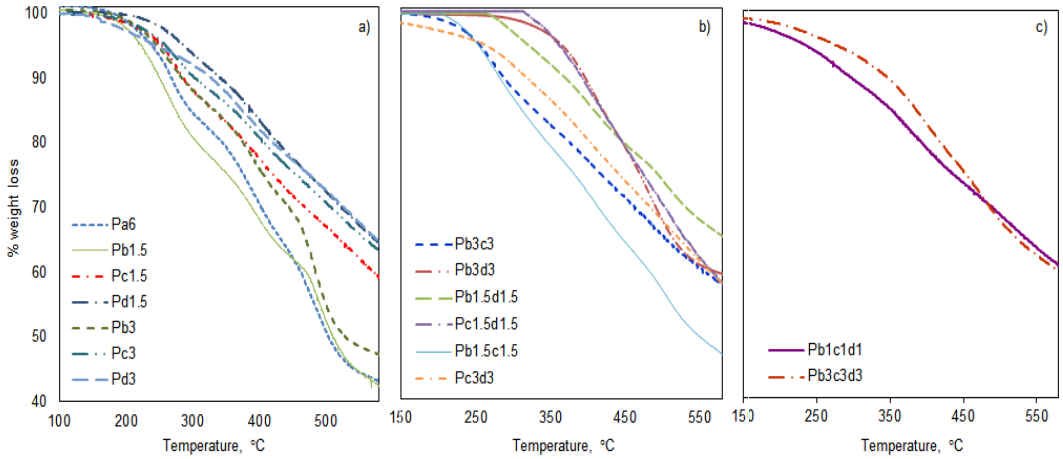

Figure 3.5 TGA curves of polybenzoxazines prepared by a) one-step, b) two-step and c) three-step curing process

TGA results reveal that thermal degradation of polybenzoxazine based on aniline occurs in two or three steps in the temperature regions 200-280, 300-400 and 480-530°C, and yields 40-60% char yield that increases as the temperature and duration of curing is increased. This behavior may either be due to a multi-step thermal degradation or a polymer sample involving chains with different structures, thus, different thermal stabilities.

In general, as the temperature and/or the duration of one-step curing process are increased, the initial degradation step of the polymer shifts to high temperatures slightly. For the sample cured at 225°C, the degradation step below 300°C disappears. The second and third steps of degradation shifts to lower temperatures for the polymers cured for longer periods.

Thermal degradation behaviors of the samples cured in two or three steps show noticeable differences. The first step of the degradation is only observed for the polymers cured at 200°C after pre-heating at 175°C for 1.5 or 3 h at each step and for the polymer cured at 225°C after preheating at 175 and 200°C for 1.5 h at each step. Furthermore, in general, the second step decomposition slightly shifts to lower

temperatures for the polymers cured at higher temperatures and/or for longer periods. The third step of the degradation is not observed for the samples cured at 225°C after pre-heating at 200°C. Thus, TGA results indicate that thermal behavior of the polymers depends on the curing program applied; the number of steps of curing, the temperature and duration at each step, affect the thermal characteristics.

The TIC curves of the samples cured at 150°C for 3 or 6h, at 175, 200 and 225°C for 1.5 or 3 h, (Pa3, Pa6, Pb1.5, Pb3, Pc1.5, Pc3, Pd1.5 and Pd3) and the pyrolysis mass spectra recorded at the maxima of the peaks present in the TIC curves are shown in Fig.3.6. In general, three peaks are present in the TIC curves in accordance with TGA data.

Table 3.2 TGA data for polybenzoxazines prepared by different curing programs

Sample*	$T_{5\%}$	T_{max}			% char yield, at 600 ˚C
		Step 1	**Step 2**	**Step 3**	
Pa3	179.8	210.1	265.8	389.9	37.2
Pa6	237.8	268.2	387.8	485.6	43.0
Pb1.5	222.4	258.7	392.3	490.5	41.9
Pb3	245.7	270.6	389.1	482.8	47.1
Pc1.5	252.7	276.1	410.2	523.5	58.2
Pc3	257.6	278.8	398.1	520.9	62.7
Pd1.5	285.8	281.3	396.3	527.4	63.9
Pd3	242.1		370.6	522.9	63.8
Pb1.5c1.5	254.6	269.7	408.5	504.3	46.5
Pb3c3	256.3	274.8	402.8	490.1	57.1
Pb1.5d1.5	321.9		402.3	500.8	64.8
Pb3d3	365.9		401.5	481.8	59.2
Pc1.5d1.5	361.9		382.3		57.2
Pc3d3	264.2		399.7		57.1
Pb1c1d1	242.5	276.8	383.6	508.9	60.1
Pb3c3d3	284.6		396.5	479.5	59.4

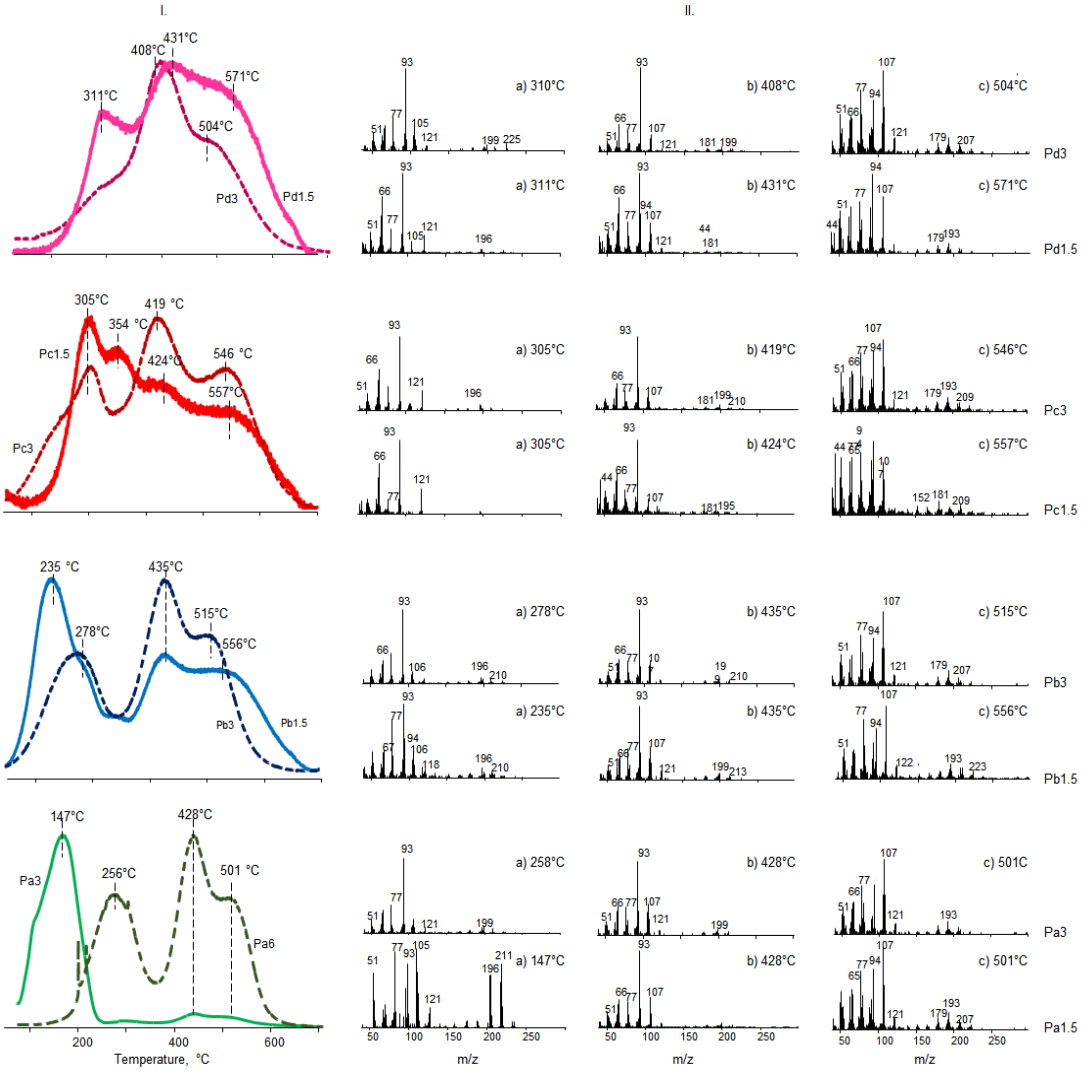

Figure 3.6 TIC curves and the mass spectra recorded during the pyrolysis of polybenzoxazines, PPh-a, cured at 150 °C for 3h (Pa3) and 6 h (Pa6), at 175°C for 1.5h (Pb1.5) and 3h (Pb3), at 200 °C for 1.5h (Pc1.5) and 3h (Pc3) and at 225 °C for 1.5h (Pd1.5) and 3h (Pd3)

The presence of an intense peak at significantly low temperature regions, at around 147°C, in the TIC curve of the sample Ma3 can be attributed to evolution of unreacted monomer and/or decomposition of low molecular weight oligomers in accordance with DSC results. The pyrolysis mass spectrum at the maximum of the peak in the TIC curve is dominated with the diagnostic peaks of the Ph-a monomer. For this sample, the relative intensities of the high temperature overlapping peaks associated

with degradation of thermally stable polymer chains, are noticeably low, pointing out that the amount of polymer chains with desirable thermal stability is almost negligible. Thus, it can be concluded that the curing of the monomer at 150℃ for 3 h (Pa3) was not sufficient for generation of thermally stable high molecular weight polymer chains. The TIC curve of the sample Pa6, prepared by curing for longer periods, for 6 h, indicates a high temperature shift for the initial step of thermal degradation. In addition, its intensity is decreased noticeably while those of the high temperature peaks are increased drastically, indicating complete polymerization in accordance with the disappearance of the exothermic peak associated with ring opening polymerization in the DSC curve. The diagnostic peaks of the monomer and the fragment ions that can also be generated during ionization of the monomer inside the mass spectrometer such as M-H (210 Da), $C_6H_5NCH_2$ (105 Da) and C_6H_5 (77 Da) still detected in the pyrolysis mass spectra at around 256°C, can then be related to decomposition of low molar mass oligomers during pyrolysis and/or ionization inside the mass spectrometer. The mass spectra recorded at the maxima of the high temperature peaks are almost identical for both samples.

Increasing the duration of curing from 1.5 to 3 h at 175 °C shifts the initial thermal degradation step of the polymer generated to high temperature regions; the evolutions of thermal degradation products are maximized at around 240 to 280℃ during the pyrolysis of the samples cured for 1.5 and 3 h respectively. However, thermal degradation is still occurred at low temperature regions and the pyrolysis mass spectra consist of diagnostic peaks of the monomer. As DSC curves indicated complete polymerization, it can be thought that the monomer and the low mass fragments are generated by the degradation of low mass oligomers, or chains that do not involve crosslinking units. The products lost at elevated temperatures become predominant during the pyrolysis of the polymer cured for 3h, but, thermal degradation of the polymer is completed at lower temperature regions indicating generation of a thermally more homogenous polymer decomposing in a narrower temperature range. Again, the mass spectra recorded at the maxima of the high temperature peaks are almost identical for both of the samples.

Overlapping peaks with maxima 305, 354, 429 and 557°C are detected in the TIC curve of the sample cured at 200°C for 1.5 h. For the sample cured for 3 h the peak at 354°C is disappeared. The diagnostic peaks of the monomer are either totally disappeared or diminished significantly in the spectra and the relative yields of the products lost at elevated temperatures are enhanced. The pyrolysis mass spectra recorded at the maxima of the peak corresponding to last step of thermal degradation show significant differences.

During the pyrolysis of the samples cured at 225°C for 1.5 and 3 h, Pd1.5 and Pd3 respectively, it has been determined that the initial step of thermal degradation is independent of the duration of curing. Yet, the relative yields of the products lost at initial stages of pyrolysis are decreased while those evolved at elevated temperatures are increased, as recorded for the samples cured at lower temperatures. Furthermore, the high temperature peaks associated with degradation of thermally more stable polymer chains are slightly shifted to lower temperature regions. In addition, the pyrolysis mass spectra at the maxima of the peaks present in the TIC curves recorded during the pyrolysis of the samples cured for 1.5 and 3 h, show noticeable differences.

Thus, it can be concluded that as the curing temperature or duration of curing at a given temperature was increased, the initial step of thermal degradation of the polymer generated shifts to high temperatures, whereas, the second and third steps of decomposition shift to low temperature regions. Furthermore, noticeable increases in the relative yields of the products evolved in the second and third steps of degradation occur during the pyrolysis of the polymers cured at higher temperatures. On the other hand, increase in the duration of curing at a given temperature causes significant decrease in the relative yields of the products lost at initial and final steps of thermal degradation.

The TIC curves and the pyrolysis mass spectra at the maximum of the peaks present in the TIC curves recorded during the pyrolysis of the samples cured at 200 °C after preheating at 175°C for 1.5h (Pb1.5c1.5), or 3 h (Pb3c3), at 225 °C after preheating

at 175°C for 1.5h (Pb1.5d1.5), or 3 h (Pb3d3) and at 225 °C after preheating at 200°C for 1.5h (Pc1.5d1.5), or 3 h (Pc3d3), are shown in Fig.3.7.

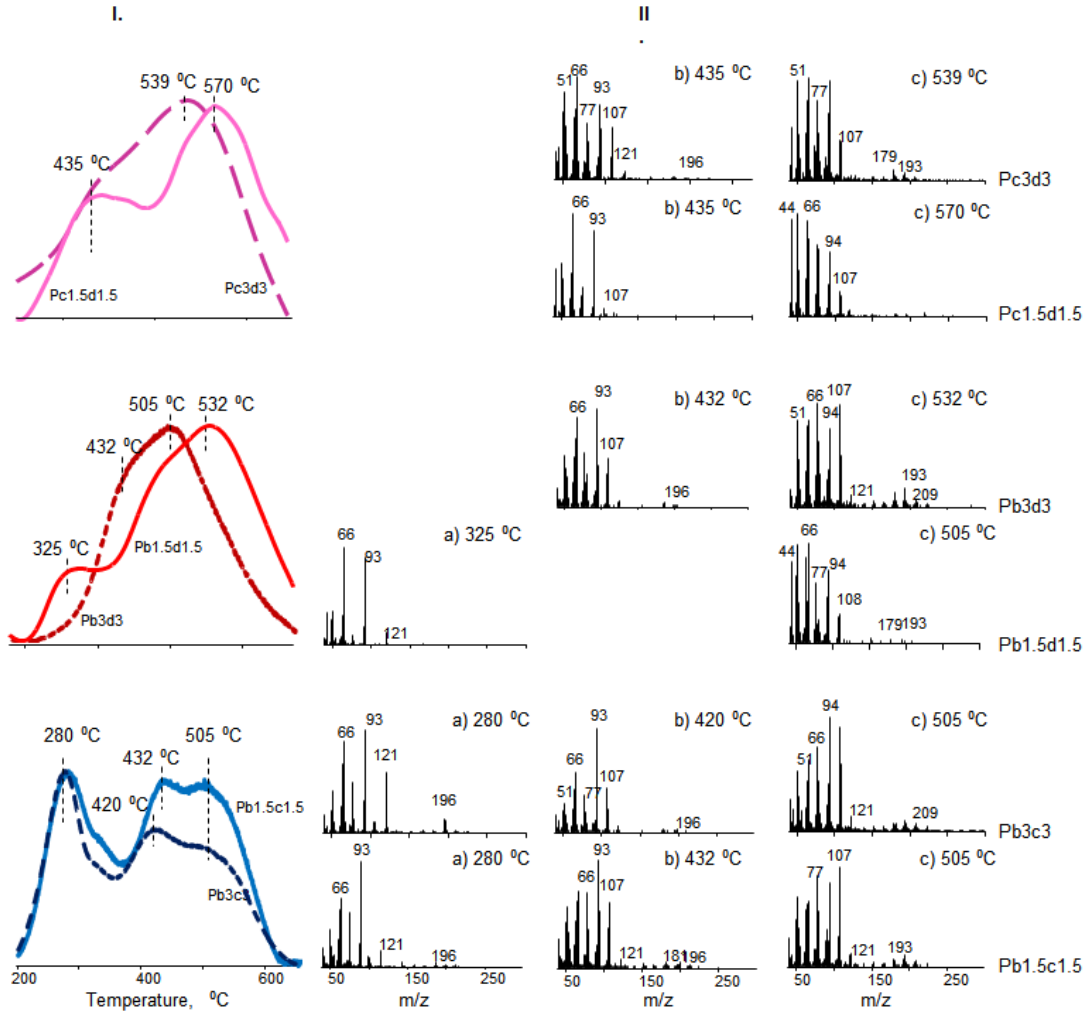

Figure 3.7 TIC curves of PPh-a cured at 200 °C after preheating at175°C for 1.5h (Pb1.5c1.5) or 3 h (Pb3c3), 225 °C after preheating at 175°C for 1.5h (Pb1.5d1.5), or 3 h (Pb3d3)and at 225 °C after preheating at 200°C for 1.5h (Pc1.5d1.5), or 3 h (Pc3d3).

For all of the samples Pb1.5c1.5 and Pb3c3, cured at 200 °C after pre-heating at 175°C for 1.5 and 3 h at each step, the initial thermal degradation peak is maximized at around 280°C as in case of the sample Pb3 cured at 175 °C for 3h. This value is lower

than the corresponding values recorded during the pyrolysis of the samples cured at 200°C for 1.5 or 3 h. The overlapping high temperature peaks show maxima at around 432 and 505°C almost similar to the corresponding ones for Pb3, but lower than the corresponding values for Pc1.5 and Pc3. Contrary to what was observed for the samples cured in a single step either at 175 or 200 °C for 1.5 or 3h, the relative intensities of the three peaks present in the TIC curve are almost identical. Furthermore, unlike the general trends observed for the samples cured in a single step, the relative intensities of the high temperature peaks are decreased during the pyrolysis of the samples cured for longer period.

Curing the monomer at 225 °C, after pre-treatment at 175 or 200°C for 1.5 or 3h at each step, yielded polymers that decompose mainly at elevated temperatures. The relative intensity of the low temperature peaks present in the TIC curves is decreased noticeably, and shifted to high temperature regions during the pyrolysis of Pb1.5d1.5 and Pc1.5d1.5. It is totally disappeared for the samples cured for 3 h cured at 225°C after pre-heating at 175 or 200°C for 3h at each step. In addition, the partially separated overlapping high temperature peaks detected in the TIC curves of the polymers cured at 200°C, cannot be resolved anymore except for Pc1.5d1.5, and broad peaks with shoulders at low temperature side and maxima at 532, 505 and 539°C are recorded in the TIC curves of Pb1.5d1.5, Pb3d3 and Pc3d3 respectively.

The pyrolysis mass spectra of the samples prepared by two-step curing process, recorded at the maxima of the peaks present in the TIC curve show identical peaks with the corresponding ones cured at different temperatures for 1.5 or 3 h. Yet, significant changes in the relative intensities are noted indicating that structure and thermal stabilities of the chains depend on both curing temperature and period.

In Fig. 3.8., the TIC curves and the pyrolysis mass spectra recorded at the maximum of the peaks present recorded during the pyrolysis of the polymers cured stepwise at 175, 200 and 225 °C for 1.5 or 3 h at each step are given.

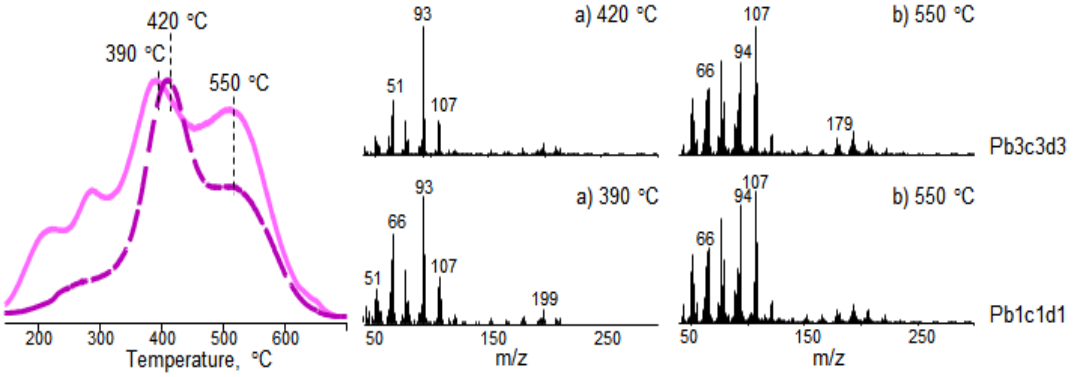

Figure 3.8 TIC curves and the mass spectra recorded at the maxima of the peaks present in the TIC curve recorded during the pyrolysis of PPh-a cured at 225 °C after preheating at 175 and 200 °C for 1 (Pb1c1d1) and 3 h (Pb3c3d3) (----)

Again four overlapping peaks with maxima at 250, 280, 390 and 550°C are present in the TIC curve recorded during the pyrolysis of the sample cured for 1.5 h as in case of the sample cured at 200 °C for 1.5 h. The polymer generated upon increasing the duration of curing decomposes mainly at around 420 C, the low and elevated temperature evolutions are diminished not noticeably. The mass spectra revealed that the evolution of high mass fragments at low temperature for Pb1c1d1 are diminished for Pb3c3d3.

The presence of more than one peak in the TGA and TIC curves may be due to a multi-step thermal degradation mechanism or presence of chains with different thermal stability and/or structure. Actually, polymerization of aniline based benzoxazine monomer may proceed through various reaction paths; the heterocyclic ring opening may be followed by attack of -NCH_2 groups to mainly para positions of phenol and pyridine rings as shown in Scheme 3.2, generating **P1** and **P2** respectively as with a bulky o, p- director and/or a bulky electrophile, para substitution predominates [24]. In addition, the dimer generated by the coupling of -NCH_2 groups may polymerize via attack of -NCH_2 groups to phenol and/or pyridine rings or through vinyl polymerization yielding **P31**, **P32** and **P4** as presented in Scheme 3.3.

Scheme 3.2 Ring-opening polymerizations of benzoxazines.

a) by attack to phenyl ring

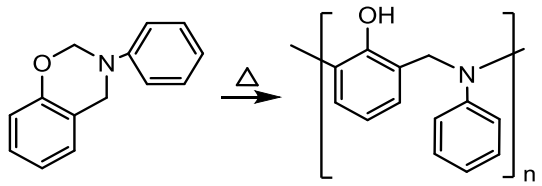

P1

b) by attack to aniline ring

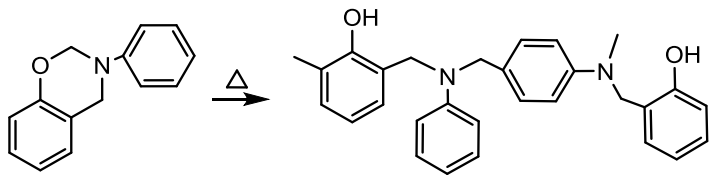

P2

Scheme 3.3

a) Generation of the dimer by coupling of $-NCH_2$ groups

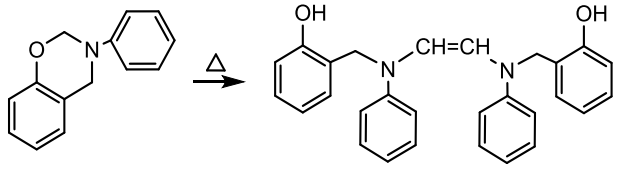

b) polymerization of the dimer

i) by attack of NCH_2 groups

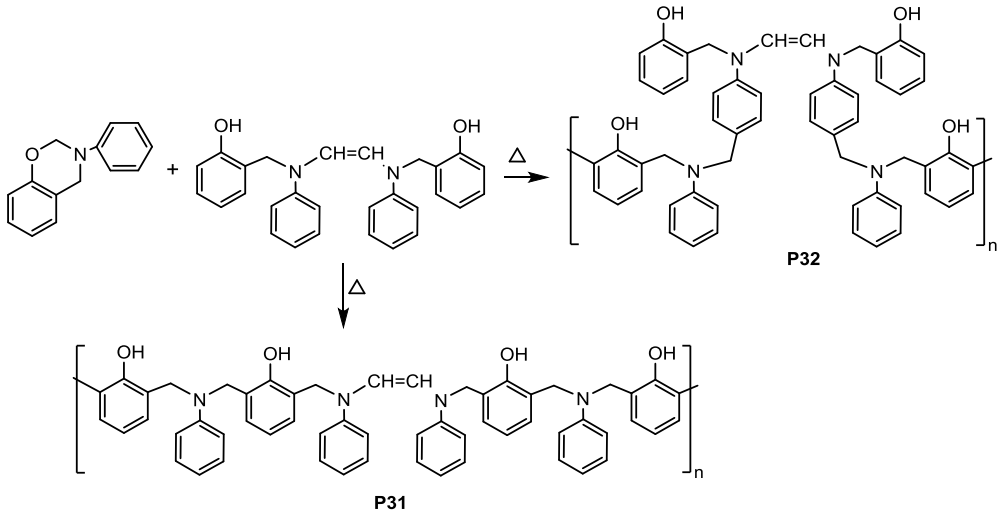

ii) by vinyl polymerization

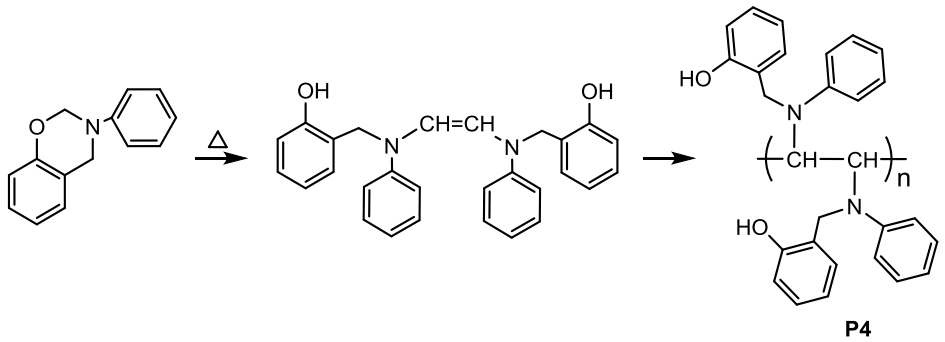

In order to get a better insight for the degradation processes of the polymers which will also supply valuable information for the polymerization routes during the curing process single ion evolution profiles of intense and/or characteristic products are analyzed. In Fig.3.9 single ion evolution profiles of some selected products recorded during the pyrolysis of Pb3c3 are given as representative examples. The single ion profiles are grouped considering the similarities in the trends observed.

Products $C_6H_5NHC_2H_2NHC_6H_5$ and/or $C_6H_4NHCH_2C_6H_4NHCH_2$ (210 Da), $HOC_6H_4CH_2NH(C_6H_5)CH_2$ (213 Da) and $HOC_6H_4CH_2NHC_6H_5$ (199 Da) are evolved at early stages of pyrolysis at around 260°C. Yet, different trends in their single ion pyrograms exit at moderate and elevated temperatures. The 210 Da fragment shows broad overlapping peaks at around 388 and 526°C, whereas, 199 and 213 Da fragments shows a relatively sharp peak at around 388°C. Although loss of 199 and 213 Da fragments occur in the same temperature regions, the relative yields observed at each region show opposite behaviors. Elimination of $HOC_6H_4CH_2NH(C_6H_5)CH_2$ is more extensive at initial stages of pyrolysis whereas, that of $HOC_6H_4CH_2NHC_6H_5$ is more pronounced at around 388°C.

The major thermal decomposition product aniline, $C_6H_5NH_2$ (93 Da) is detected at slightly higher temperatures at around 270°C. A weak peak at around 270°C is also present in the evolution profile of fragment with m/z value 91 Da that can be attributed to $C_6H_5CH_2$. The evolution of aniline is detected over a broad temperature range, reaching maximum yield at around 390 °C as do 213, 210 and 199 Da fragments and is completed just above 450°C. The loss of 91 Da fragment is also observed at elevated temperatures, two overlapping peaks with maxima at around 415 and 555°C are present in its pyrogram.

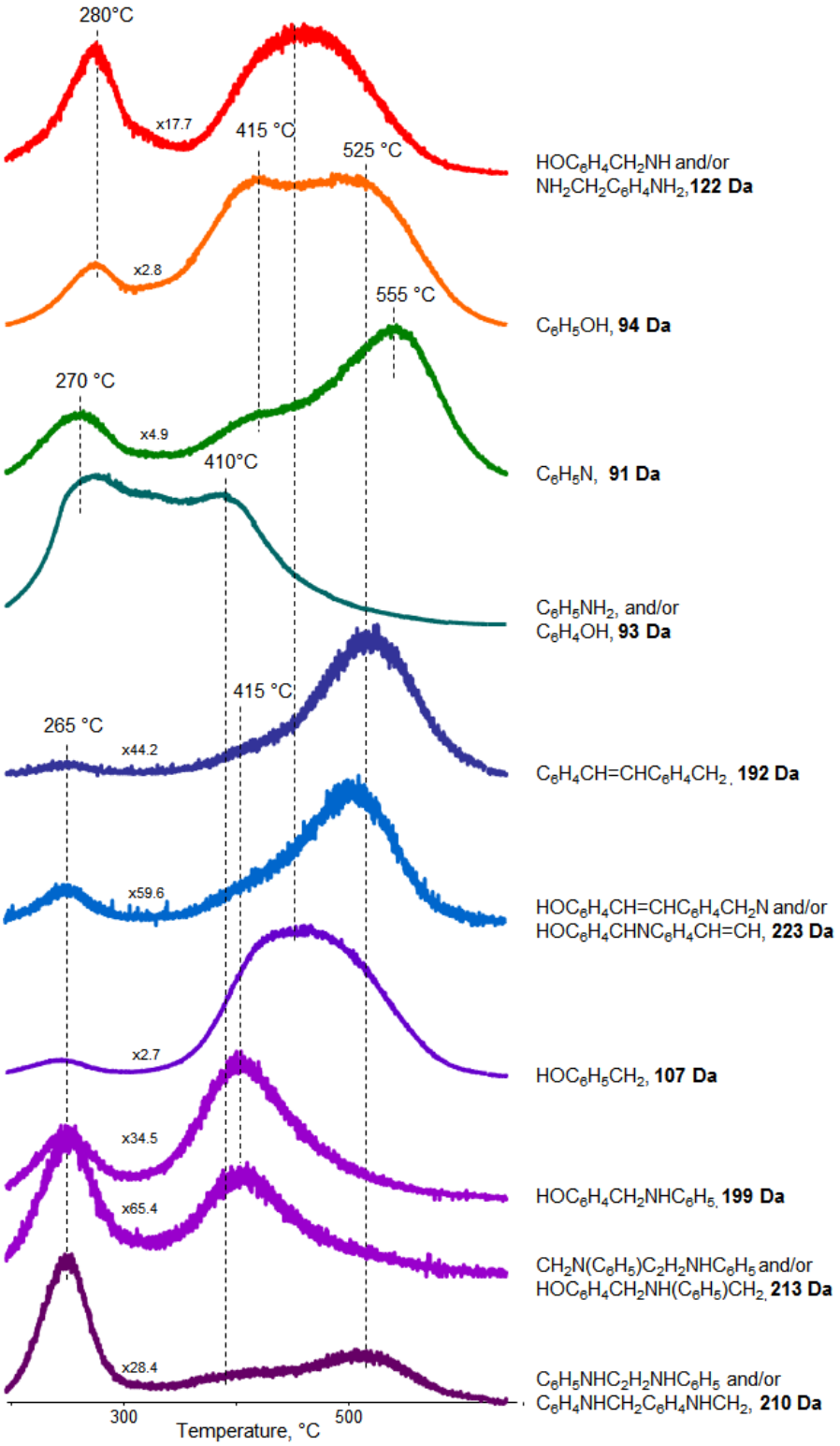

Figure 3.9 Single ion evolution profiles of selected products detected during the pyrolysis of Pb3c3.

The evolution profiles of phenol, C_6H_5OH (94 Da) and the 122 Da fragment assigned to $NH_2CH_2C_6H_4NH_2$ and/or $HOC_6H_4CH_2NH$ involve a low temperature peak maximizing at around 280°C. Among these, loss of phenol is also detected at elevated temperatures at around 415 and 525°C. On the other hand, extensive evolution of 122 Da fragment is observed over a broad temperature region at around 465°C as does $C_6H_5NH_2CH$.

Taking into consideration all the possible polymeric structures, the low-temperature evolutions at around 260, 270 and 280°C can be attributed decomposition of chains due to elimination of aniline units. It may be proposed that loss of $C_6H_5NHCH{=}CHNHC_6H_5$ (210 Da) occurs at around 260°C, due to the degradation of the chains generated by the coupling of $C_6H_5NCH_2$ groups, **P3** while that of aniline takes place at around 270°C as a consequence of decompositions of the chains generated by attack of $C_6H_5NCH_2$ groups to phenol and/or aniline rings, **P1** and **P2** respectively. On the other hand, The products C_6H_5OH (94 Da) and $NH_2CH_2C_6H_4NH_2$ and/or $HOC_6H_4CH_2NH$ (122 Da) evolving at around 280°C may be attributed to further cleavages of **P1** and **P2** chains after elimination of aniline.

The decomposition of P1 and P2 chains may also proceed via random cleavages at the β-carbon to phenol or nitrogen atom yielding fragments such as HOC_6H_4 (93 Da), HOC_6H_5 (94 Da), $HOC_6H_4CH_2NHC_6H_5$ (199 Da), $C_6H_5NHCH_2C_6H_4NHCH_2$ (210 Da) and $HOC_6H_4CH_2NH(C_6H_5)CH_2$ (213 Da) as in the case of the EI dissociation of the monomer and dimer. The peaks at around 390, 400 or 415 °C in their evolution profiles may be associated with random chain cleavages of **P1**, **P2**, **P31** and **P32**.

In addition, the low-mass products such as $HOC_6H_4CH_2$ (107 Da) and $HOC_6H_4CH_2NH$ (122 Da) evolved in a broad temperature region at around 465°C may also be related to the decomposition of these units. The broad peak in their evolution profiles may be associated with extensive loss of these fragments from chains involving some crosslinking.

It may be proposed that the radicals generated upon loss of aniline and substituted aniline dimers from **P1**, **P2, P31** and **P32** at initial stages of pyrolysis and/or during curing may couple to produce an unsaturated polymer backbone (Scheme 3.4). The detection of fragments presumably assigned to $HOC_6H_4CH{=}CHC_6H_4CHNH$ and/or $HOC_6H_4CHN(C_6H_4CH{=}N)$ (223 Da), $C_6H_4CH{=}CHC_6H_4CH_2$ (192 Da) and C_6H_5OH (94 Da) at around 525 °C supports this proposal.

Scheme 3.4 Elimination of aniline

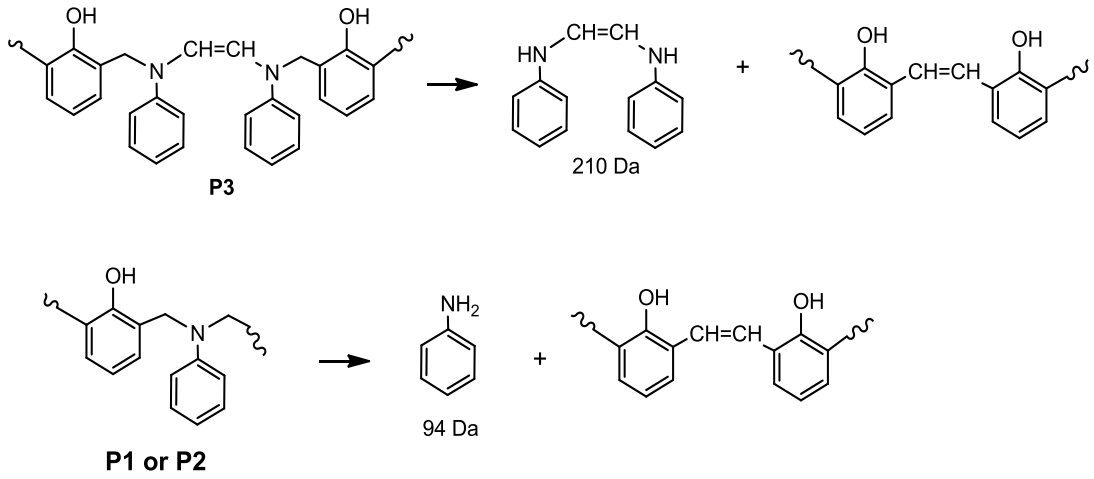

And finally, the evolution of $C_6H_5CH_2$ at slightly higher temperatures, at around 555 °C may be associated with chains with highly crosslinked structures that dissociate with loss of CO.

To investigate the effects of curing conditions on polymerization and/or thermal degradation characteristics of polybenzoxazines, single ion evolution pyrograms of characteristic thermal degradation products of each polymer synthesized by different curing programs are analyzed in detail. In Fig.3.10, single ion evolution of profiles of aniline (93 Da), $C_6H_5NHC_2H_2NHC_6H_5$ and/or $C_6H_4NHCH_2C_6H_4NHCH_2$ (210 Da) and $HOC_6H_4CH_2NHC_6H_5$ (199 Da) detected during the pyrolysis of the samples prepared by different curing programs are shown.

Evolution of the major decomposition product, aniline (93 Da) is detected in two distinct temperature regions, at around 300 and 400 °C. Detection of aniline below 250 °C may be regarded as an evidence for the presence of unreacted monomer and/or low molecular weight oligomers as polymerization was not completed due to the inefficient curing process. In general, the loss of aniline shifts to high temperature regions during the pyrolysis of the polymers cured at higher temperatures or for longer periods at a given temperature. Two overlapping peaks are detected in the evolution profile of aniline evolved during the pyrolysis of Pb1.5 and Pc1.5 at around 240 and 255 °C, for Pb1.5 and 290 and 310°C for Pc1.5. Whereas, a single peak at around 340°C is present in its single ion pyrogram when generated during the pyrolysis of Pd1.5. Low temperature loss of aniline is detected at around 240 and 295, and 340 °C for Pb3, Pc3 and Pd3 respectively. In addition, the relative yield of aniline evolved at initial stages of pyrolysis is decreased for the samples cured for longer periods. The decrease is more pronounced for the samples cured at higher temperatures. For Pd3, low temperature evolution of aniline is almost totally disappeared. On the other hand, during the pyrolysis of all the samples cured in one step, the evolution aniline is also detected at around 415°C, independent of the duration and temperature of the curing process used for polymerization.

Evolution of $C_6H_5NHC_2H_2NHC_6H_5$ and/or $C_6H_4NHCH_2C_6H_4NHCH_2$ (210 Da) is detected in three temperature regions, at around 270, 400 and above 500°C. The evolutions at low and moderate temperatures are almost independent of the temperature and the duration of curing used for polymerization, whereas, the high temperature evolutions shift to high temperature regions as the curing temperature was increased. On the other hand, the relative yields are affected by both the temperature and duration of curing; the low temperature evolutions are diminished, whereas the evolutions at around 400°C are enhanced during the pyrolysis of the samples cured at higher temperatures and for longer periods at a given temperature.
The loss of $HOC_6H_4CH_2NHC_6H_5$ (199 Da) is detected in two regions at around 270 and 415°C almost independent of the temperature and duration of curing used for

polymerization. Yet, the amount lost at initial stages of pyrolysis diminishes significantly during the pyrolysis of the polymers cured at higher temperatures.

Single ion evolution profiles of some representative pyrolysis products evolved mainly at moderate and/or elevated temperature, such as phenol (94 Da), $CH_2C_6H_5$ and/or C_6H_4N (91 Da) and $C_6H_4CH{=}CHC_6H_4CH_2$ (192 Da) are depicted in Fig.3.11.

Phenol is one of the common thermal degradation products of all the chains with different structures. Thus, overlapping peaks that can be used to determine the thermal behavior of these chains are present in its evolution profiles. As the curing was performed at higher temperature or for prolonged periods, the evolution of phenol is reduced noticeably below 300 °C. On the other hand, the extensive loss of phenol at around 425°C is independent of the curing conditions of the polymer pyrolyzed. The evolution of phenol at elevated temperatures at around 520°C is also independent of temperature of curing. However, when the curing was performed for short periods at 200 and 225°C, the loss of phenol is shifted to high temperature regions.

The evolution of $CH_2C_6H_3CHNC_6H_5$ and/or $C_6H_4CH{=}CHC_6H_4CH_2$ (192 Da) is predominantly detected at elevated temperatures above 500°C during the pyrolysis of all the polymers cured in single step and is independent of the temperature of curing. However, as the duration of curing was increased, its single ion pyrogram shifts to lower temperature regions. The weak shoulders in its evolution profiles at around 400°C are attributed to $CH_2C_6H_3CHNC_6H_4$ that may be generated by degradation of **P1**, **P31** and **P32**.

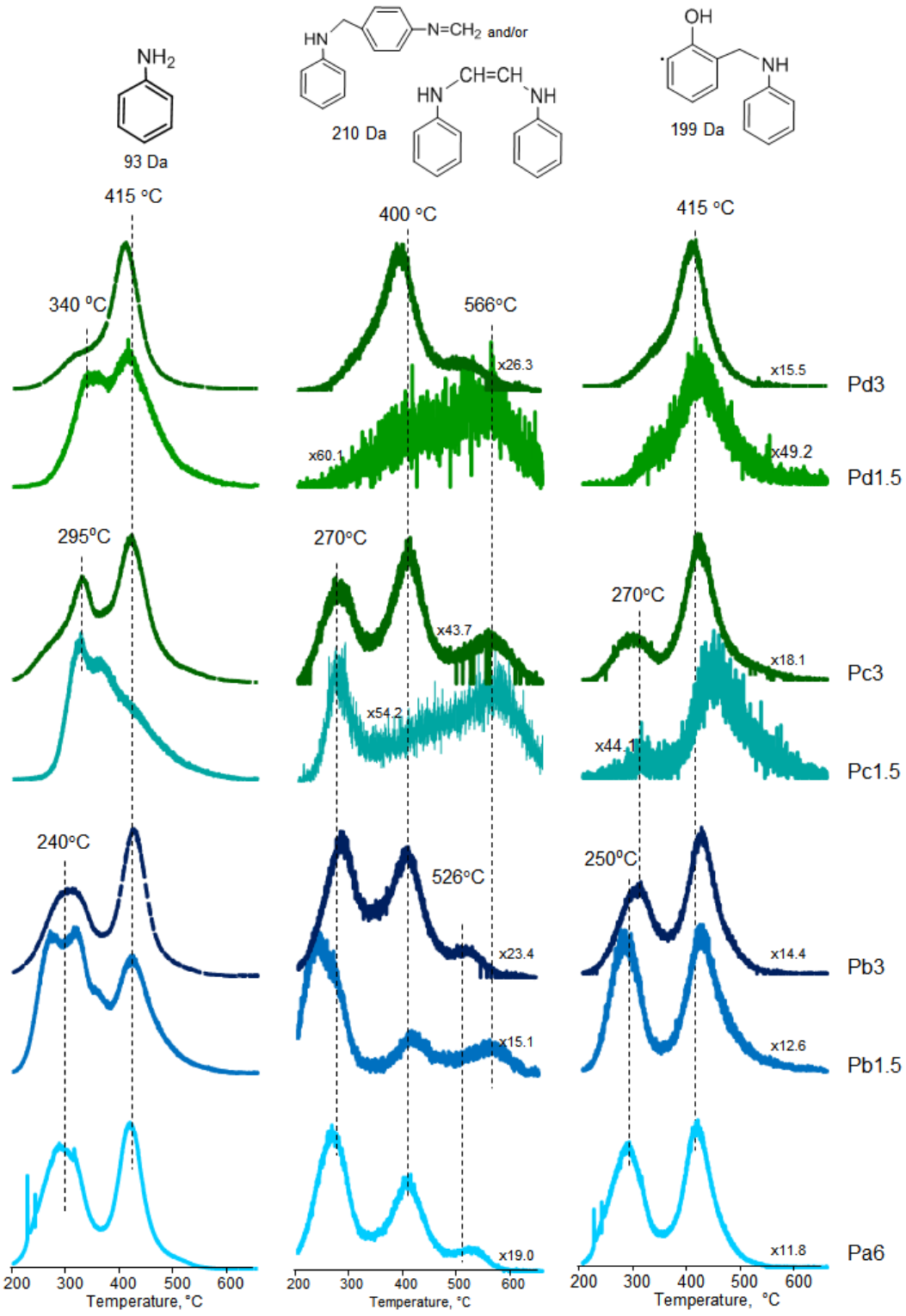

Figure 3.10 Single ion evolution profiles of aniline (93 Da), $C_6H_5NHC_2H_2NHC_6H_5$ and/or $C_6H_4NHCH_2C_6H_4NHCH_2$ (210 Da) and $HOC_6H_4CH_2NHC_6H_5$ (199 Da) detected during the pyrolysis of PPh-a prepared by applying one-step curing programs.

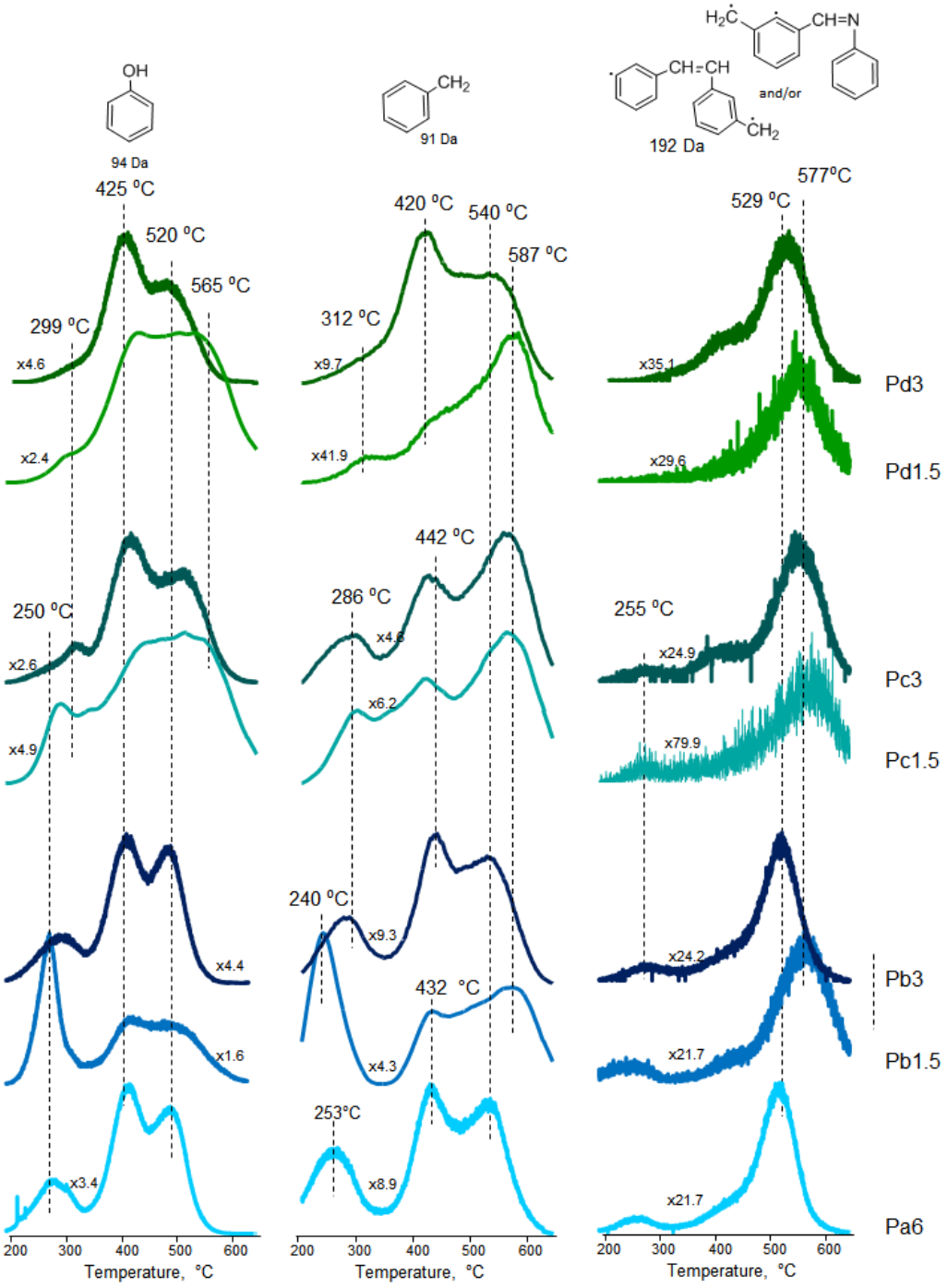

Figure 3.11 Single ion evolution profiles of phenol (94 Da), $C_6H_5CH_2$ (91 Da) and $C_6H_5C_2H_2C_6H_5$ (192 Da) detected during the pyrolysis of PPh-a prepared by applying one-step curing programs

The fragment with m/z value 91 Da is directly associated with $C_6H_5CH_2$, a common ion detected in the mass spectra of molecules involving alkyl substituted benzene rings and may be generated during the ionization and/or decomposition of segments with different structures. Again, three broad overlapping peaks maximizing at distinct temperature regions are present in its evolution profile. The low temperature evolutions shifting slightly to higher temperature region as the duration of curing increased, are maximized in the temperature region 240-312°C. Loss of $C_6H_5CH_2$ is diminished significantly at low temperatures as the polymer pyrolyzed was cured at higher temperatures. The evolutions at around 440 and 565 °C are increased as the temperature and duration of curing were increased. However, its evolution is shifted to low temperatures slightly when the duration of curing was increased.

The normalized ion yields at the maxima of the peaks present in the single ion evolution profiles of aniline (93 Da), $C_6H_5NHC_2H_2NHC_6H_5$ and/or $C_6H_4NHCH_2C_6H_4NHCH_2$ (210 Da), phenol (94 Da), $CH_2C_6H_5$ and/or C_6H_4N (91 Da) and $C_6H_4CH{=}CHC_6H_4CH_2$ (192 Da) detected during the pyrolysis of the polybenzoxazines based on aniline prepared by curing in one step are collected in Table 3.3 for a better comparison.

Table 3.3 Normalized ion yields of aniline (93 Da), $C_6H_5NHC_2H_2NHC_6H_5$ and/or $C_6H_4NHCH_2C_6H_4NHCH_2$ (210 Da), phenol (94 Da), $CH_2C_6H_5$ and/or C_6H_4N (91 Da) and $C_6H_4CH{=}CHC_6H_4CH_2$ (192 Da) detected during the pyrolysis of the PPha prepared by curing in one step.

	93 Da		210 Da			199 Da		94 Da			91 Da			192 Da
	T1	T2	T1	T2	T3	T1	T2	T1	T2	T3	T1	T2	T3	T1
a6	844	1000	52	32	7	74	83	103	277	234	65	111	95	43
b1	1000	784	60	21	15	72	78	601	275	206	226	125	151	44
b3	595	1000	408	367	8	392	65	68	216	217	47	103	79	39
c1	1000	828	12	7	10	2	14	119	183	177	85	108	130	8
c3	722	1000	278	428	131	23	77	80	325	211	48		133	33
d1	857	1000	2	9	13	10	30	87	450	415	50	98	243	29
d3	253	1000	7	36	6	1	64	29	210	139	17	99	64	2

The trends in the single ion pyrograms of diagnostic products reveal that thermal degradation of polybenzoxazines cured in a single step based on aniline starts by elimination of $C_6H_5NHC_2H_2NHC_6H_5$ (210 Da) and aniline (93 Da). This step of decomposition highly depends on the temperature and duration of the curing process used for the polymerization of the benzoxazine monomer. For the samples cured at higher temperatures and/or for longer periods, loss of aniline and substituted aniline dimer does not observed at initial stages of pyrolysis.

The products reaching maximum yield in the temperature region 400- 425°C are related to degradation via random cleavages. Considering the bond energies, it may be thought that the polymer chains generated by attack of $C_6H_5NCH_2$ to *ortho* or *para* positions of aniline rings, **P2** and **P32** degrade mainly at around 400 °C, whereas the chains produced by attack of $C_6H_5NCH_2$ to *ortho* or *para* positions of phenol rings, **P1** and **P31** degrade mainly at around 415°C. The 210 Da fragment that can also be associated with $C_6H_5NHCH_2C_6H_4NCH_2$ evolves at around 400 °C due the degradation of chains generated by attack of $C_6H_5NCH_2$ to *ortho* or *para* positions of aniline rings **P2** and **P32.** Whereas, evolutions of $HOC_6H_4CH_2NHC_6H_5$ (199 Da) and aniline (93 Da) at around 415 °C, are attributed to decomposition of chains generated by attack of $C_6H_5NCH_2$ to *ortho* or *para* positions of phenol rings, **P1** and **P31**. Losses of $C_6H_5CH_2$ (91) and phenol (94 Da) at around 420 and 425 °C respectively, seem to be maximizing at slightly higher temperatures most probably due to the overlap of high temperature evolutions, are also associated with degradation of polymer chains **P1**, **P2**, **P31** and **P32**. The trends in the single ion pyrograms reveal that the thermal degradations of the chains **P1** and **P2** are not affected by the temperature and duration of the curing process used for polymerization, are detected in the same temperature region.

Evolutions of phenol (94 Da) and $C_6H_5CH_2$ (91 Da) at elevated temperatures are associated with degradation of crosslinked units or segments involving unsaturation. As the extent of crosslinking increases, the char yield is increased. It may be thought that elimination of CO takes place yielding only unsaturated carbon residue, the

limited amount of 192 Da fragment, $C_6H_4C_2H_2C_6H_4CH_2$ may be correlated with this possible process.

On the other hand, elimination of the products at elevated temperatures associated with chains involving unsaturated segments and/or crosslinking is affected mainly by the duration of curing process performed. As the duration of curing at a given temperature was increased, the evolution of these products during the pyrolysis of the polymer generated is shifted to lower temperatures.

Thus, it can be concluded that elimination of aniline and substituted dimer during the curing process most probably, mainly due to the decomposition of low mass oligomers generated, yields chains involving unsaturation and thus, having higher thermal stabilities, As a consequence of the coupling of the chains generated, polymer segments involving unsaturation are formed (Scheme 3.3). As the curing process was performed for longer periods, mainly high molar mass products with higher thermal stabilities were produced. However, as unsaturated segments cannot be produced during the curing process, a thermally more homogenous polymer that decomposes in a narrower temperature region is generated.

In Fig.3.12, single ion evolution of profiles of aniline (93 Da), $C_6H_5NHC_2H_2NHC_6H_5$ and/or $C_6H_4NHCH_2C_6H_4NHCH_2$ (210 Da) and $HOC_6H_4CH_2NHC_6H_5$ (199 Da) detected during the pyrolysis of the samples prepared by two or three step curing programs are shown.

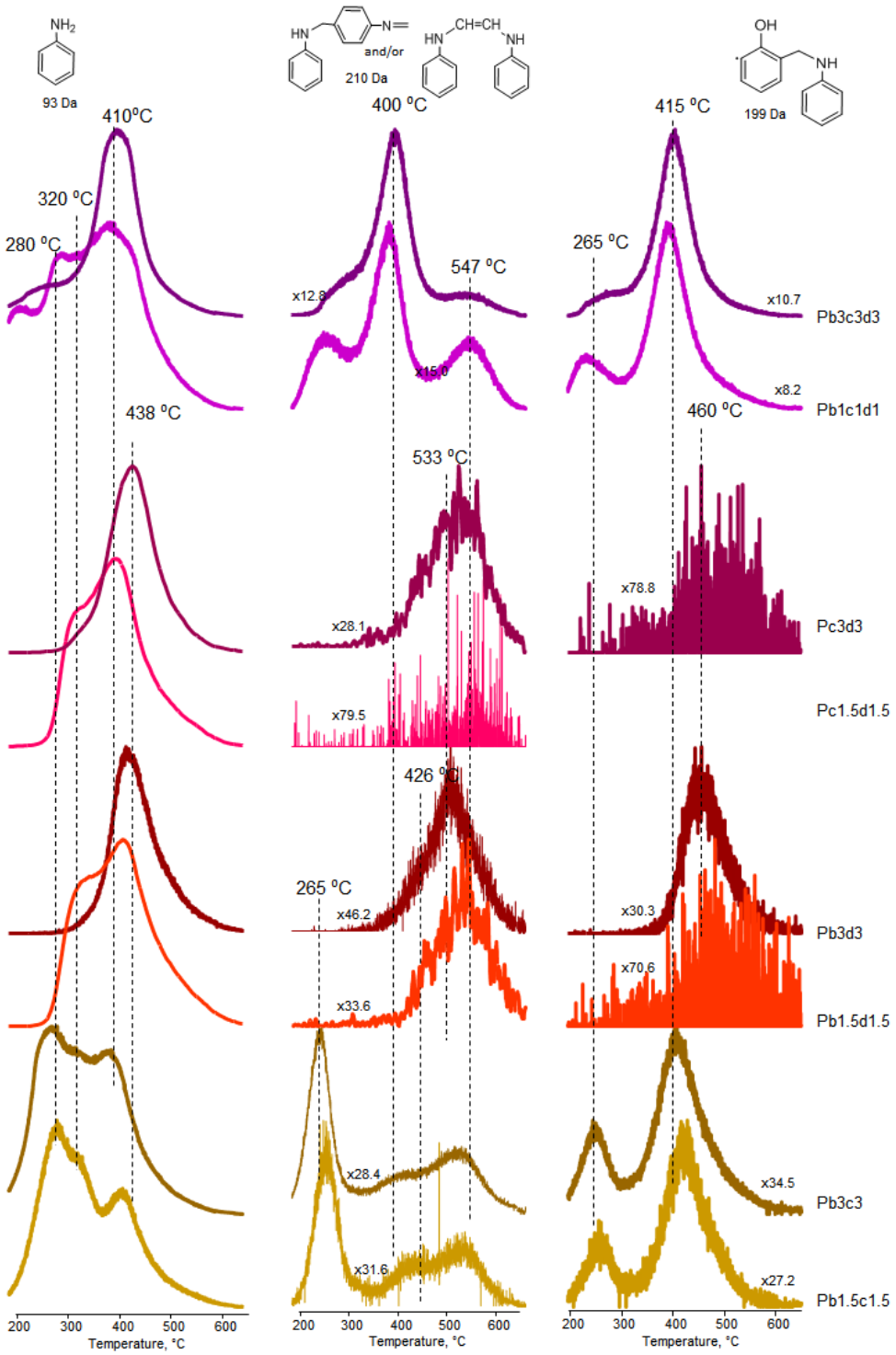

Figure 3.12 Single ion evolution profiles aniline (93 Da) $C_6H_5NHC_2H_2NHC_6H_5$ and/or $C_6H_4NHCH_2C_6H_4NHCH_2$ (210 Da) and $HOC_6H_4CH_2NHC_6H_5$ (199 Da) detected during the pyrolysis of PPh-a prepared by applying two or three-step curing programs

Extensive evolutions of aniline (94 Da) and $C_6H_5NHC_2H_2NHC_6H_5$ (210 Da) below 300°C are only detected during the pyrolysis of the samples cured at 200 °C after pre-heating at 175 °C for 1.5 and 3 h. A shoulder at around 320°C is present in the evolution profile of aniline during the pyrolysis of all the samples cured for 1.5 h at each step independent of the temperature and the steps of curing. However, its relative yield is decreased as the polymer pyrolyzed was prepared at high curing temperatures. The evolution of aniline is again observed at around 410°C during the pyrolysis of the samples cured for 1.5 h at each step independent of the temperature and the steps of curing, as in case of the samples cured in a single step. However, during the pyrolysis of the samples cured at 225°C after preheating at 175 or 200°C for 3h at each step, the high temperature loss of aniline shifts to high temperature regions. On the other hand, the elimination of 210 Da fragment is not observed at low and moderate temperature regions and diminishes drastically at elevated temperature regions, during the pyrolysis of the polymers cured at 225°C, without preheating at least for 3 h at lower temperatures,

Almost a similar behavior is observed for the evolution of $HOC_6H_4CH_2NHC_6H_5$ (199 Da). During the pyrolysis of the samples cured at 225°C, without preheating at least for 3 h at lower temperatures, the evolution of 199 Da fragment totally disappears at low temperature regions and diminishes drastically at high temperatures. On the other, the pyrolysis of the samples cured at 200°C after preheating at 175°C and those cured at 225°C after preheating at both 175 and 200 °C, yields 199 Da fragment in two distinct regions at around 265 and 415°C. In general its relative yield is higher at around 415 °C and its low temperature evolutions during the pyrolysis of the samples cured in three steps diminishes noticeably, being more pronounced when the duration of curing was increased.

Single ion evolution profiles of phenol (94 Da), $CH_2C_6H_5$ and/or C_6H_4N (91 Da) and $C_6H_4CH{=}CHC_6H_4CH_2$ (192 Da) detected during the pyrolysis of the polymers cured stepwise in two or three steps are depicted in Fig.3.13.

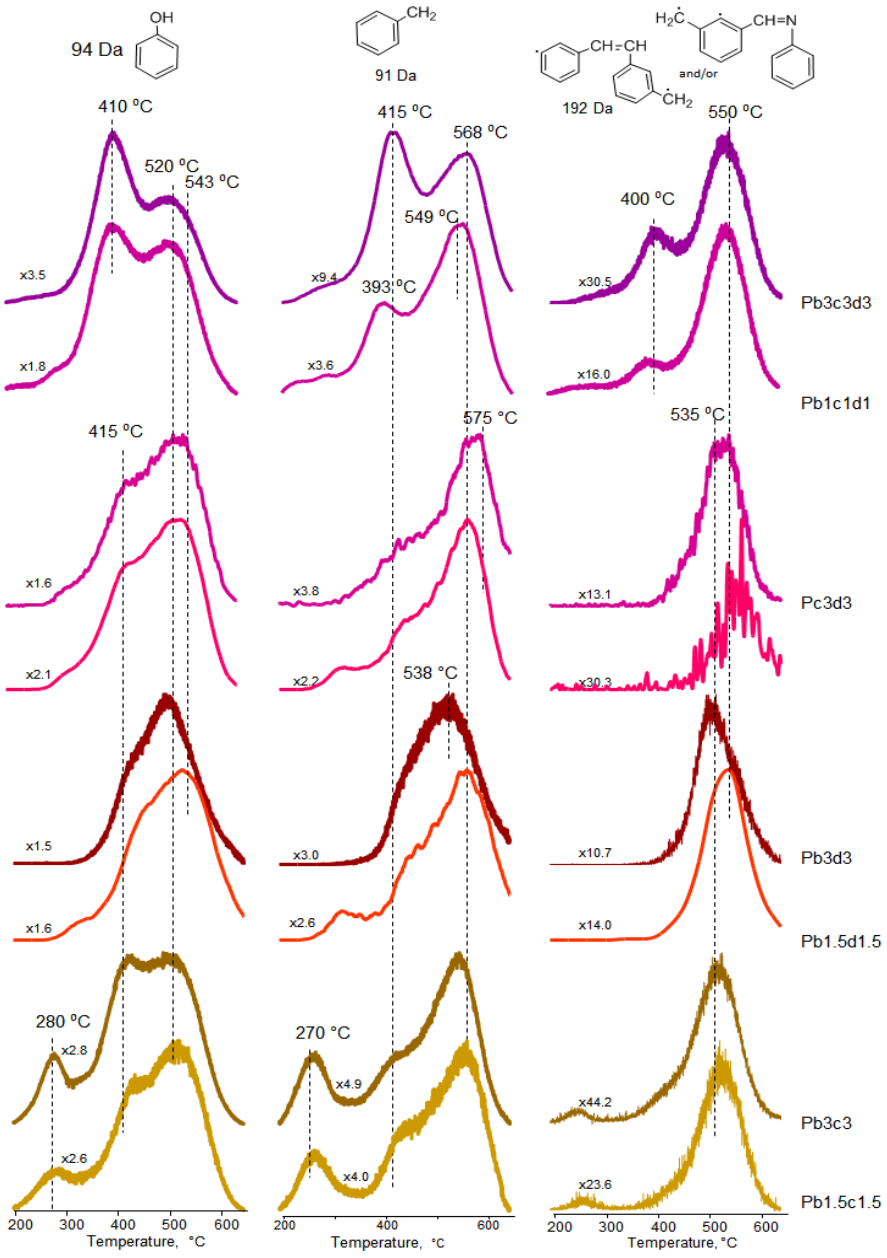

Figure 3.13 Single ion evolution profiles of phenol (94 Da), $C_6H_5CH_2$ (91 Da) and $C_6H_5C_2H_2C_6H_5$ (192 Da) detected during the pyrolysis of PPh-a prepared by applying two or three-step curing programs.

Evolution of phenol at initial stages of pyrolysis is only detected for the samples cured at 200°C after preheating at 175 °C. For the samples preheated at 175 °C loss of phenol is detected at around 410 and 520 °C. Its evolution is slightly shifted to high

temperatures during the pyrolysis of the sample cured at 225°C after preheating at 200°C. However a low temperature shift is detected during the pyrolysis of the samples cured in three steps. Furthermore, contrary to what was observed for the polymers cured in two-steps the relative yield of phenol lost at around 410°C is more pronounced during the pyrolysis of the samples cured in three steps.

Almost exactly the same behavior is observed for evolution of $C_6H_5CH_2$ (91 Da) fragment. Low temperature evolutions are only detected during the pyrolysis of the samples cured at 200°C after preheating at 175 °C. Its evolution is slightly shifted to high temperatures during the pyrolysis of the samples cured at 225°C after preheating at 200°C, reaching maximum yield at around 575°C. However a low temperature shift is detected during the pyrolysis of the samples cured in three steps. In addition, the evolutions at around 415 °C are significantly decreased for the samples cured at 225°C after preheating at 175 or 200°C. Evolutions at around 415°C are enhanced during the pyrolysis of the samples cured at 175 and 200°C in two steps or cured at 225°C after preheating at both 175 and 200°C.

The 192 Da fragment associated with $C_6H_5C_2H_2C_6H_5$ mainly eliminated at around 535 and 550 °C. Again its evolution shifts slightly to high temperature regions during the pyrolysis of the sample cured at 225 °C after pre-heating at 200 °C and shifts to lower temperatures during the pyrolysis of the sample cured in three steps. For these samples evolutions at around 400°C are also noted and associated with loss of $CH_2C_6H_3CHNC_6H_4$ (192 Da) that may be generated by degradation of **P1**, **P31** and **P32**.

The normalized ion yields at the maxima of the peaks present in the single ion evolution profiles of aniline (93 Da), $C_6H_5NHC_2H_2NHC_6H_5$ and/or $C_6H_4NHCH_2C_6H_4NHCH_2$ (210 Da), phenol (94 Da), $CH_2C_6H_5$ and/or C_6H_4N (91 Da) and $C_6H_4CH{=}CHC_6H_4CH_2$ (192 Da) detected during the pyrolysis of the polybenzoxazines based on aniline prepared by curing in two or three steps are collected in Table 3.4 for comparison.

Table 0.4 Normalized ion yields at the maxima of the peaks present in the single ion evolution profiles of aniline (93 Da), $C_6H_5NHC_2H_2NHC_6H_5$ and/or $C_6H_4NHCH_2C_6H_4NHCH_2$ (210 Da), phenol (94 Da), $CH_2C_6H_5$ and/or C_6H_4N (91 Da) and $C_6H_4CH{=}CHC_6H_4CH_2$ (192 Da) detected during the pyrolysis of the polybenzoxazines based on aniline prepared by curing in two or three steps.

	93 Da		**210 Da**			**199 Da**		**94 Da**			**91 Da**			**192 Da**
	T1	**T2**	**T1**	**T2**	**T3**	**T1**	**T2**	**T1**	**T2**	**T3**	**T1**	**T2**	**T3**	**T1**
b1c1	157	1000	39	11	15	2	48	16	456	606	154	176	367	53
b3c3	1000	859	366	71	119	144	286	157	358	351	92	91	205	57
b1d1	866	1000	3	3	14		5	81	463	554	56	179	365	37
b3d3		1000		6	19		28		380	639		219	319	82
c1d1	690	1000		2	9		1	62	416	671	50	131	388	42
c3d3		1000			0	3			303	420		66	163	16
b1c1d1	808	1000	25	67	25	37	120	87	551	474	5	162	277	62
b3c3d3	177	1000	15	76	8	12	87	23	282	160	14	108	91	32

The trends in the single ion pyrograms of these diagnostic products indicate that thermal degradation of polybenzoxazines based on aniline cured in two or three single step again starts by elimination of $C_6H_5NHC_2H_2NHC_6H_5$ (210 Da) and aniline (93 Da). The early stage evolutions highly depends on the temperature and duration of the curing process used for the polymerization of the benzoxazine monomer. For the samples cured at 225 °C after pre-heating at 175 or 200°C, especially for the samples cured for longer periods, loss of aniline and substituted aniline dimer are either diminished or totally disappeared at initial stages of pyrolysis.

In general, the evolution of diagnostic products at moderate temperatures occurs almost in the same temperature range, almost in dependent of the curing program applied. Loss of $C_6H_5NHC_2H_2NHC_6H_5$ (210 Da) occurs at around 400°C, those of aniline (93 Da) and $HOC_6H_4CH_2NHC_6H_5$ (199 Da) are observed at around 410°C and

those of phenol (94 Da) and $C_6H_5CH_2$ (91 Da) are eliminated at around 415 °C. However, for the samples cured at 225°C after pre-heating at 175 or 200°C, the relative yields of $C_6H_5NHC_2H_2NHC_6H_5$ and/or $C_6H_4NHCH_2C_6H_4NHCH_2$ (210 Da) and $HOC_6H_4CH_2NHC_6H_5$ (199 Da) evolved at around 400 °C diminished drastically. Thus, the proposed process for the loss of 199 Da fragment, degradation of chains with **P31** and **P32** structures is supported. On the other hand for these samples, the relative yields of $C_6H_5CH_2$ (91 Da), phenol (94 Da) and $C_6H_4CH{=}CHC_6H_4CH_2$ (192 Da) are increased significantly. It can further be suggested that upon curing at 225°C, without pre-heating for sufficiently long periods, vinyl polymerization takes place yielding **P4** that can eliminate mainly phenol and aniline readily at elevated temperatures, leaving an unsaturated polymer backbone that decomposes at higher temperatures.

It may be thought that the pre-heating process at low temperatures allows polymerization of the dimers generated by coupling of $C_6H_5NCH_2$ groups via attack of $C_6H_5NCH_2$ groups to ortho and para positions of phenol and/or aniline rings, generating **P31** and **P32** segments. Furthermore, the polymers produced involves un-crosslinked segments that can eliminate aniline and $C_6H_5NHC_2H_2NHC_6H_5$ during the pyrolysis process. The increase in the temperature and/or duration of curing at low temperatures yielded highly crosslinked structures. Under this condition vinyl polymerization was inhibited.

3.1.2. Benzoxazine monomer based on 4-nitroaniline, Ph-na

Benzoxazine monomer was synthesized from phenol, 4-nitroaniline and paraformaldehyde via solventless method (Scheme 3.5).

Scheme 3.5 Synthesis of benzoxazine monomer based on 4-nitroaniline and phenol

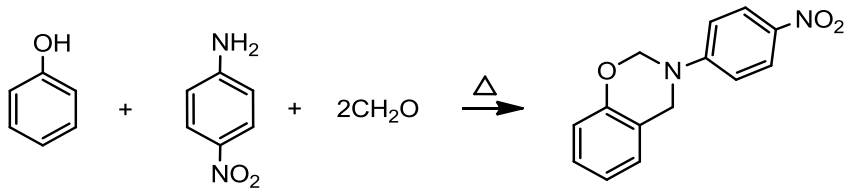

The proton NMR spectrum of the monomer shows strong resonances at 4.75 and 5.42 ppm corresponding to the methylene protons (C1 and C2) of Ar-CH_2-N and O-CH_2-N of the oxazine ring, respectively (Fig.3.5). The strong resonances at 4.88 and 5.61 ppm correspond to the methylene protons (H1 and H2) of Ar-CH_2-N and O-CH_2-N of the oxazine ring, respectively. The resonance signals in the range of 6.88–7.08 ppm are typical region for the phenyl ring; the chemical shifts (ppm) at 6.88 ppm (2H, H5 and H6), 6.96 ppm (1H, H7), 7.06 ppm (2H, H10 and H14), 7.08 ppm (1H, H4) are assigned to the aromatic protons. The signals at 8.15 ppm (2H, H11 and H13) are assigned to the aromatic protons next to nitro group. The resonances at 49.49 and 77.02 ppm correspond to the methylene carbons (C1 and C2) of Ar-CH_2-N and O-CH_2-N of the oxazine ring, respectively. Other chemical shifts (ppm) are assigned to the resonances of the carbons: 115.08 (C7), 117.31 (C10, C14), 120.07 (C5), 121.62 (C3), 125.84 (C11, C13), 126.76 (C4), 128.36 (C6), 140.48 (C12), 152.94 (C9), 154.05 (C8). Anal. calcd. for C14H12N2O3: C, 65.62; H, 4.72; N, 10.93; O,18.73%. Found: C, 65.43; H, 4.60; N, 10.99; O,18.98%.

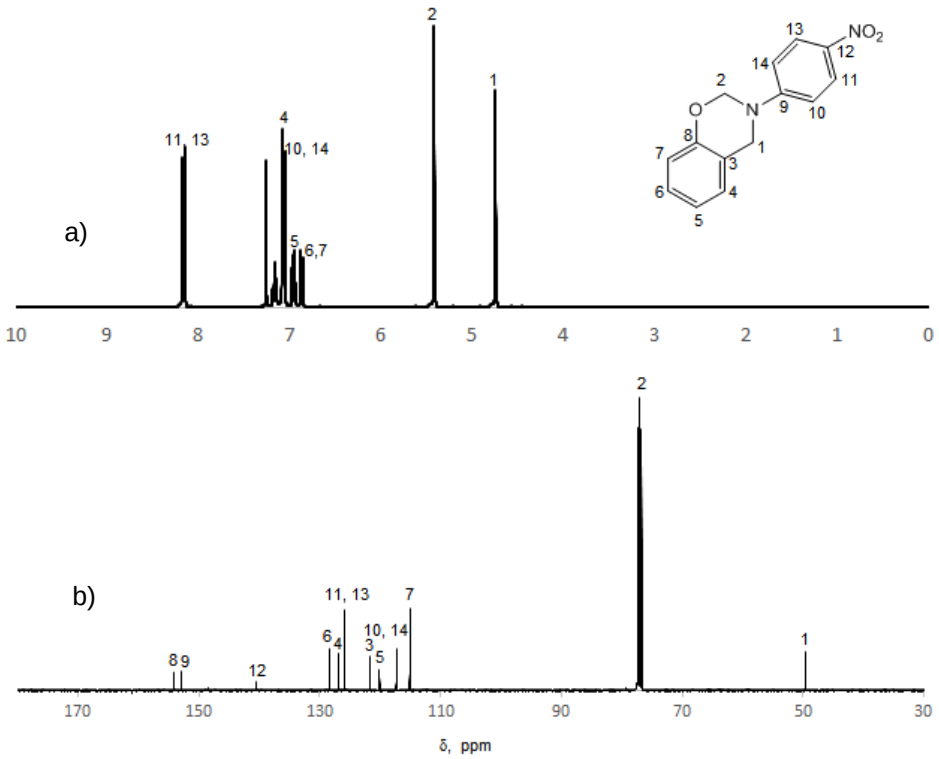

Figure 3.14 a) Proton-NMR and b)13C-NMR spectra of benzoxazine monomer.

The FTIR spectrum of the benzoxazine monomer is shown in Fig. 3.15a. The typical absorption bands for the benzoxazine are observed at 1487, 1366, 1227, 1039 and 959 cm^{-1}, corresponding to the di-substituted benzene rings, CH_2 wagging, Ar-O-C anti-symmetric stretching, C-O-C symmetric stretching and vibration modes of cyclic substituted benzene rings, respectively. The peak at 1447 cm^{-1} is associated with di-substituted benzene of 4-nitroaniline.

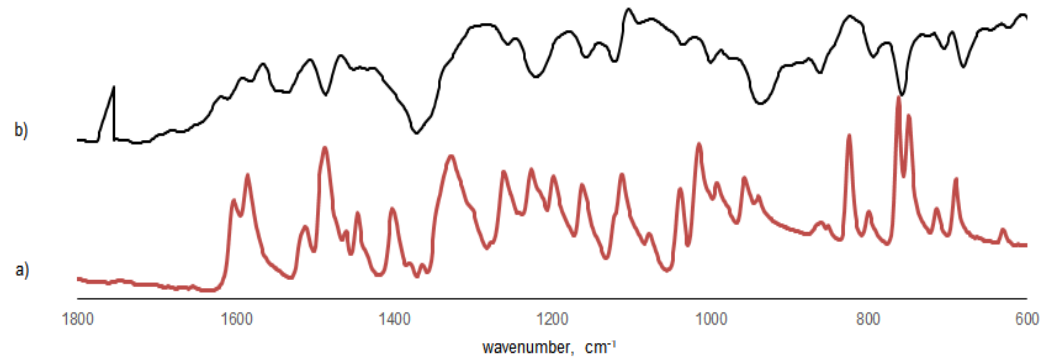

Figure 3.15 FTIR spectra of a) benzoxazine monomer and b) polybenzoxazine

In general, the peaks in the region 1600-1585 and 1500-1400 cm^{-1} are assigned to C-C stretching vibrations in aromatic compounds. The ring C-C stretching vibrations occur in the region 1600-1350. The peaks at 1603, 1584 and 1402 cm^{-1} are related to C-C stretching vibrations. The aromatic C-H in plane bending and out-of-plane deformation modes of benzene and its derivatives are observed in the region 1300-1000 cm^{-1}, and 1000-600 cm^{-1} regions respectively. Thus, several peaks present in these regions are associated with both of the di-substituted benzene rings present in the structure.

Aromatic nitro compounds show peaks in the region 1550-1500 and 1360-1290 cm^{-1} due to symmetric and symmetric stretching vibrations. Thus, the absorption at 1510 cm^{-1} is assigned to the asymmetric vibration of NO_2. But the peak due to symmetric stretching vibration of NO_2 cannot be differentiated because of the overlaps of absorptions of C-H in plane bending mode of aromatic ring, yielding a broad peak at around 1329 cm^{-1}.

In Fig. 3.16 the mass spectrum of the benzoxazine monomer, Ph-na, is depicted. For comparison those of the reactants p-nitroaniline and phenol are also included. The mass spectrum of Ph-na shows the base peak at 78 Da due to C_6H_6, the molecular ion peak at 256 Da, and moderate peaks at 150, 120 and 52 that can be associated with $O_2NC_6H_4NCH_2$, $OC_6H_4NCH_2$ and C_4H_4 respectively. The weak peaks at 106, 104,

92, 66 and 65 Da can be attributed to $OC_6H_4CH_2$ and/or OC_6H_4N, $C_6H_4NCH_2$, $C_5H_4NCH_2$ and/or OC_6H_4, C_3HNCH_2, C_5H_6, C_5H_5 fragment ions respectively. Hence, the fragmentation pattern observed is in accordance with the general expected fragmentation pattern for a molecule involving aromatic nitro group.

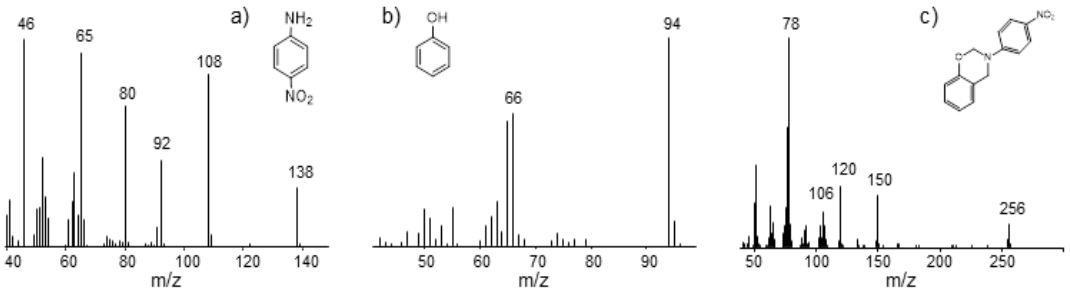

Figure 3.16 Mass spectra of a) p-nitroaniline, b)phenol and c) benzoxazine based on p-nitroaniline and phenol, Ph-na

Thus, the NMR, FTIR and MS spectra for the monomer are in good agreement with the expected chemical structure.

Polymerization of p-nitroaniline based benzoxazine monomer may be expected to proceed through various reaction paths. It is known that with a bulky *ortho – para* director, para substitution predominates. Thus, the heterocyclic ring opening is followed by the attack of $NO_2C_6H_4NCH_2$ groups to mainly *para* positions of phenol ring as shown in Scheme 3.6, generating **P1** [25, 26]. On the other hand, the attack of $NO_2C_6H_4NCH_2$ groups to aniline rings is almost impossible contrary to aniline based benzoxazine. It is expected that being also a bulky directing group, substitution to *para* positions should almost exclusively predominate. However, as *para* position of aniline ring is already occupied by the NO_2 group, polymerization via attack of NCH_2 groups to aniline ring should be negligible.

On the other hand, the dimer generated by the coupling of -NCH_2 groups may polymerize via attack of -NCH_2 groups to phenol rings (**P31**) or through vinyl polymerization (**P4**) (Scheme 3.7). As a consequence of these competing reaction pathways, generation of chains with various structures involving also cross-linking is also expected.

Scheme 3.6 Ring-opening polymerizations of benzoxazines by attack to phenyl ring

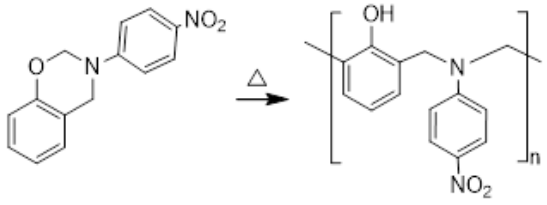

P1

Scheme 3.7

a) Generation of the dimer by coupling of –NCH_2 groups

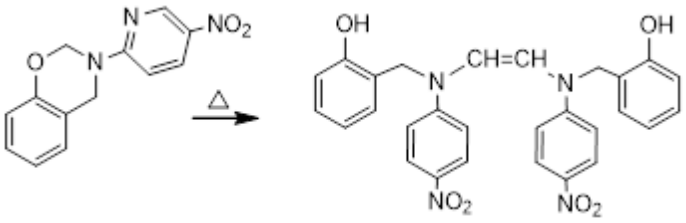

b) polymerization of the dimer

i) by attack of NCH_2 groups to phenol ring

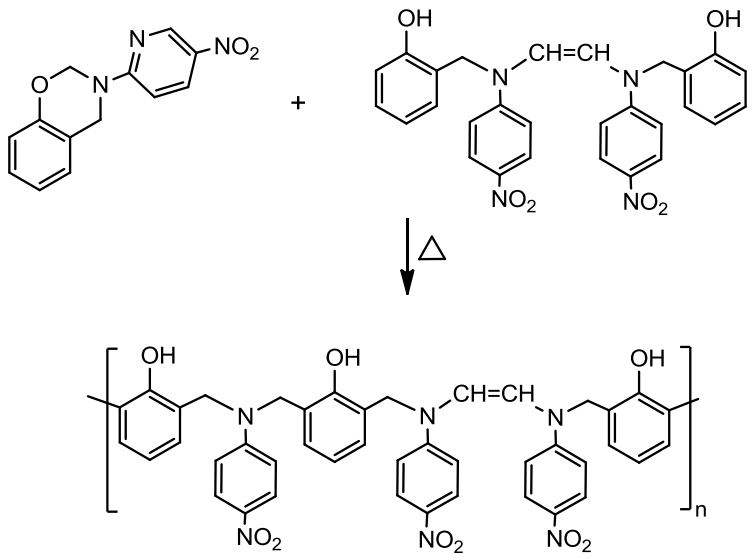

P3

ii) by vinyl polymerization

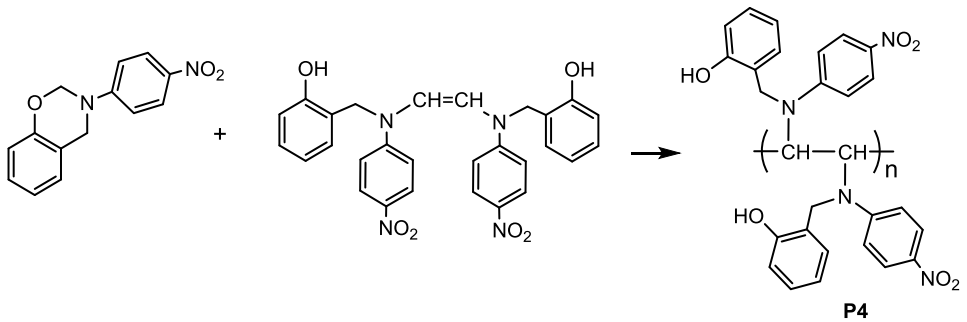

P4

It is known that as the electron withdrawing character of the group at the para position to the N of the aniline group increases, the imine group is destabilized and the polymerization temperature of benzoxazine is increased [58]. Thus, as a consequence

of the highly electron withdrawing character of the nitro group, the curing temperature of benzoxazine based on p-nitroaniline, Ph-na is relatively high and significantly close to its degradation temperature. Hence, the curing program applied is very crucial.

The exothermic ring opening polymerization peak in the temperature range of 230-270°C is observed for the samples Ma1 to Ma8 which were cured at 160℃ for 1 to 8 hours, indicating that the polymerization was not completed for these samples (Fig. 3.17). The disappearance of this peak in the DSC curves of the rest of the samples confirmed polymerization of the Ph-na monomer by the applied curing programs. As representative examples DSC profiles for Pa10 and Pa12 cured at 160°C for 10 and 12 hours, respectively, Pb3 cured at 180°C for 3 hours and Pc1 cured at 200°C for 1 hour are also shown.

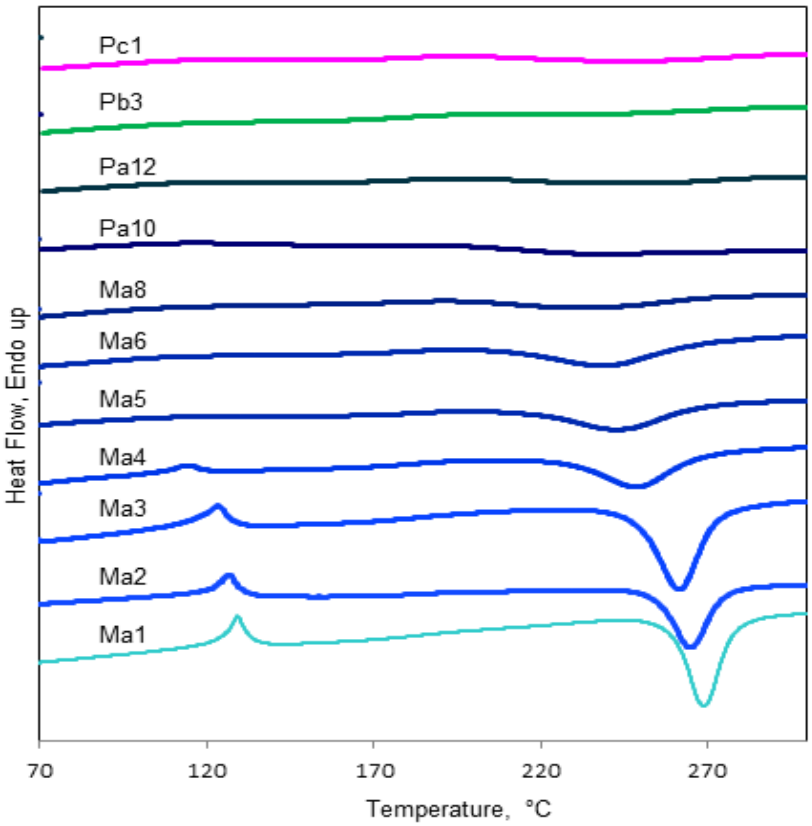

Figure 3.17 DSC profiles of benzoxazines Ma1 to Ma8 cured at 160°C for 1 to 8 h, Pa10 and Pa12 cured at 160°C for 10 to 12 h and Pb3 cured at 180°C for 3 h.

Polymerization of the monomer is also confirmed by FTIR analyses. As an example, the FTIR spectrum of the polymer prepared by curing at 200 °C for 2 h after preheating at 180°C for 3 h is shown in Fig.3.15b. The polymer spectrum exhibits disappearance of the characteristic peaks of oxazine and di-substitute benzene rings at 1487, 1366, 1227, 1039 and 959 cm^{-1} indicating complete polymerization via ring opening of oxazine ring. The peaks in the region 1600-1550 and 1500-1400 cm^{-1} assigned to C-C stretching vibrations are also diminished significantly. This behavior may be related to crosslinked structure of the polymer generated. The characteristic asymmetric streching peak of NO_2 group is detected at 1506 cm^{-1}. The aromatic C-H in plane bending and out-of-plane deformation modes of aromatic rings are detected again in the range 1250-1050 and 900-700 cm^{-1}. In addition, a new peak at 1772 cm^{-1} in the region of C=O absorptions, is appeared in the spectrum. Low and his coworkers also detected generation of various carbonyl derivatives due to oxidation at the methylenes of Mannich base and tentatively assigned the band at 1754 cm^{-1} to an imide structure. Another possibility for this absorption is the presence of a COOH group bonded to an aromatic ring. It may be thought that, under the curing conditions, the NO_2 radicals may be eliminated and being strong oxidizing agent may oxidize the methylenes of Mannich base to COOH as shown in Scheme 3.8.

Scheme 3.8 Generation of COOH end groups

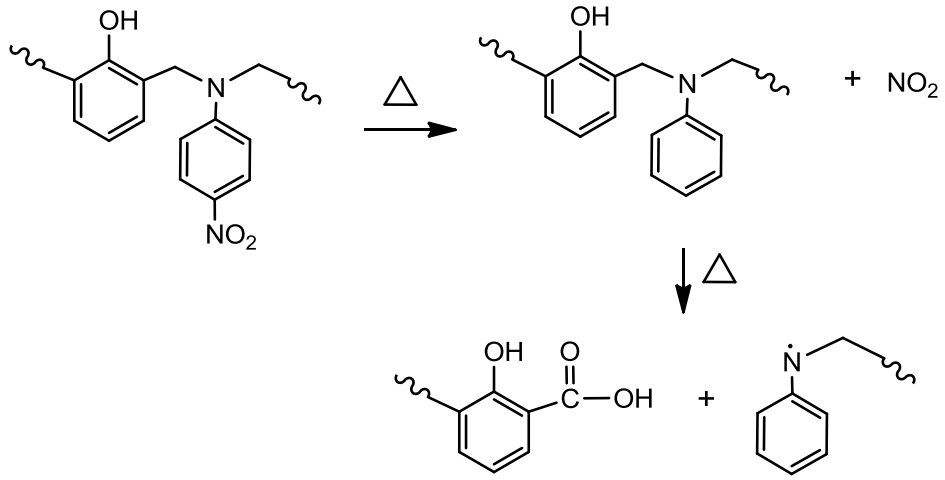

It may be thought that certain polymerization routes may be predominant under certain curing conditions. As thermal degradation mechanism depends on the structure of the polymer, investigation of thermal characteristics, especially thermal degradation products and mechanism of polybenzoxazines prepared by different curing programs, also gives valuable hints for polymerization mechanism.

Thus, thermal analyses of the samples, for which complete polymerization was indicated by DSC findings by different curing programs, were performed systematically via TGA and DP-MS techniques not only to determine thermal behavior but also to elucidate the predominant polymerization routes under certain curing condition.

The TGA curves of these polymers are shown in Fig. 3.18 and the results are tabulated in Table 3.5.

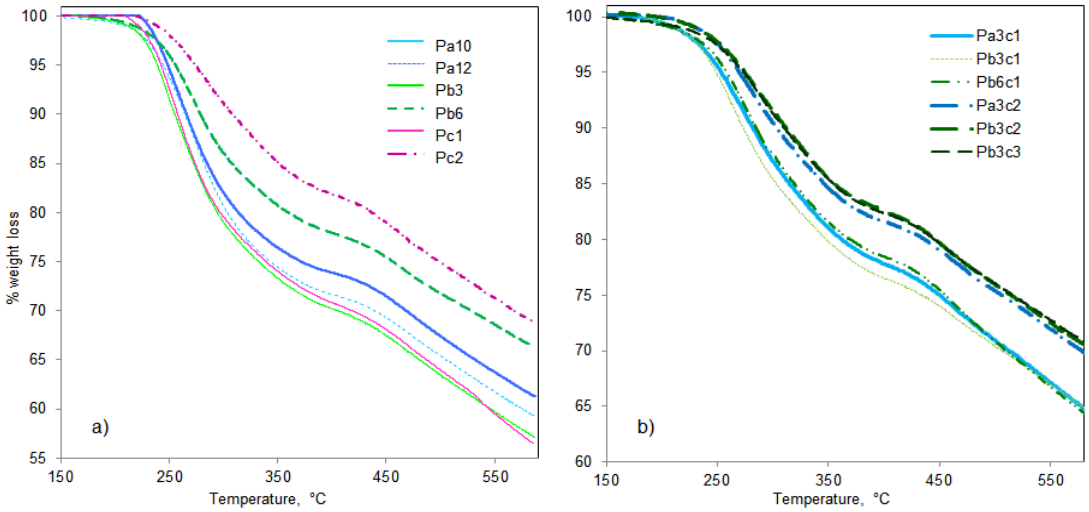

Figure 3.18 TGA curves of polybenzoxazines cured a) in one step and b) at 200°C after preheating at 160 and 180°C (a=160°C, b=180°C and c=200°C for given durations in hours).

For all the samples, the TGA curves show two or three step decompositions, indicating presence of chains with different structures and/or thermal stabilities and/or a multi-step thermal degradation mechanism. It can be noted from Fig.3.18 that as the curing was performed at higher temperatures or continued for prolonged periods, the char yields of the polymers produced are increased and the temperature at which 5% weight losses occurred, $T_{5\%}$ and the temperature at which maximum weight loss detected, $T_{max,1}$ are shifted to higher temperatures. The char yield of the samples cured at 200°C after pretreatment at 160 or 180 °C are somewhat higher than the ones cured without preheating. In addition, the increase in the duration of curing at 200°C provides an increase in the ultimate char yield. On the other hand, when the duration of pre-treatment at 180°C is increased from 3 h to 6 h, a lower char yield is obtained. In general, a high temperature shift for the initial weight loss step is also recorded in the same sequence.

Table 3.5 TGA data for polybenzoxazines

	$T_{5\%}$	T_{max}	

Sample*		Step 1	**Step 2**	**Step 3**	% char yield, at 600 ˚C
Pa10	247.5	258.6	476.4		61.5
Pa12	244.2	273.5	470.0		59.5
Pb3	238.5	248.5	476.3		57.4
Pb6	255.8	270.9	462.5		66.2
Pc1	242.6	261,3	460.3		56.5
Pc2	273.5	279.6	459.3		68.8
Pa3c1	271.1	268.2	459.9		67.5
Pa3c2	279.2	275.9	4593		71.0
Pb3c1	249.3	261.9	472.9		64.7
Pb3c2	274.8	282.4	454.7	536.9	70.4
Pb3c3	274.5	287.2	455.4	533.3	70.6
Pb6c1	258.9	275.8	463.4		64.0

* Samples prepared by curing at a=160°C, b=180°C and c=200°C for given periods in hours.

The TIC curves of the polybenzoxazines prepared by applying one step curing program is shown in Fig. 3.19. The mass spectra of the samples detected at the maxima of the peaks present in the TIC curves are given in the figures. For all the samples, the TIC curves show an intense peak in the temperature region 200-350°C and two overlapping weak peaks at around 400-650°C revealing a multi-step thermal degradation process and/or presence of chains with different thermal stabilities in accordance with TGA results. The trends indicated that the curing program used affected both the thermal stability and the yields of the products lost at different temperature regions.

In general, the initial step of thermal degradation of polybenzoxazines shifts to high temperatures as the temperature or the duration of curing used for polymerization is increased. Similarly, a high temperature shift for the overlapping peaks present in the TIC curves at elevated temperatures is observed in the same sequence. In addition, the relative yields of the products lost at elevated temperatures are increased during

the pyrolysis of the samples cured at higher temperatures. However, as the curing period at a given temperature is increased, the relative yields of high temperature pyrolysis products eliminated in the final step of degradation are decreased.

The pyrolysis mass spectra of all the samples at the maximum of the low temperature peak in the corresponding TIC curves are dominated with diagnostic peaks of p-nitroaniline, molecular ion (M) peak at 138 Da, and peaks due to its diagnostic fragment ions $[M\text{-}NO]^+$ (108 Da), $[M\text{-}NO_2]^+$ (92 Da), $[M\text{-}NO\text{-}CO]^+$ (80 Da) and $C_5H_5^+$ (65 Da) (Fig.3.19) confirming the elimination of nitroaniline during the pyrolysis and/or ionization inside the ion source. For the samples Pa10, Pa12, Pb3, Pb6 and Pc1 moderate or weak peaks at 256 and 242 Da that can directly be associated with $HOC_6H_4CH_2N(C_6H_4NO_2)CH_2$ and $HOC_6H_4CH_2NC_6H_4NO_2$ respectively are also observed. Upon expansion the spectrum, weak peaks at 514 and 648 Da that can be attributed to di-protonated dimer and $NO_2C_6H_4NCH_2MC_6H_4(OH)CH_2NC_6H_4NO_2$ (648 Da) are recorded. As the exothermic ring opening polymerization peak in the temperature region of 230-270°C in the DSC curves is not detected for these samples it may be thought that these fragments are generated by degradation of low mass oligomers (Fig. 3.19). For the samples cured for longer periods and at higher temperatures, these peaks are either totally disappeared or diminished significantly.

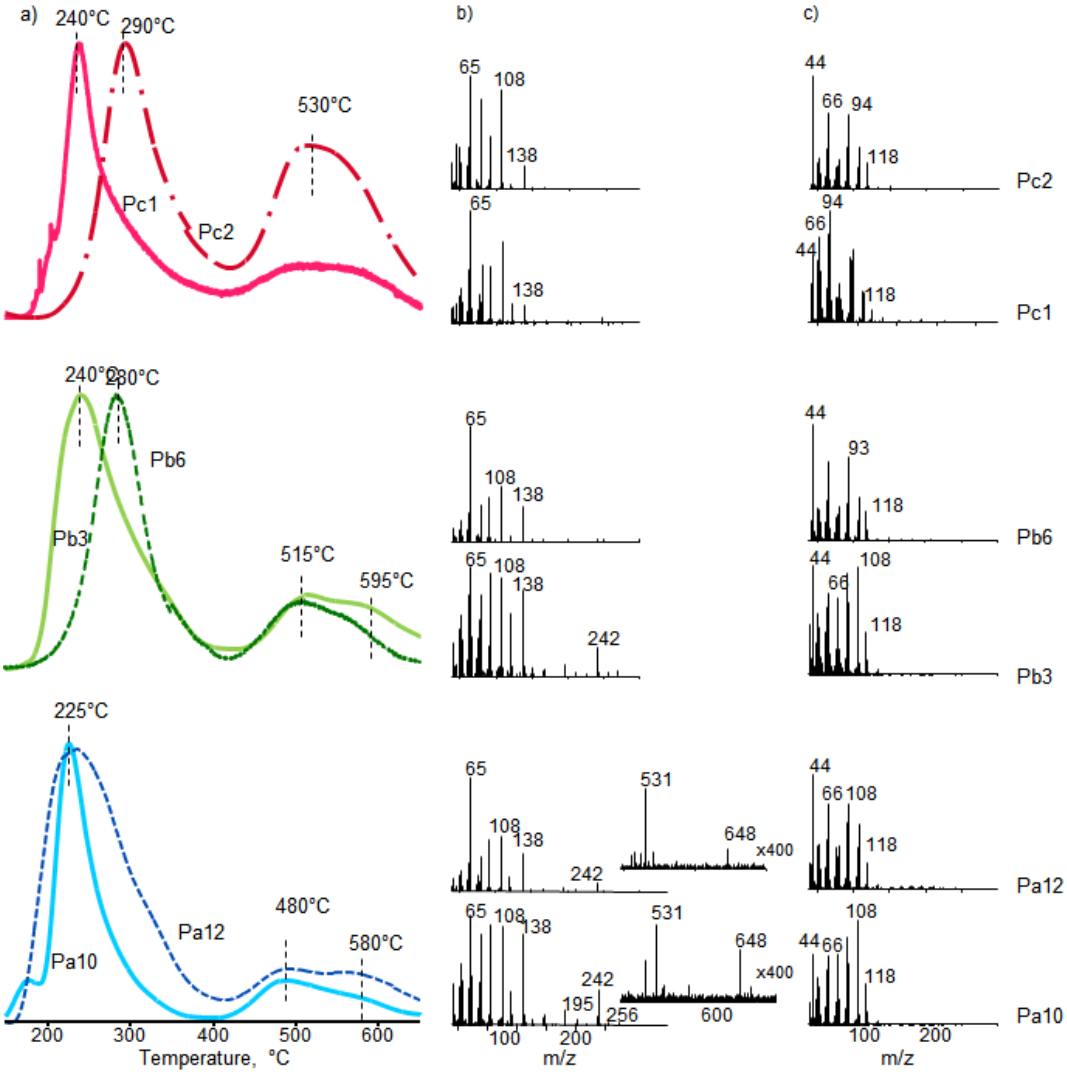

Figure 3.19 TIC curves of PPh-na cured at 160°C for 10h (Pa10) and 12 h (Pa12), at 180°C for 3h (Pb3) and 6 h (Pb6) and 200 °C for 1h (Pc1) and 2h (Pc2)

The pyrolysis mass spectra of the samples recorded at elevated temperatures are dominated with identical peaks. Yet, significant variations in the relative intensities of the peaks that can be associated with products involving phenyl ring or their fragments generated mostly during ionization, such as C_5H_6 and/or NC_4H_3 (66 Da), C_6H_6 and/or NC_5H_4 (78 Da), C_7H_7 and/or NC_6H_5 (91 Da), HOC_6H_5 (94 Da), $HOC_6H_4CH_2$ (107 Da) and $HOC_6H_3C_2H_2$ and/or $CH_2NC_6H_4CH_2$ (118 Da) are

detected. The base peak is at 108 Da ($OC_6H_4NH_2$ and/or $HOC_6H_4CH_3$) for the samples cured at 160 °C, for the samples cured at 180°C, for rest of the samples, it is at 44 Da that can be associated with loss of CO_2. The decrease in the relative intensities of the peaks at 108 and 118 Da is followed by the increase in the relative intensities of the peaks at 93 and 94 Da in the pyrolysis mass spectra of the samples cured at higher temperatures and/or for longer periods.

The initial decomposition of the polymer samples Pa10, Pa12, Pb3 and Pc1 in the temperature region 225-250℃ corresponding to the region where ring opening polymerization of Ph-na takes place and the presence of monomer peak in their pyrolysis mass spectra indicate elimination of monomer and decomposition of low molar mass oligomers. For these samples, char yields are relatively low, less than 60% except that of Pa10, and the relative intensity of the high temperature peak associated with degradation of thermally more stable polymer chains, is noticeably low. Thus, it can be concluded that the curing of the monomer at low temperatures, even for prolonged periods or curing at elevated temperatures for short periods, is not sufficient for complete polymerization and low molar mass oligomers exit in the product. When DP-MS and TGA results are analyzed together, it can be noticed that the increase in the char yield and the decrease in the relative yields of the products eliminated in the final stages of thermal decomposition occur subsequently.

The TIC curves of the samples cured at 200°C for 1 or 2 h, after preheating for 3 h at 160°C (Pa3c1, and Pa3c2) and 3 or 6 h at 180°C (Pb3c1, Pb3c2 and Pb6c1) and the pyrolysis mass spectra recorded at the maximum of the peaks present in the TIC curves are shown in Fig. 3.20. The thermal decomposition of all these samples occurs above the temperature regions where polymerization of Ph-na takes place. In addition, for these samples, the weak overlapping peaks at elevated temperatures present in the TIC curves are shifted to higher temperature regions, and their relative intensities are increased revealing presence of chains with significantly high thermal stabilities. For the samples cured at 200 °C for one hour, as the temperature of pre-treatment or duration of preheating is increased, the evolution of thermal degradation products

both at initial and final stages of pyrolysis shifts to high temperatures. A similar behavior is observed when the duration at 200°C is increased from one hour to two hours. However, when the duration at 200°C is increased to three hours, the thermal degradation products evolve at lower temperature regions indicating a decrease in thermal stability of the polymer generated. Thus, it can be concluded that curing the monomer at 200 °C for 3 h after pre-heating at 180°C for 3 h initiate the degradation of the polymer chains during the curing process to a certain extent.

The pyrolysis mass spectra recorded at the peak maximum of the low temperature peak present in the TIC curves are almost identical and dominated with diagnostic peaks of p-nitroaniline indicating elimination of p-nitroaniline during the initial stages of pyrolysis. For these pre-heated samples, elimination of the monomer or any higher mass fragments is not detected. The pyrolysis mass spectra recorded at elevated temperatures are also almost similar showing small variations in the relative intensities of the peaks.

Among all the samples prepared, the thermally most stable polybenzoxazine with highest char yield is the one produced by curing at 200°C for 2 h after pre-heating at 180°C for 3 h. The sample Pb6c1 also shows desirable thermal behavior. But, further curing of this sample at 200°C was not tried considering the significantly long curing period.

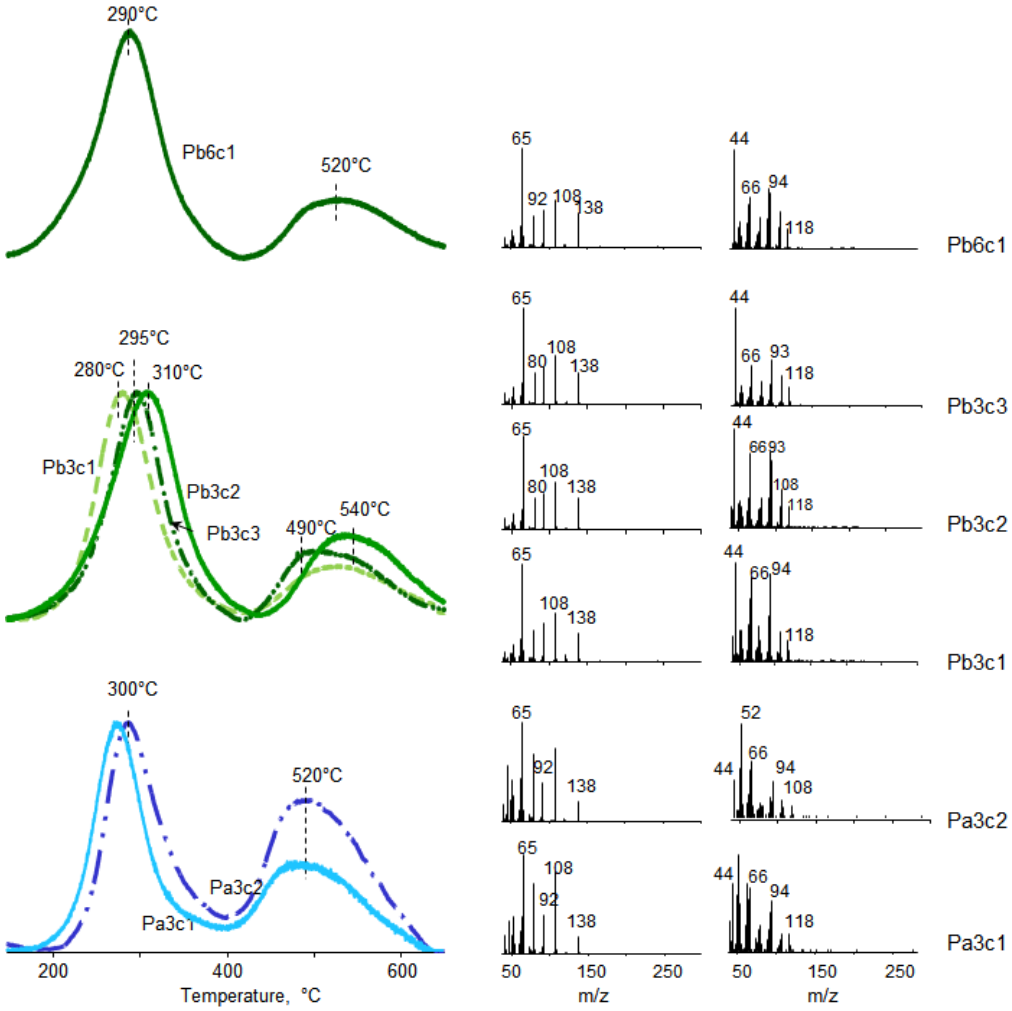

Figure 3.20 TIC curves of PPh-na cured at 200°C after curing at 160 and 180°C for 3 h (Pa3c1 and Pb3c1) and at 180°C for 6 h (Pa6c1)

The trends detected in the TIC curves reveal that thermal decomposition of the polybenzoxazines based on nitroaniline takes place in two distinct temperature regions. The yield of monomer and nitro aniline maximizes in the temperature region 225-300 depending on the temperature and duration of curing used for polymerization. Evolution of products such as phenol and CO_2 are detected in a broad temperature region above 500°C. Thus, contrary to what was observed for

polybenzoxazines based on aniline, loss of degradation products at around 400°C is not observed for polybenzoxazines based on nitroaniline.

Unfortunately, further dissociation of thermal degradation products in the mass spectrometer during ionization and contribution of all the fragments that are structural isomers and the products involving different combinations of C, N, O and H, with the same m/z values, to the intensity of the same m/z peak in the mass spectrum, the interpretation of pyrolysis mass spectra of polymers is usually very difficult. Thus, in order to minimize dissociation during ionization low energy DP-MS analysis were also performed. Furthermore, the variation of the intensity of almost all products as a function of temperature were analyzed and grouped according to the similarities in their evolution profiles, to determine the source of the related product, or the mechanism of thermal degradation which also supplies valuable information for the polymerization routes during the curing process.

In order to minimize dissociation of thermal degradation products during ionizations, the pyrolysis analyses were also utilized at electron energies of 20 eV. As expected, reproducibility decreased noticeably. In addition, the ion yields are diminished drastically and few product peaks can be detected in the 20 eV pyrolysis mass spectra. Thus, only limited information can be obtained. In Fig. 3.21, as a representative example, the TIC curves and the pyrolysis mass spectra at selected temperatures recorded during the pyrolysis of Pb3c2 at 70 and 20 eV ionization energies are shown. Although, almost identical peaks are detected, significant variations in the relative intensities exist. The significant increase in the relative intensities of the peaks at 138 and 108 Da at around 310 C, and those at 94, 93 and 78 Da confirm elimination of nitroaniline, $NH_2C_6H_4O$ and/or $HOC_6H_4CH_3$ (108 Da), HOC_6H_5 (94 Da), $H_2NC_6H_5$ (93 Da), C_6H_6 (78 Da) and CO_2 (44 Da) directly during the thermal decomposition process.

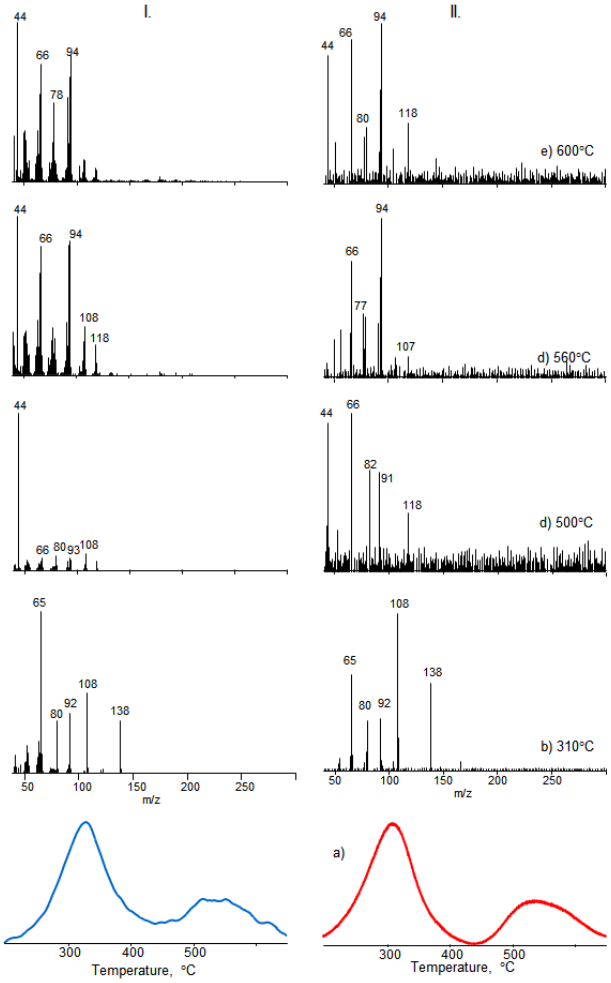

Figure 3.21 a) The TIC curves and b to e) mass spectra recorded during the pyrolysis of Pb3c2 at I. 70eV and II. 20 eV ionization energies.

In Fig. 3.22, single ion evolution profiles of some selected products recorded during the pyrolysis of Pa10 and Pb3c2 are given for comparison. The single ion profiles are grouped considering the similarities in the trends observed especially in the high temperature regions. As can be noticed from Fig. 9, the relative yields of products evolved at around 225°C during the pyrolysis of Pa10, are significantly high. Evolutions of monomer (256 Da) and high mass products such as $NO_2C_6H_4NCH_2MC_6H_4(OH)CH_2NC_6H_4NO_2$ (648 Da), di-protonated dimer (514 Da) p-nitroaniline (138 Da) and low mass fragments that can be associated with dissociation of these products mainly during ionization inside the mass spectrometer,

such as $C_6H_5NHC_2H_2NHC_6H_5$ (210 Da), $HOC_6H_4C_2H_2C_6H_4$ and/or $HNC_6H_4CH_2NC_6H_4$ (195 Da), $CH_2C_6H_4CH_2NC_6H_4$ and/or $HOC_6H_4C_2H_2C_6H_4$ (184 Da), $C_6H_4CHNC_6H_4$ and/or $C_6H_5C_2H_2C_6H_4$ (179 Da), $H_2NC_6H_4O$ and/or $HOC_6H_4CH_3$ (108 Da), HOC_6H_5 (94 Da), $H_2NC_6H_4$ and/or OC_6H_4 (92 Da), $C_6H_5CH_2$ and/or NHC_6H_4 (91 Da), C_6H_6 (78 Da) and C_5H_5 (65 Da) are recorded. Evolutions of high mass products (648, 514, 195 Da), monomer and p-nitroaniline are only detected at around 225°C. Loss of CO_2 is detected at moderate temperatures, two overlapping intense peaks with maxima at around 362 and 449°C are present in its single ion pyrogram. CO_2 elimination usually occurs during the ionization processes of molecules involving ester linkages or acid end-groups inside the mass spectrometer. The fragments with m/z values 184, 179, 108, 91 and 78 Da are lost at high temperature regions. A broad, relatively weak peak at around 475, 550 and 570 °C are present in the evolution profiles of fragments with m/z values 108, 210 and 179 Da respectively. On the other hand, the fragments with m/z value 91 Da and 78 Da show two overlapping weak peaks with maxima at around 475 and 570°C in their single ion pyrograms. On the other hand, evolutions of $HOC_6H_3C_2H_2$ and/or $CH_2NC_6H_4CH_2$ (118 Da) and HOC_6H_5 (94 Da) mainly occur at elevated temperatures, and are maximized at around 475 and 530°C respectively.

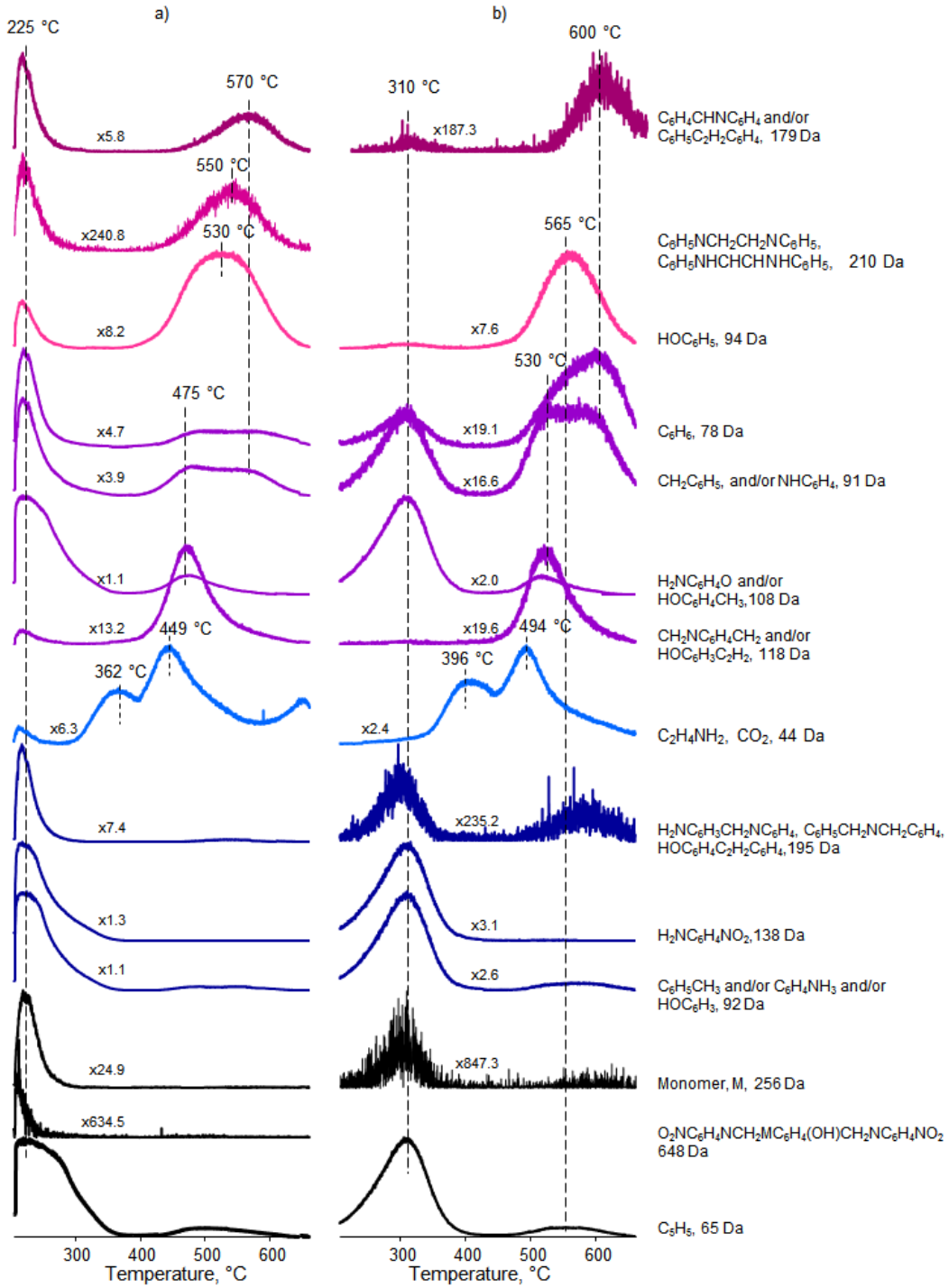

Figure 3.22 Single ion evolution profiles of selected products detected during the pyrolysis of a) Pa10 and b) Pb3c2.

A high temperature shift is detected in the evolution profiles of almost all the products generated during the pyrolysis of Pb3c2 cured at 200 °C after pre-heating at 180°C for 3h. No monomer or high mass fragment that can be associated with degradation of oligomers is detected. Yet, evolution of nitroaniline is again extensive at initial stages of pyrolysis. Diagnostic fragments of nitroaniline, $H_2NC_6H_4O$ (108 Da), OC_6H_4 (92 Da) and C_5H_5 (65 Da) show similar trends in their evolution profiles in the low temperature regions, reaching maximum yield at around 310°C confirming that thermal degradation of polybenzoxazine is initiated by elimination of nitroaniline. The evolutions of fragments such as $C_6H_4CHNC_6H_4O$ (179 Da), $CH_2NC_6H_3CH_2$ (118 Da) and HOC_6H_5 (94 Da) are almost exclusively detected only at elevated temperatures. Again, loss of fragments with m/z values 91 and 78 Da are detected in two temperature regions. Yet, their relative yields are increased significantly at high temperatures. Similarly, the low temperature evolutions of fragments with m/z values 118 and 94 Da, diminish noticeably.

The single ion pyrograms of the abundant degradation products show broad overlapping peaks with maxima at different temperatures indicating either a multi-step complex thermal degradation process and/or presence of chains with different thermal stabilities and structures.

In Fig. 3.23, the pyrograms of nitroaniline (m/z=138 Da) and $HOC_6H_4C_2H_2C_6H_4$ and/or $C_6H_5CH_2NC_6H_4CH_2$ (m/z=195 Da), that mainly evolved at initial stages of pyrolysis of the samples prepared by different curing programs are shown. The evolution of nitroaniline below 250℃ may be associated with the decomposition of monomer and low molecular weight oligomers as polymerization cannot be completed due to the inefficient curing process. In general, the evolution of nitroaniline is suppressed and is shifted to higher temperature regions during the pyrolysis of the samples cured at higher temperatures or cured for longer periods.

Unlike nitroaniline, evolution of fragment with m/z value 195 Da is also observed at elevated temperatures. This fragment may be associated with degradation of chains with different structures. In general, its single ion pyrograms follow almost identical trends with that of nitroaniline at low temperatures. The low temperature evolutions may be related with loss of fragments $C_6H_5CH_2NCH_2C_6H_4$ and/or $H_2NC_6H_3CH_2NC_6H_4$, whereas, those at elevated temperatures may be associated with elimination of $HOC_6H_4C_2H_2C_6H_4$. The relative yield of the fragment lost at elevated temperatures increases for the samples polymerized by curing at higher temperatures or for longer periods.

The single ion evolution profiles of some representative pyrolysis products, $CH_2C_6H_5$ and/or HNC_6H_4, (91 Da), C_6H_5OH (94 Da), $HOC_6H_3C_2H_2$ and/or $CH_2NC_6H_4CH_2$ (118 Da) and $C_6H_5C_2H_2C_6H_4$ and/or $C_6H_4CHNC_6H_4$ (179 Da) evolved predominantly at elevated temperatures are depicted in Fig. 3.24. Among these, losses of 91 and 179 Da fragments are also detected in low temperature regions. On the other hand, losses of C_6H_5OH (94 Da), $HOC_6H_3C_2H_2$ and/or $CH_2NC_6H_4CH_2$ (118 Da) are mainly observed at elevated temperatures.

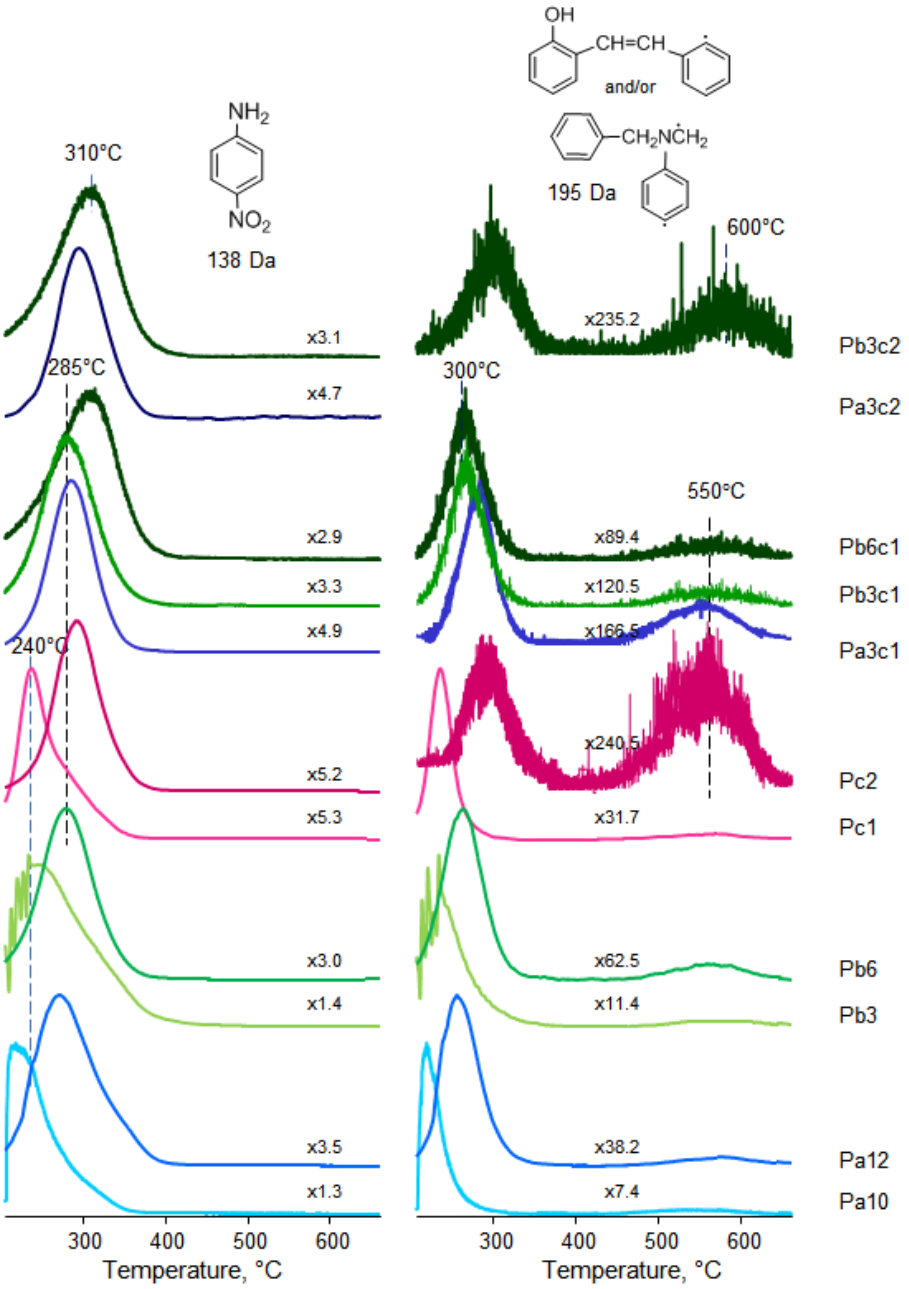

Figure 3.23 Single ion evolution profiles of nitroaniline (138 Da) and $C_6H_5CH_2N(C_5H_4)CH_2$ and/or $HOC_6H_4C_2H_2C_5H_4$ (m/z=195 Da) detected during the pyrolysis of PPh-na prepared by different curing programs

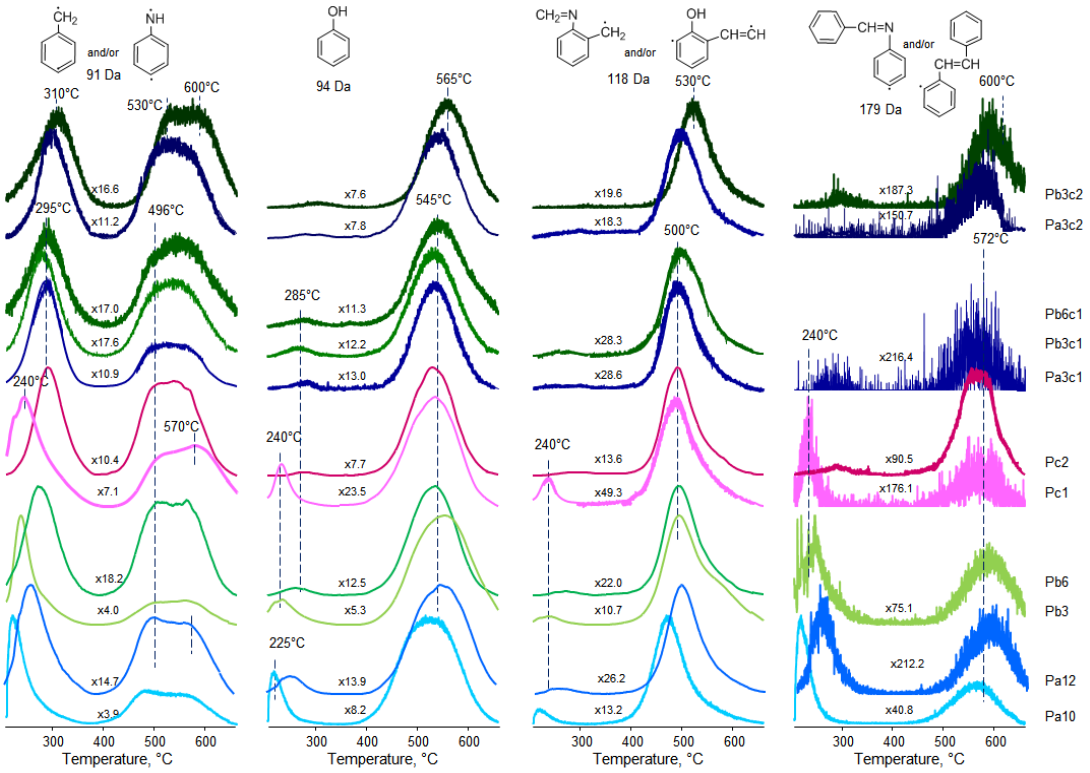

Figure 3.24 Single ion evolution profiles of some selected products detected during the pyrolysis of PPh-na prepared by different curing programs

A relatively sharp peak in the temperature region 200-350°C and two overlapping peaks at elevated temperatures are present in the single ion profile of fragment with m/z value 91 Da evolved during the pyrolysis of all the polymers prepared by different curing programs. This fragment can be associated with $CH_2C_6H_5$ which is a diagnostic fragment generated during the ionization of methylene substituted phenyl compounds. The presence of three peaks in its evolution profile indicates that it is generated from units of different structures and/or thermal stabilities. The loss of 91 Da fragment is diminished and shifted to high temperature regions during the pyrolysis of the polymers cured at higher temperature regions or for longer periods. The low temperature peak in its evolution profile maximizes in the temperature region 225-310°C, whereas, the two overlapping peaks show maxima in the temperature region 475-530 and 530-600°C respectively.

Elimination of 179 Da fragment, $C_6H_4CHNC_6H_4$, is also extensive at initial stages of pyrolysis for the samples cured in one step. The evolution of 179 Da fragment, diminishes drastically for the samples cured at higher temperatures, especially at initial stages of pyrolysis. For the samples cured in two steps, loss of $C_6H_4CHNC_6H_4$ at low temperatures is almost disappeared while those at high temperature regions are relatively enhanced.

On the other hand, the loss of C_6H_5OH (94 Da), predominantly occurs only at elevated temperatures and its yield is maximized in the temperature region 530-565°C. Similarly, evolution of $HOC_6H_3C_2H_2$ and/or $CH_2NC_6H_4CH_2$ (118 Da) is also observed mainly at elevated temperatures, reaching maximum yield in the temperature region 475-525°C.

Among these representative fragments the ones with m/z values 195 and 179 Da are maximized at temperatures corresponding to the high temperature peak in the evolution profile of 91 Da fragment.

The fragmentation patterns detected in the pyrolysis mass spectra and the trends in the evolution profiles reveal that thermal degradation of polybenzoxazines based on nitroaniline starts by evolution of nitroaniline, similar to loss of aniline in case of polybenzoxazines based on aniline in the temperature region 225 to 310°C. However, for this case, elimination $NO_2C_6H_4NHCHCHNHC_6H_4NO_2$ corresponding to $C_6H_5NHCHCHNHC_6H_5$ analogue or any other product that can be associated with decomposition of segments involving coupling of $NO_2C_6H_4NCH_2$ groups (Scheme 3.a) is not detected. During the pyrolysis of PPh-a, thermal degradation products attributed to degradation of P2 via random cleavages were detected at around 400 °C, independent of the temperature and the duration of curing process used for preparation of the polymer. However, for PPh-na, no product that can be associated with decomposition of such chains is recorded as expected. For the samples cured at high temperatures for prolonged periods, evolution of CO_2 during the pyrolysis is also enhanced and shifted to high temperature regions, indicating oxidation of methylene units. The oxidation methylenes most probably affects the generation of dimer via

Scheme 3.a more than the attack of NCH_2 groups to *para* positions of the phenol rings as two NCH_2 groups are involved in the coupling process. Thus, the probability of the existence of segments involving unsaturated dimer is reduced. Thus, the generations of **P3** structure is not very likely. Hence, it may be concluded that polymerization of nitroaniline based benzoxazine mainly proceed via attack of NCH_2 groups to *para* positions of the phenol ring.

The very high char yield indicates that the radicals generated by the elimination of nitroaniline combined to form unsaturated linkages as shown in Scheme 3.9, that decompose at elevated temperatures.

Scheme 3.9 Generation of unsaturated linkages during curing and/or pyrolysis

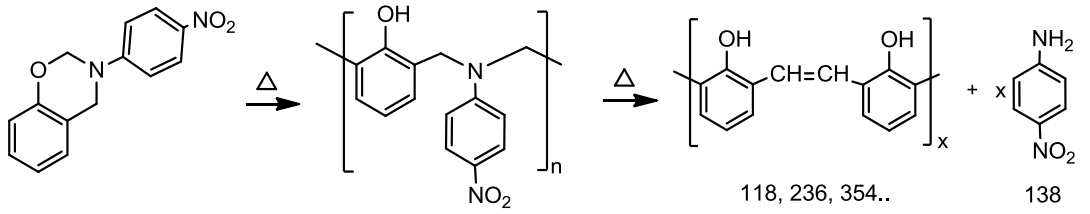

It may further be thought that if the loss of nitroaniline during the curing process is very extensive then the polymer sample does not involve chains with **P1** structure degrading via random cleavages.

The presence of peaks in the single ion evolution profiles of the fragments with m/z values 195, 179, 94 and 91 Da, that may be presumably associated with $HOC_6H_4C_2H_2C_6H_4$, $C_6H_5C_2H_2C_6H_4$, $HOC_6H_5$and $C_6H_5CH_2$ respectively, in the temperature region 500-600°C supports this proposal. In order to investigate the extent of loss of nitroaniline during the curing process, the monomer was cured while performing TGA analyses continuously. At the end of the process a weight loss of about 40% was detected. The TGA curve recorded during the process is given in Fig. 3.25. Considering the weight percent of nitroaniline (~54%) in the monomer, it can be concluded that about 75% of the nitroaniline groups are lost during the curing process.

The char yield for the polymer produced is about 70 % supporting the coupling of the radicals generated as shown in Scheme 3.9.

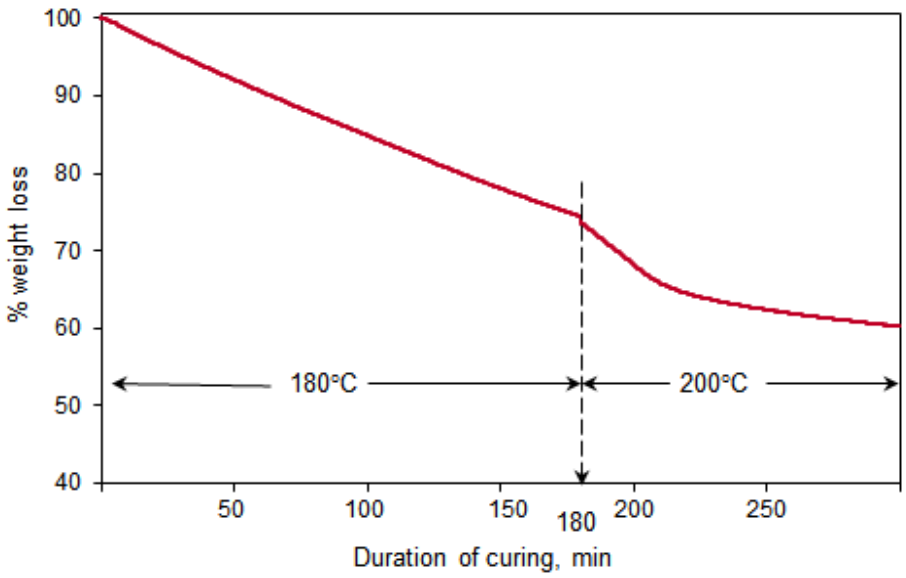

Figure 3.25 TGA curve recorded during the curing process

As the temperature and/or duration of curing is increased, evolution of aniline, phenol, $CH_2C_6H_5$ and products involving cross-linked and/or unsaturated linkages during the pyrolysis of the polymer produced shifts to high temperatures. However, although the relative yield of aniline is increased in the same sequence, decrease in relative yields of $CH_2C_6H_5$ and $C_6H_5C_2H_2C_6H_4$ is recorded. The increase in the relative yield of nitroaniline lost during pyrolysis indicates, decrease in the amount of nitroaniline eliminated during the curing process, which in turn leads to reduction in extend of unsaturated linkages formed via Scheme 3.9. On the other hand, as the temperature and duration of preheating is increased for the samples cured at 200 °C, the ultimate char yield is also increased. Then, it may be suggested that crosslinking reactions that inhibits loss of nitroaniline groups predominates under these conditions increasing the char yield.

3.1.3. Benzoxazine monomer based on 3-aminobenzonitrilei Ph-abn

Benzoxazine monomer was synthesized from phenol, 3-aminobenzonitrile and paraformaldehyde via solventless method (Scheme 3.10).

Scheme 3.10 Synthesis of benzoxazine monomer based on 3-aminobenzonitrile and phenol

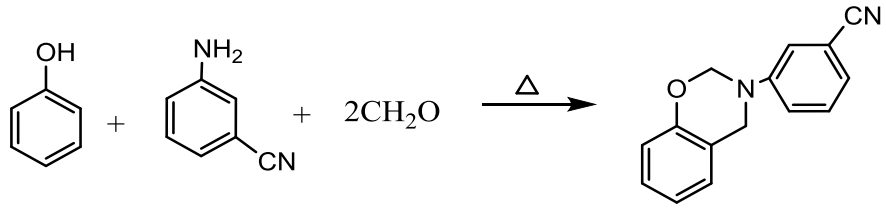

The resonances at 4.62 and 5.33 ppm correspond to the methylene protons (H1 and H2) of Ar-CH_2-N and O-CH_2-N of the oxazine ring, respectively. The chemical shifts (ppm) at 6.80 (3H, H6, H7 and H14), 6.90 (1H, H5), 7.00 (1H, H4), 7.13 (2H, H10 and H12) and 7.30 (H, H11) are assigned to the aromatic protons. The resonances at 50.43 and 77.43 ppm correspond to the methylene carbons (C1 and C2) of Ar-CH_2-N and O-CH_2-N of the oxazine ring, respectively. Other chemical shifts (ppm) are assigned to the resonances of the carbons: 113.20 (C7), 117.15 (C13), 118.98 (C14), 120.13 (C10, C15), 120.89 (C5), 121.30 (C3), 122.30 (C12), 124.61 (C6), 126.80 (C4), 128.30 (C11), 148.90 (C9), 154.0 (C8). Anal. calcd. for C15H12N2O: C, 76.27; H, 5.09; N, 11.86; O, 6.77%. Found: C, 76.31; H, 4.96; N, 12.02; O,6.71%.

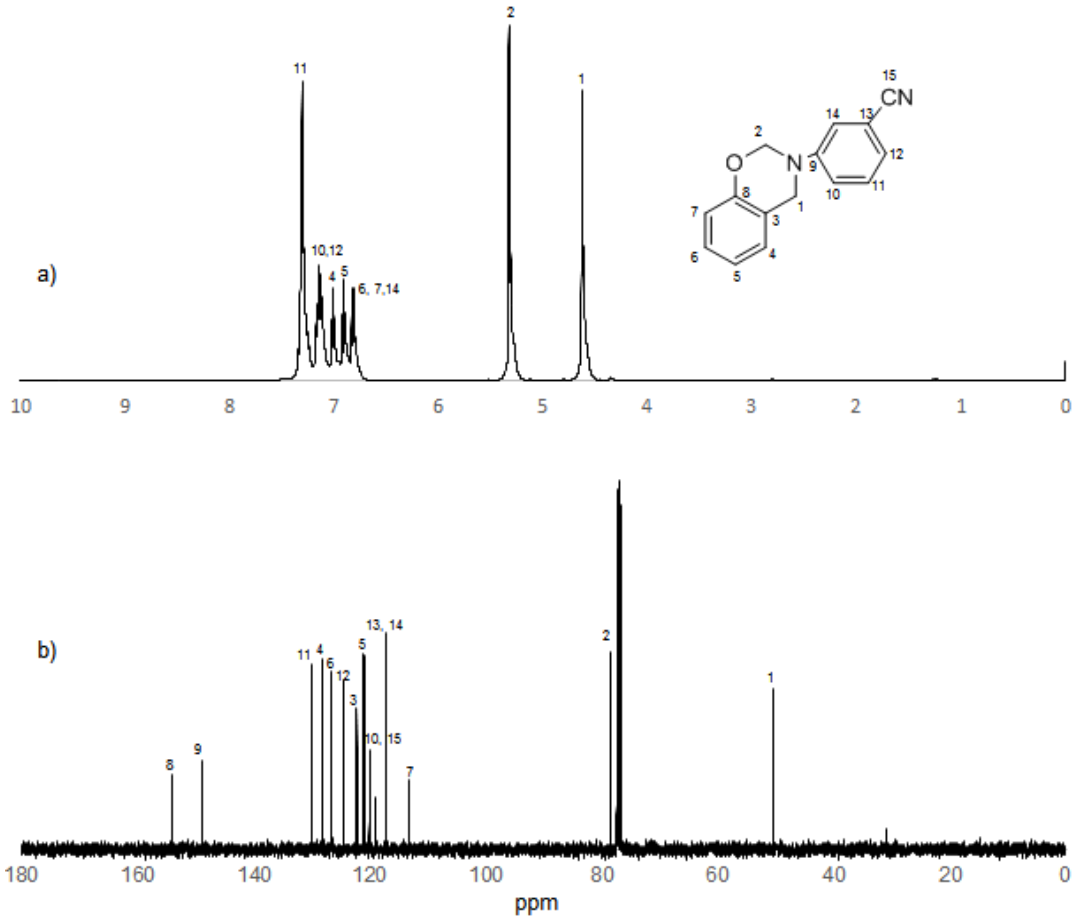

Figure 3.26 a) Proton-NMR and b)13C-NMR spectra of benzoxazine monomer.

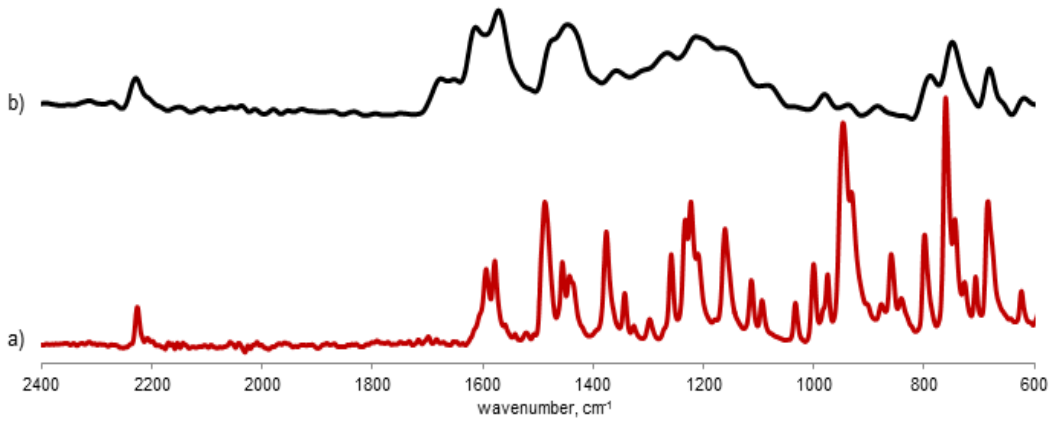

Figure 3.27 FTIR spectra of a) benzoxazine monomer and b) polybenzoxazine

The FTIR spectrum of the benzoxazine monomer is shown in Fig.3.27a. The typical absorption bands for the benzoxazine are observed at 1484, 1374, 1230, 1030 and 948 cm^{-1}, corresponding to the di-substituted benzene rings, CH_2 wagging, Ar-O-C anti-symmetric stretching, C-O-C symmetric stretching of oxazine ring and vibration modes of benzene ring with an oxazine ring, respectively. The band at 823 cm^{-1} corresponds to the symmetric stretching vibration of C-N-C of the oxazine ring and the C-H out-of-plane bending of the aromatic ring, whereas the band at 750 cm^{-1} is ascribed to the benzoxazine ring breathing. The absorptions at 2224 cm^{-1} are belong to the stretching vibrations of C≡N.

In general, the peaks in the region 1600-1585 and 1500-1400 cm^{-1} are assigned to C-C stretching vibrations in aromatic compounds. The ring C-C stretching vibrations occur in the region 1600-1350 cm^{-1}. The peaks at 1595, 1576 and 1434 cm^{-1} are related to C-C stretching vibrations. The aromatic C-H in plane bending and out-of-plane deformation modes of benzene and its derivatives are observed in the region 1300-1000 cm^{-1}, and 1000-600 cm^{-1} regions respectively. Thus, several peaks present in these regions are associated with both of the di-substituted benzene rings present in the structure.

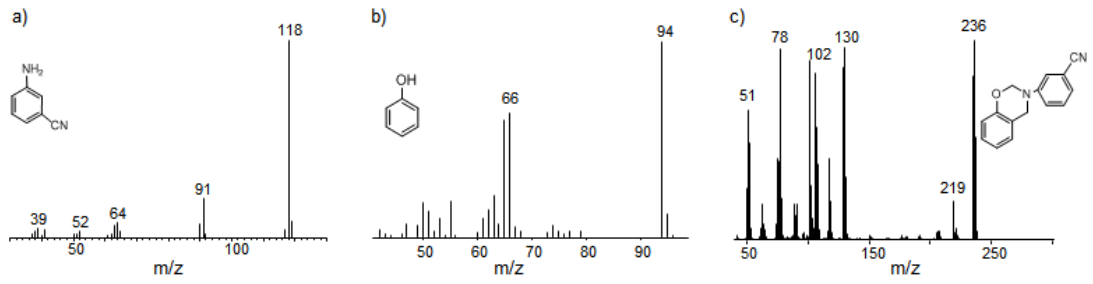

Figure 3.28 Mass spectra of a)aminobenzonitrile, b)phenol and c)benzoxazine based on aminobenzonitrile and phenol, Ph-abn

Phenol and 3-aminobenzonitrile based benzoxazine polymer was prepared by applying the curing conditions given in the literature[4][5][59,60].

The exothermic ring opening polymerization peak in the temperature range of 230-250 °C is observed for the samples prepared by curing at 160°C for 6h, Pa6 and at 180°C for 3 h, Pb3, indicating that the polymerization was not completed for these samples (Fig. 3.29). The disappearance of this peak in the DSC curves of the sample prepared by curing the monomer at 200 °C for 2h after preheating at 180 °C for 3 h confirmed polymerization of Ph-abn monomer. This polymer is abbreviated by Pb3c2.

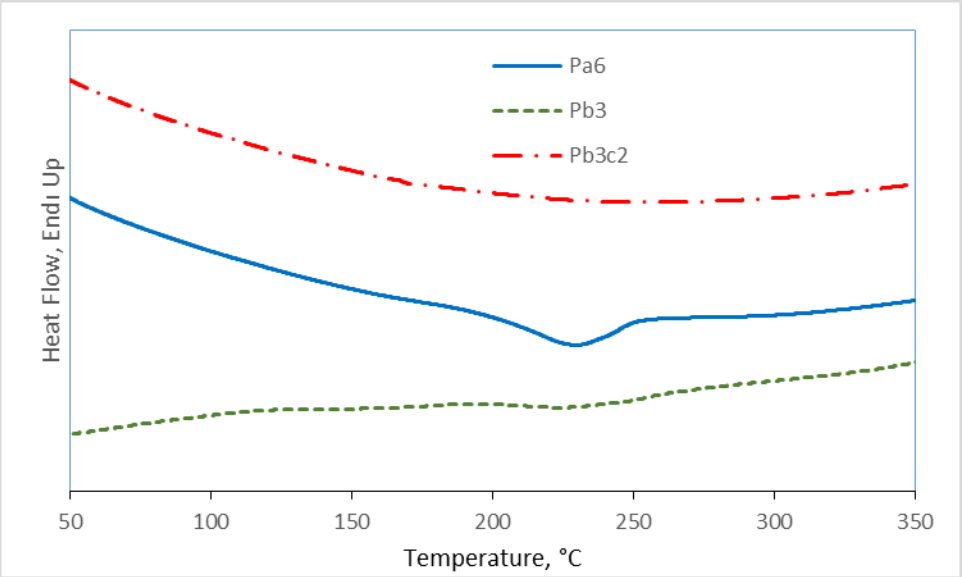

Figure 3.29 DSC profiles of DSC profiles of benzoxazines Pa6 and Pb3cured at 150 °C for 6 h and 180 ° C for 3h, respectively and Pb3c2 cured at 200 °C for 2h after preheating at 180 °C for 3h.

Polymerization of the monomer is also confirmed by FTIR analyses. As an example, the FTIR spectrum of the polymer prepared by curing at 200 °C for 2 h after preheating at 180°C for 3 h is shown in Fig.3.27b. The absorption intensity of the characteristic peaks at 1374, 1230, 1030, 948, 856, and 750 cm^{-1} decreased

significantly, indicating that the oxazine ring opening reaction is complete. At the same time, the peak at 2224 cm^{-1} the stretching vibrations of C≡N does not change. The peaks in the region 1600-1550 and 1500-1400 cm-1 assigned to C-C stretching vibrations are also diminished significantly. This behavior may be related to crosslinked structure of the polymer generated.

To determine the thermal characteristics of the polymers generated were analyzed by TGA and DP-MS techniques. The TGA curves of these polymers are shown in Fig.3.30 and the results are tabulated in Table 3.6.

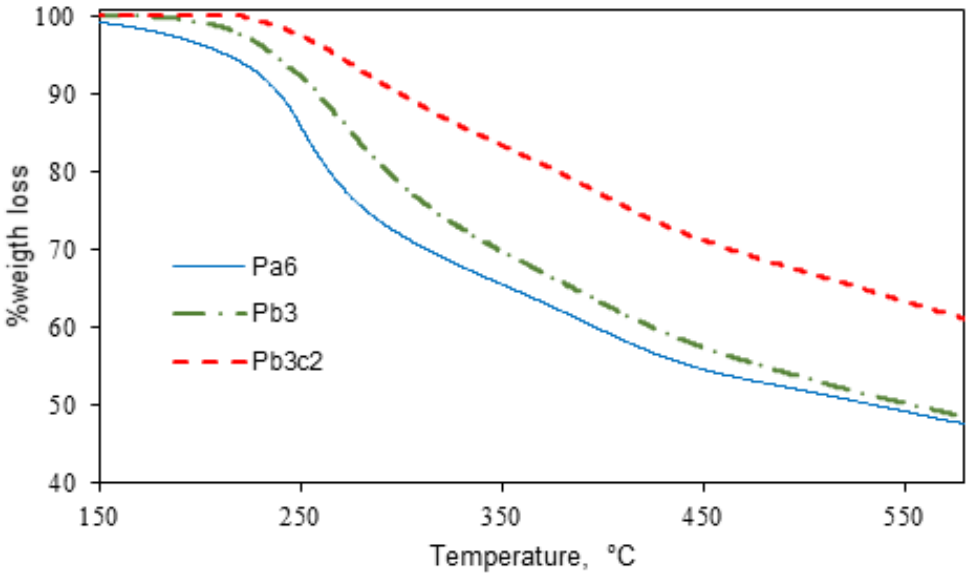

Figure 3.30 TGA curves of polybenzoxazines Pa6 and Pb3cured at 150°C for 6 h and 180° C for 3h, respectively and Pb3c2 cured at 200 °C for 2h after preheating at 180 °C for 3h.

TGA results reveal that the thermal degradation of polybenzoxazine based on 3-aminobenzonitrile occurs in two or three steps in the temperature regions 200-280, 300-400 and 480-530°C. This behavior may either be due to a multi-step thermal degradation or a polymer sample involving chains with different structures, thus, different thermal stabilities. The char yield of Pa6 and Pb3 are almost identical and

relatively lower than that of Pb3c2. As the temperature of curing process is increased, the initial degradation step of the polymer shifts to high temperatures slightly.

Table 3.6 TGA data for polybenzoxazines prepared by different curing programs

Sample	$T_{5\%}$	T_{max}		%Char yield at 600 °C
		Step 1	**Step 2**	
Pa6	213.8	250.5	397.0	47.6
Pb3	237.0	269.1	398.9	48.4
Pb3c2	268.4	274.6	399.9	60.9

The TIC curves and mass spectra at each peak maxima present in the TIC curve are shown in Fig.3.31. Pa3 and Pb3 exhibits an intense peak at around 226 °C and a weak peak at 425 °C. The high temperature peaks that can be associated with the degradation of thermally stable polymer chains are quite weak, pointing out the polymerization cannot be completed due to the inefficient curing programs used. Evolution of monomer and the characteristic fragments of the monomer can be seen in the mass spectrum of Pa3 at 226 °C. The monomer evolution at 226 °C was diminished for Pb3; however, the diagnostic peaks of the monomer and the fragment ions that can also be generated during ionization of the monomer inside the mass spectrometer such as $HO_6H_5CH_2NC_6H_4CN$ (222 Da), C_6H_4CN (102 Da) and $NH_2C_6H_5CNCH_2$ (130 Da) are still present in the mass spectrum.

The initial thermal degradation temperature is shifted to 296 °C during the pyrolysis of the polymer prepared by curing for 2h at 200 °C after preheating at 180 °C for 3h. The relative intensities of the high temperature peaks associated with the degradation of thermally more stable polymer chains are increased. Thus, it can be concluded that the polymerization of the benzoxazine monomer was completed during the curing

process involving post-heating at 200°C. When the TIC curves are compared, it can be said that the curing program applied did not affect the thermal characteristics of the polymer produced, in other words, degradation in three distinct temperature regions, but affected the amount of products evolved at each stage, indicating variations in degree of polymerization generating different structures.

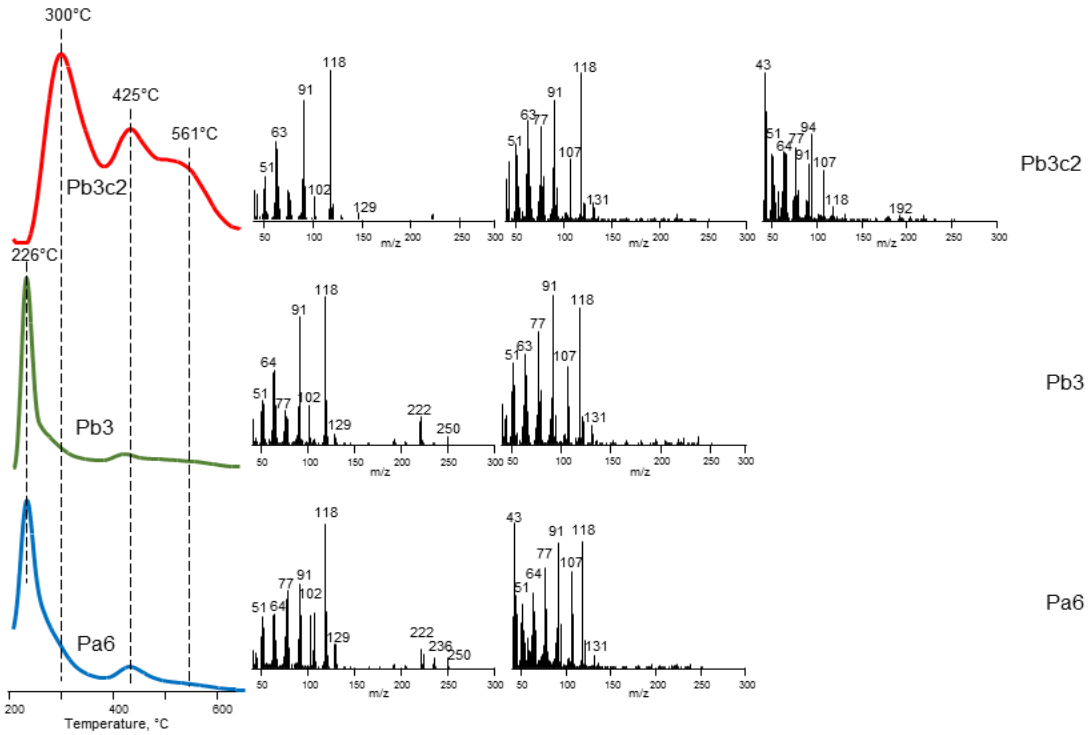

Figure 3.31 The TIC curves and mass spectra at each peak maxima present for Pa6, Pb3 and Pb3c2

In order to get a better insight for the degradation processes of the polymers which will also supply valuable information for the polymerization routes during the curing process single ion evolution profiles of intense and/or characteristic products are analyzed. In Fig.3.32, single ion evolution profiles of some selected products recorded during the pyrolysis of Pb3c2 are given. The single ion profiles are grouped

considering the similarities in the trends observed especially in the high temperature regions.

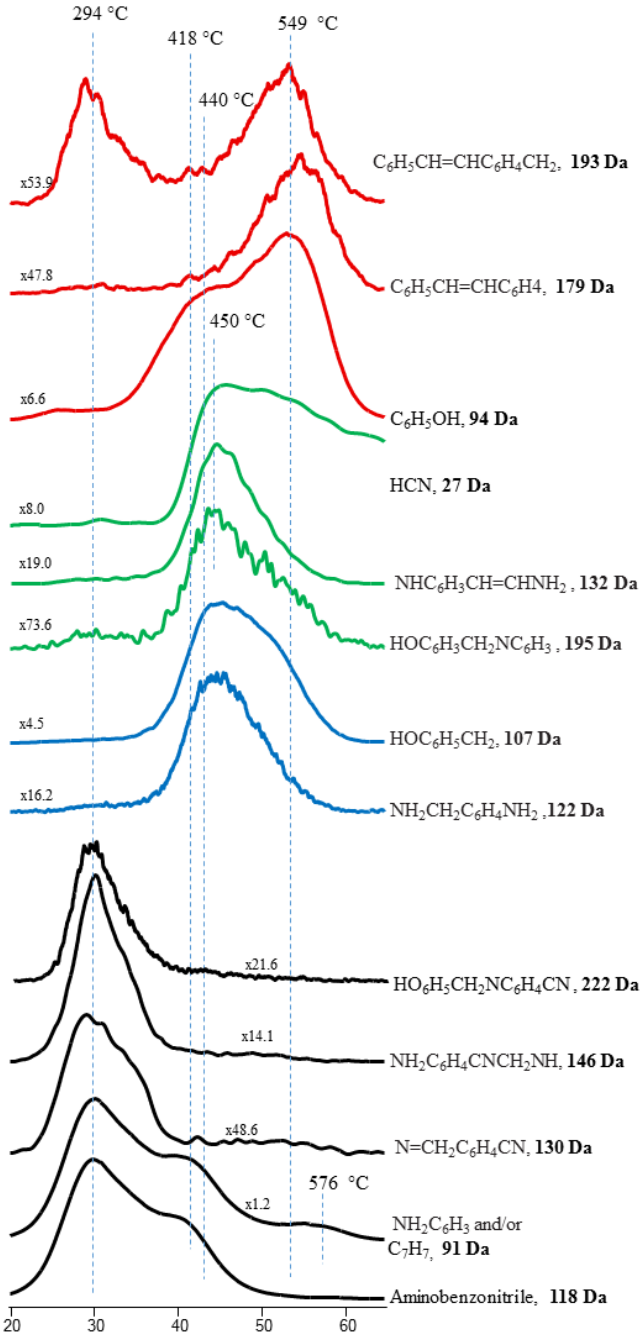

Figure 3.32 Single ion evolution profiles of selected products detected during the pyrolysis of Pb3c2.

Polymerization of benzoxazine monomers based on aniline may proceed through various reaction paths; the heterocyclic ring opening followed by attack of -NCH_2 groups to *ortho* and *para* positions of phenol and aniline rings is accepted as the main polymerization path in the literature [24]. In case of benzoxazine based on aminobenzonitrile, being a bulky o, p- director and a bulky electrophile, para substitution predominates. Actually, presence of nitrile at meta position to N atom deactivates substitution to both ortho and para positions of the aniline ring. However, the activating effect of amine group predominates the deactivating effect of nitrile group and thus polymerization may proceed as shown in Scheme 3.11 to a certain extent. In addition, the dimer generated by the coupling of -NCH_2 groups may polymerize via attack of -NCH_2 groups to phenol and/or benzonitrile rings or through vinyl polymerization yielding **P31**, **P32** and **P4** as presented in Scheme 3.12.

Scheme 3.11 Ring-opening polymerizations of benzoxazines.

a) by attack to phenyl ring

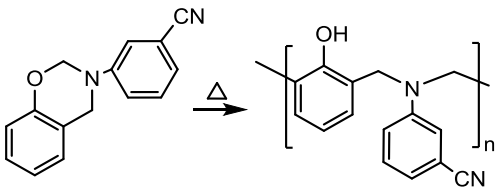

P1

b) by attack to benzonitrile ring

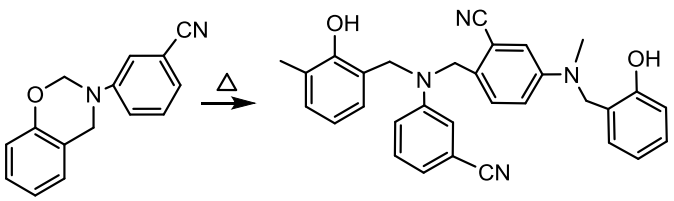

P2

Scheme 3.12

a) Generation of the dimer by coupling of $-NCH_2$ groups

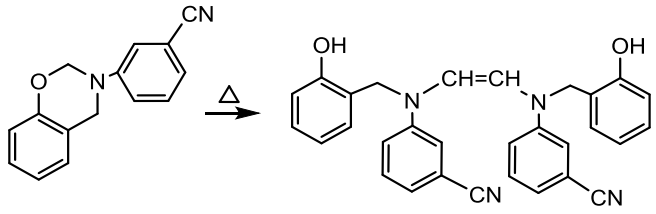

b) polymerization of the dimer

i) by attack of NCH_2 groups

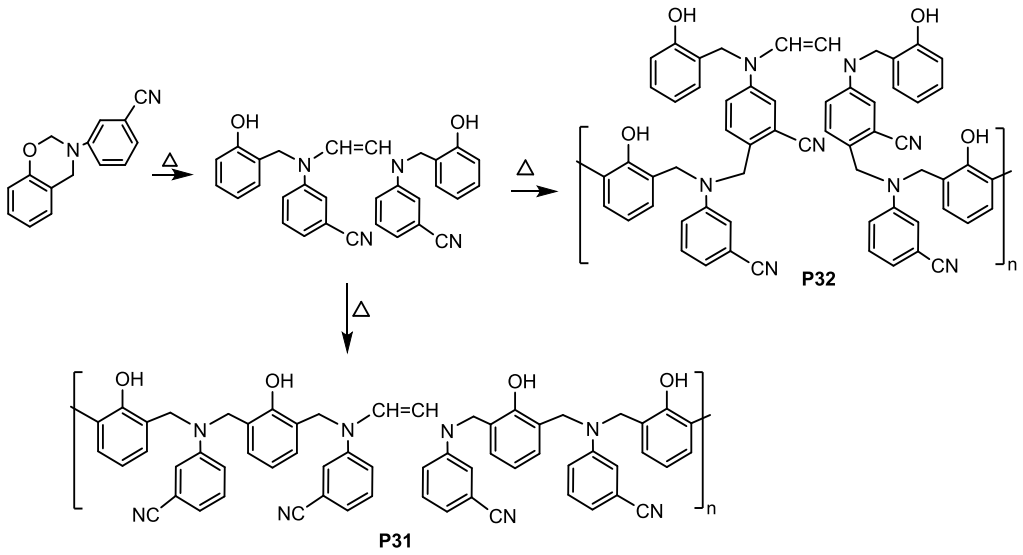

ii) by vinyl polymerization

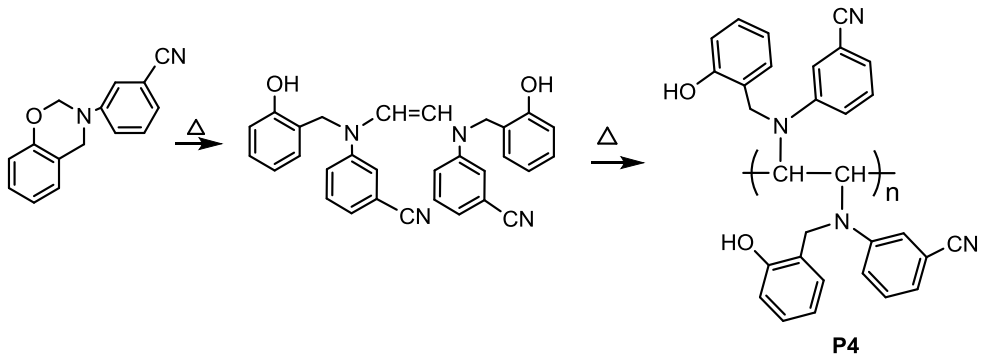

The detection of $HO_6H_5CH_2NC_6H_4CN$ (222 Da) in the mass spectra of Pa3 and Pb3 at low temperature regions, can be related to evolution of monomer in accordance with the incomplete polymerization indicated by DSC analyses. It may also be due to the decomposition of the low mass oligomers or chains that do not involve crosslinking units.

Generally, thermal degradation of polybenzoxazines starts with the evolution of amine groups. The evolution of major thermal decomposition product aminobenzonitrile, $CNC_6H_4NH_2$ (118 Da) is detected at around 294°C. Its evolution is detected over a broad temperature range, reaching maximum yield also at around 418 °C as do 91 Da and is completed just above 450°C. The fragments evolve at around 294 °C are mainly the characteristic fragments of aminobenzonitrile and substituted aminobenzonitriles such as $NH_2C_6H_4CN$ (118 Da), $NH_2C_6H_3$ and/or C_7H_7 (91 Da), $NCH_2C_6H_4CN$ (130 Da) and $NH_2C_6H_4CNCH_2NH$ (146 Da). In contrast, the loss of 91 Da fragment is also observed at elevated temperatures; two overlapping peaks with maxima at around 418 and 576 °C are present in its pyrogram.

The decomposition of P1 and P2 chains may also proceed via random cleavages at the *β*-carbon to phenol or nitrogen atom yielding low-mass fragments such as HOC_6H_4 (93 Da), HOC_6H_5 (94 Da), $NH_2CH_2C_6H_4NH_2$ (122 Da) and $C_6H_5OHCH_2$ (107 Da) as in the case of the EI dissociation of the monomer and dimer [R]. The peaks at around 420, 440, 550 and 576 °C in the evolution profiles of these species may be associated with random chain cleavages of **P1**, **P2**, **P31** and **P32**. The broad peak in their evolution profiles may be associated with extensive loss of these fragments from chains involving different extents of crosslinking.

HCN evolution starts at above 400 °C, reaches maximum yield at around 450 °C. The fragments showing maximum at this temperature region in their evolution profiles such as $NHC_6H_3CH{=}CHNH_2$ and/or $H_2N(C_6H_3CN)CH_3$ (132 Da) and $HOC_6H_3CH_2NC_6H_3$ and/or $HOC_6H_4CH{=}CHC_6H_4$ (195 Da) are mainly the ones that can be generated by elimination of HCN from the polymer chains P1, P2, P31 and P32.

It may be proposed that the radicals generated upon loss of aniline and substituted aniline dimers from P1, P2, P31 and P32 at initial stages of pyrolysis and/or during curing may couple to produce an unsaturated polymer backbone (Scheme 3.12). The detection of fragments presumably assigned to $C_6H_5CH{=}CHC_6H_4$ (179 Da), $C_6H_5CH{=}CHC_6H_4CH_2$ (193 Da), $HOC_6H_4CH{=}CHC_6H_4$ and/or $C_6H_4CH_2NHC_6H_4CH_2$ (195 Da) and C_6H_5OH (94 Da) at around 550 °C supports this proposal.

And finally, the evolution of $C_6H_5CH_2$ at slightly higher temperatures, at around 576 °C may be associated with chains with highly crosslinked structures.

In Fig.3.33, the pyrograms of aminobenzonitrile (118 Da), $NCH_2C_6H_4CN$ (130 Da) and $NH_2C_6H_4CNCH_2NH$ (146 Da) and $NH_2C_6H_3$ and/or C_7H_7 (91 Da) that mainly evolved at initial stages of pyrolysis of the samples prepared by different curing programs are shown.

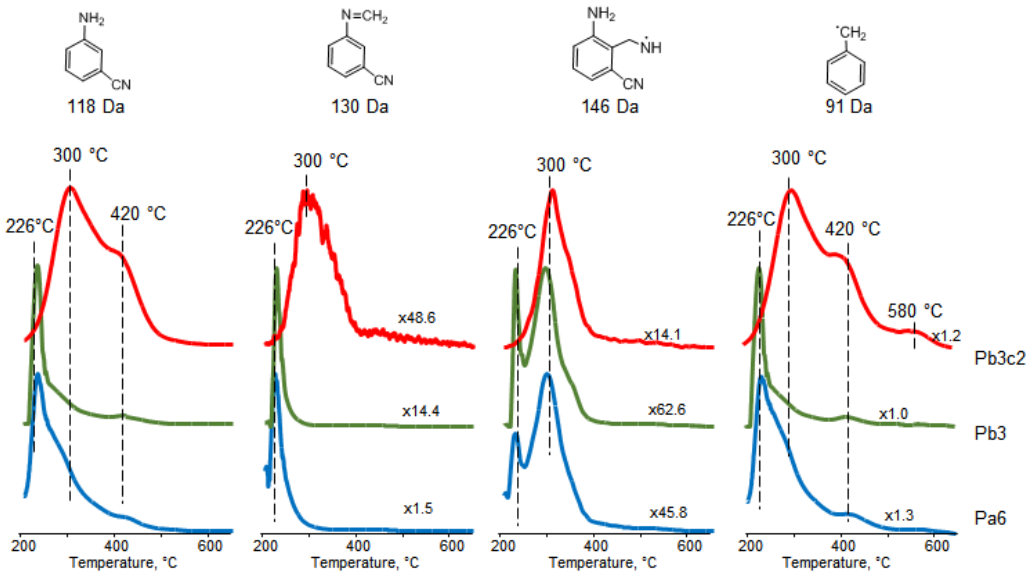

Figure 3.33 Single ion evolution profiles of some selected products detected during the pyrolysis of PPh-abn prepared by different curing programs

As the curing temperature was increased, the low temperature peaks with a maximum at around 226°C in the single ion evolution profiles of aminobenzonitrile and methyleneaminobenzonitrile (130 Da) which are characteristic fragments of the monomer generated during ionization inside the mass spectrometer, are disappeared detected during the pyrolysis of the polymer. On the other hand, the evolution of aminobenzonitrile is increased significantly at around 300 and 420 °C, in the temperature regions where no monomer evolution is detected, pointing out that it is mainly produced during the thermal decomposition of the polymer chains formed. The limited amount of aminobenzonitrile and methyleneaminobenzonitrile (130 Da) lost at moderate and high temperature regions during the pyrolysis of Pa6 and Pb3, reveals generation of negligible amounts of polymer chains with higher thermal stability by the curing programs applied for these samples. Unlike aminobenzonitrile, the relative yield of methyleneaminobenzonitrile (130 Da) lost at moderate and elevated temperatures is quite low, for Pb3c2 indicating that it is mainly produced during the ionization of the monomer inside the mass spectrometer not by degradation of the polymer. On the contrary, the evolution of $NH_2C_6H_4CNCH_2NH$ (146 Da) due to the thermal degradation of polymer chains P2 at around 300 °C was increased. The evolution of $C_6H_5CH_2$ (91 Da), is detected in three regions, at around 300, 420 and 580 °C. $C_6H_5CH_2$ (91 Da) is a common fragment detected at elevated temperatures during the pyrolysis of polybenzoxazines with crosslink structure. Its relative intensity at around 420 and 580 °C is increased noticeably for Pb3c2, pointing out the increase in crosslink structure.

In Fig.3.34, the pyrograms of phenol (94 Da), $C_6H_5OHCH_2$ (107 Da), $H_2N(C_6H_3CN)CH_3$ and/or $NHC_6H_3CH=CHNH_2$ (132 Da) and $C_6H_5CH=CHC_6H_4$ and/or $C_6H_4CH=NC_6H_4$ (179 Da) that mainly evolved at final stages of pyrolysis of the samples prepared by different curing programs are shown.

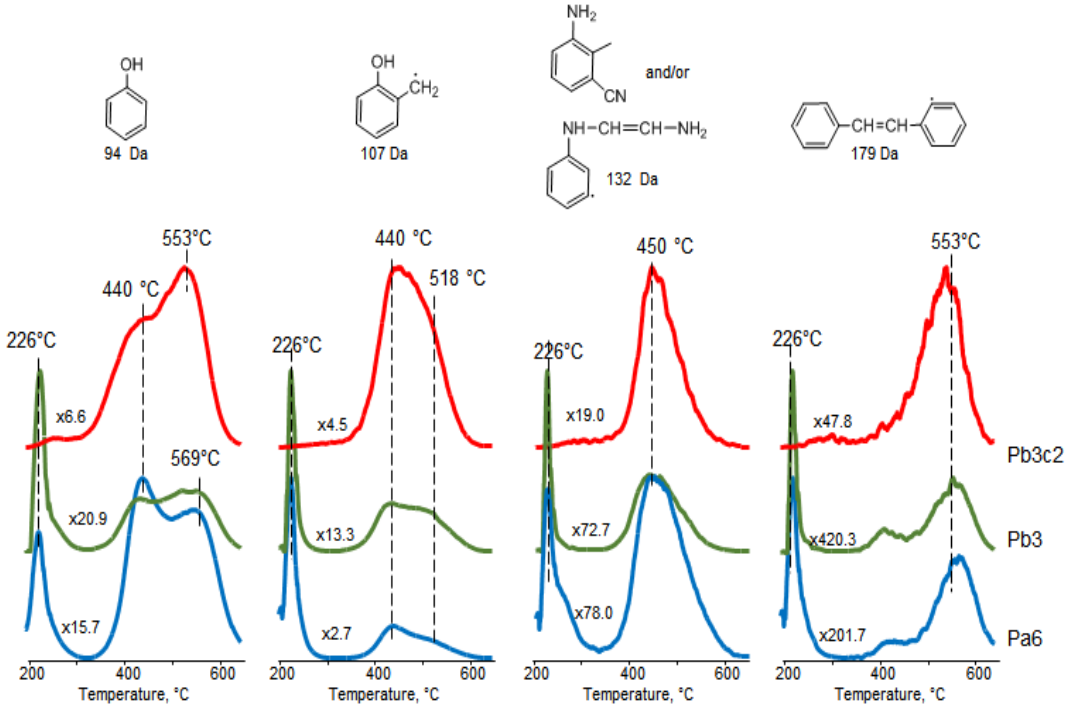

Figure 3.34 Single ion evolution profiles of some selected products detected during the pyrolysis of PPh-abn prepared by different curing programs

Phenol is one of the common fragments that can be generated through all polymeric structures. The evolutions of C_6H_5OH (94 Da) and $C_6H_5OHCH_2$ (107 Da) also occur during the ionization of the monomer. The high intensity of these fragments for Pa6 is due to the ionization of the unreacted monomer inside the mass spectrometer. The evolution of 94 and 107 Da are reduced noticeably below 400 °C during the pyrolysis of Pb3c2, whereas, its relative yield at around 440 °C is increased significantly. Yet, the evolution of phenol at elevated temperatures at around 570 °C is shifted to 550 °C for Pb3c2.

The evolution of $C_6H_5CH{=}CHC_6H_4$ and/or $C_6H_4CH{=}NC_6H_4$ (179 Da) is predominantly detected at elevated temperatures above 500°C during the pyrolysis of all polymers. The low temperature peak for Pa6 and Pb3 can be related to the unreacted monomer and low mass oligomers. As the temperature and duration of

curing was increased, the relative yield is increased noticeably and its single ion pyrogram shifts to lower temperature regions.

The fragment with m/z value 132 Da tentatively assigned to methyl substituted aminobenzonitrile $NHC_6H_3CH{=}CHNH_2$ and/or $H_2N(C_6H_3CN)CH_3$ is also lost mainly at around 450°C as does 107 Da fragment.

Thus, it can be concluded that thermal degradation of polybenzoxazine based on aminobenzonitrile also starts by elimination of amino groups as in case of polybenzoxazines based on aniline and nitroaniline at around 300°C. Coupling of the radicals generated yields thermally stable polymer chains involving unsaturated linkages that decompose at elevated temperatures (Scheme 3.12). No evidence for polymerization via coupling of NCH_2 groups, (P31 and P32) is detected as in case of polybenzoxazine based on nitroaniline. On the other hand, as deactivating effect of CN group is less than that of $-NO_2$, and as the para position is available in meta-aminobenzonitrile, unlike para-nitroaniline, polymerization via attack of NCH_2 groups to aniline ring, P2 also takes place, that decomposes mainly by random cleavages yielding products such as $H_2N(C_6H_3CN)CH_3$ and $HOC_6H_4CH_2$ at around 450 °C, as loss of aminobenzonitrile is not possible.

3.1.4. Benzoxazine monomer based on 2-aminopyridine, Ph-ap

Benzoxazine monomer was synthesized from phenol, 2-aminopyridine and paraformaldehyde via solventless method (Scheme 3.13).

Scheme 3.13 Synthesis of benzoxazine monomer based on phenol and 2-aminopyridine

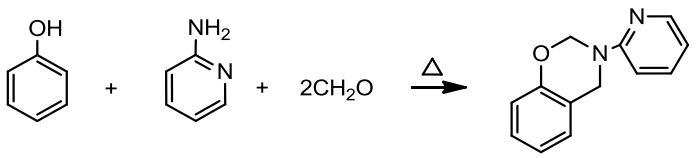

The proton NMR spectrum of the neat benzoxazine is presented in Fig.3.35. The strong resonances at 4.88 and 5.61 ppm correspond to the methylene protons (C1 and C2) of Ar-CH_2-N and O-CH_2-N of the oxazine ring, respectively. The resonance signals (labeled 3 and 4) in the range of 6.90–7.54 ppm are typical region for the phenyl ring. In addition, the signals at around 6.71, 7.53 and 8.35 ppm (labeled 5, 6 and 7 respectively) are attributed to the protons of the pyridyl ring. The resonances at 46.24 and 75.25 ppm correspond to the methylene carbons (C1 and C2) of Ar-CH_2-N and O-CH_2-N of the oxazine ring, respectively. Other chemical shifts (ppm) are assigned to the resonances of the carbons: 108.0 (C10), 115.0 (C7), 117.22 (C12), 121.0 (C5, C3), 126.69 (C6), 127.78 (C4), 137.95 (C11), 148.21(C13), 154.52 (C9), 157.58 (C8). Anal. calcd. for C13H12N2O: C, 73.58; H, 5.66; N, 13.21; O,7.67%. Found: C, 72.46; H, 5.85; N, 13.29%.

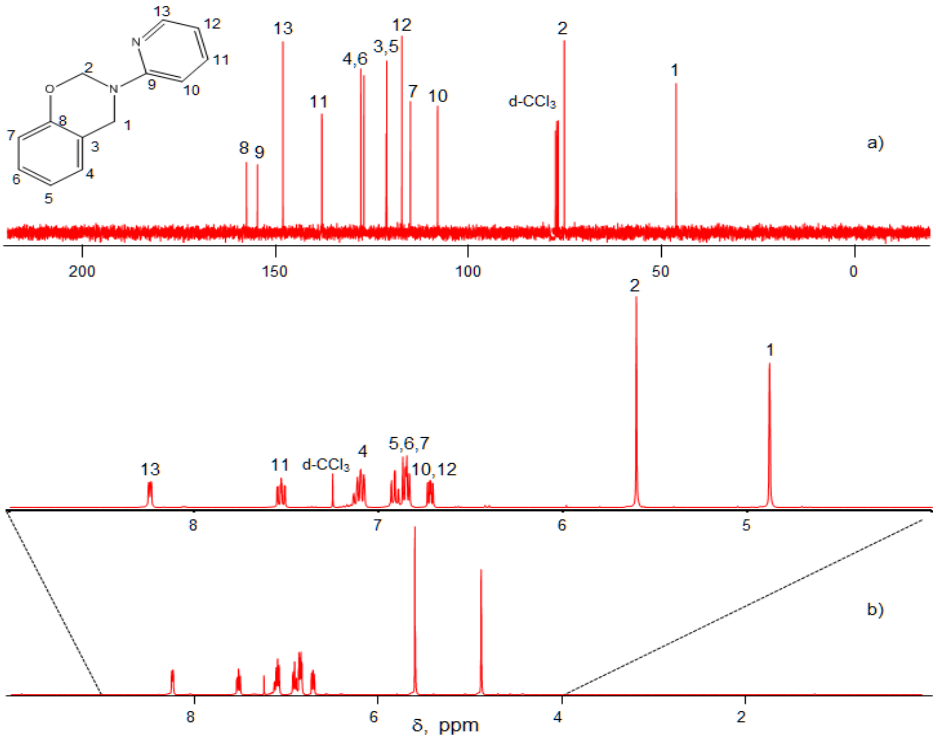

Figure 3.35 a) 13C NMR and b) proton NMR spectra of benzoxazine monomer.

The DSC profiles of the monomer and polybenzoxazine are shown in Fig.3.36a and b. The pure monomer mainly exhibits a single exothermic peak with an onset at 225 ˚C and a maximum at 262 ˚C, corresponding to ring-opening polymerization. The disappearance of this peak in the DSC curves of the sample prepared by curing confirmed polymerization of Ph-ap monomer.

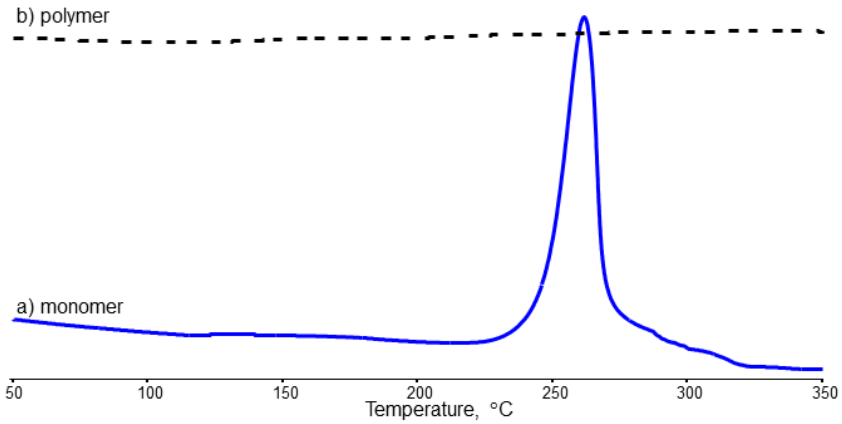

Figure 3.36 DSC profiles of monomer and polymer based on aminopyridine.

The FTIR spectra of the benzoxazine monomer and the polymer are shown in Fig.3.37. Typical absorption bands for the benzoxazine monomer are observed at 1480, 1380, 1230, 1033 and 946 cm^{-1}, corresponding to the di-substituted benzene rings, CH_2 wagging, Ar-O-C antisymmetric stretching, C-O-C symmetric stretching and vibration modes of cyclic substituted benzene rings, respectively. The absorptions at 1597, 1584 and 1564 cm^{-1} are assigned to the C-H stretching vibrations and the ones at 1436 and 947 cm^{-1} are associated to C=N and C-N stretching vibrations of the pyridine ring. The absorption bands of the oxazine ring at 1380, and 946 cm^{-1} are totally vanished in the FTIR spectrum of polybenzoxazine (Fig.3.37b). Furthermore, bands due to di-substituted benzene and pyridine rings are decreased or totally disappeared, indicating that polymerization is proceeded via ring opening of the benzoxazine ring followed by attack of NCH_2 groups to both phenyl and pyridyl rings.

Significant broadening of the absorption bands is in accordance with the cross-linked structure generated due to competing and parallel polymerization processes.

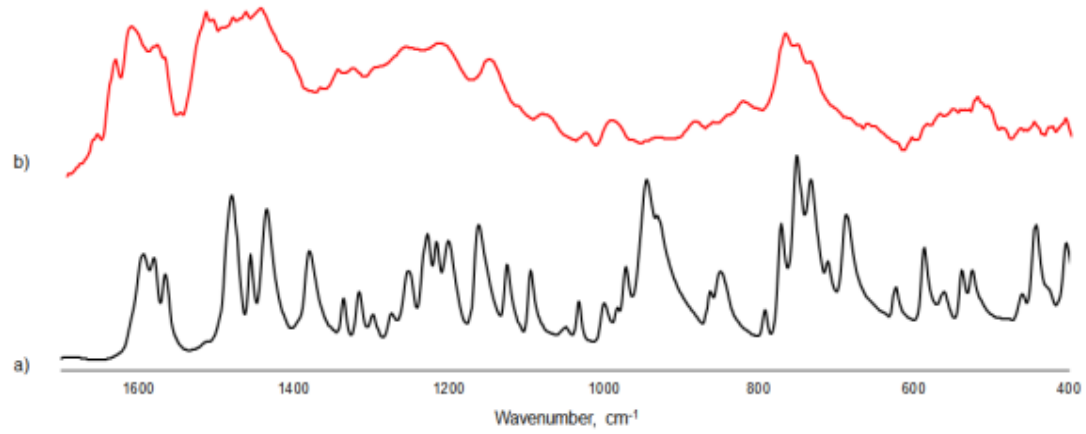

Figure 3.37 FTIR spectra of a) benzoxazine monomer and b) polybenzoxazine

To determine the thermal characteristics of the polymers generated were analyzed by TGA and DP-MS techniques. The TGA curve of the polymer is shown in Fig.3.38

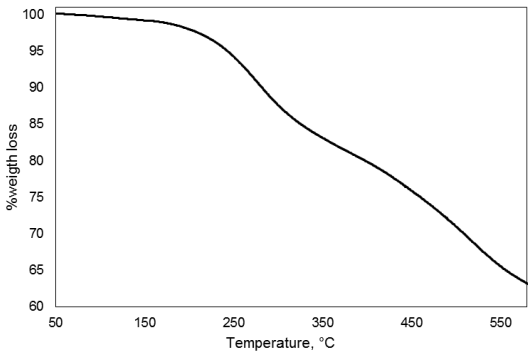

Figure 3.38 TGA curve of polybenzoxazine based on aminopyridine

TGA curve indicates multi-step weight loses. This behavior may either be due to a multi-step thermal degradation or a polymer sample involving chains with different structures, thus, different thermal stabilities. The char yield is %63.2 at 600 °C.

TIC curve and the spectra at the peak maxima at around 307, 469 and 547°C recorded during the pyrolysis pf PPh-2ap are shown in Fig.3.39.

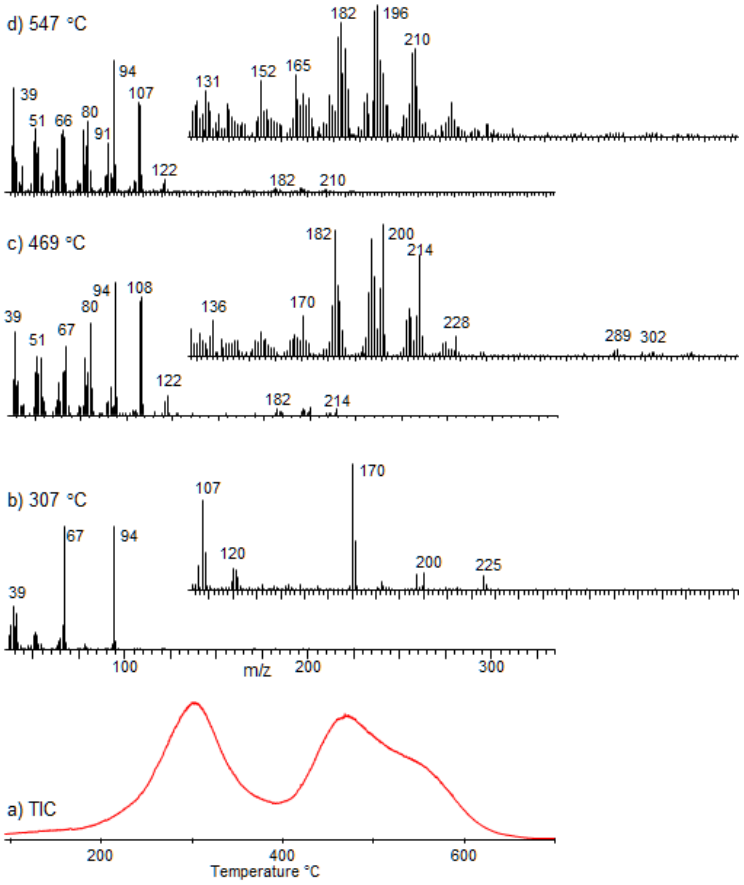

Figure 3.39 TIC curve and the spectra at the maxima recorded during the pyrolysis of PPh-2ap

The pyrolysis mass spectra recorded just above 300 °C of the neat polybenzoxazine show only few peaks. The presence of more than one peak in the TGA and TIC curves may be due to a multi-step thermal degradation mechanism or presence of chains with different thermal stability and/or structure. Actually, polymerization of 2-

aminopyridine based benzoxazine monomer may proceed through various reaction paths; the heterocyclic ring opening may be followed by attack of -NCH_2 groups to ortho and para positions of phenol and pyridine rings as shown in Scheme 3.14, generating P1 and P2 respectively [24]. In addition, the dimer generated by the coupling of -NCH_2 groups may polymerize via attack of -NCH_2 groups to phenol and/or pyridine rings or through vinyl polymerization yielding P31, P32 and P4 as presented in Scheme 3.15. As a consequence of these competing reaction pathways, generation of a cross-linked structure is expected.

Scheme 3.14 Ring-opening polymerizations of benzoxazines.

a) by attack to phenyl ring

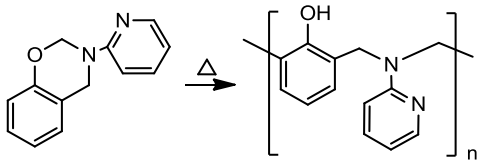

P1

b) by attack to pyridyl ring

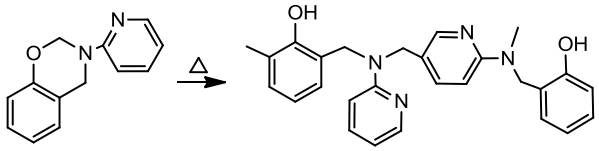

P2

Scheme 3.15

a) Generation of the dimer by coupling of –NCH_2 groups

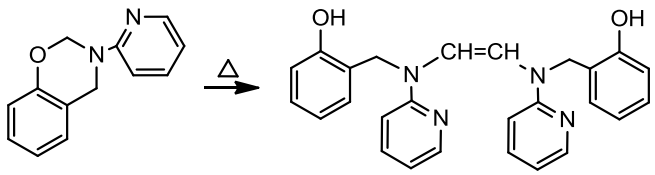

b) polymerization of the dimer

i) by attack of NCH_2 groups

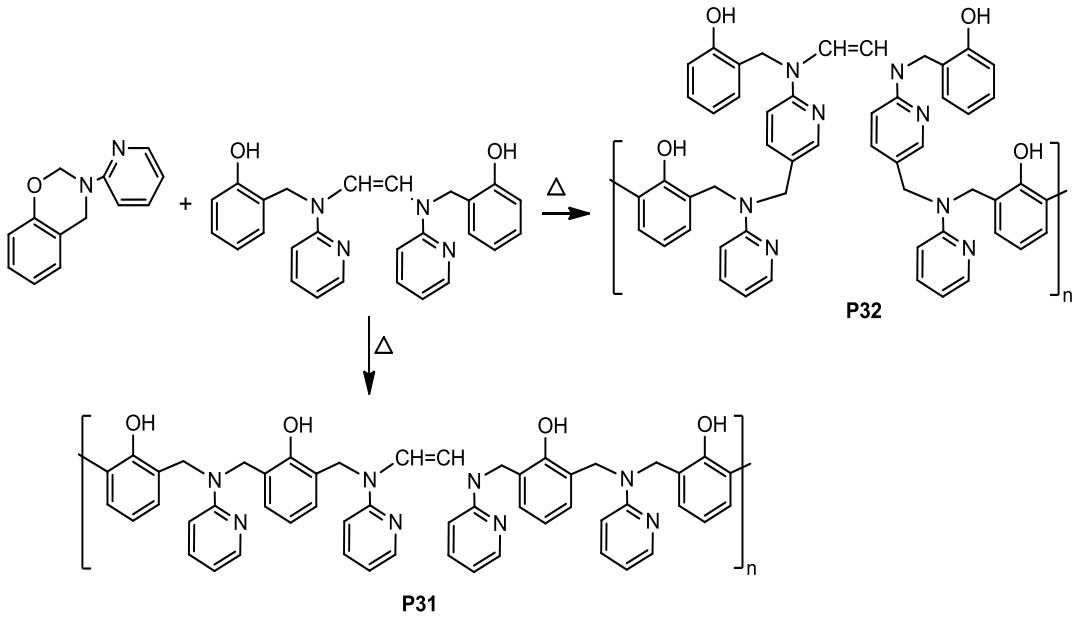

ii) by vinyl polymerization

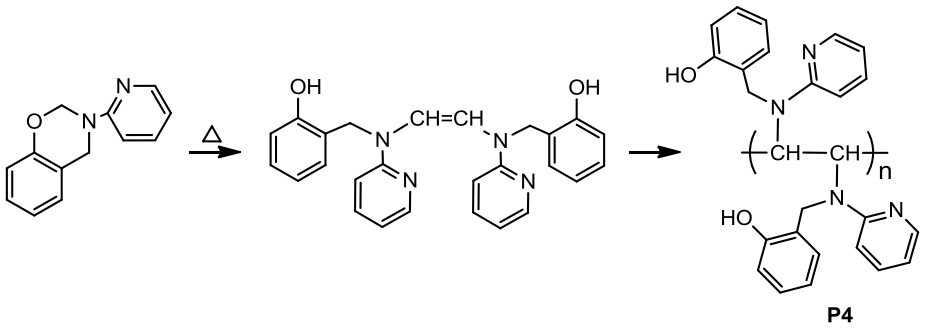

P4

In Fig.3.40, the single ion pyrograms of dominant fragment ions grouped according to the trends in their evolution profiles are given. The most abundant product is the one with m/z value 94 Da that may be associated with elimination of aminopyridine and/or phenol. The fragmentation patterns recorded in the low temperature pyrolysis mass spectra reveal that the first steps of thermal degradation involve loss of aminopyridine, $H_2NC_5H_4N$. Its evolution is continued at elevated temperatures, however, elimination of phenol at least at elevated temperatures cannot be totally excluded.

Losses of several fragments are detected in the temperature region of 400-500°C during the pyrolysis of the neat polybenzoxazine. The peak maxima in their single ion pyrograms show slight differences and either a high temperature peak or a shoulder is also present in their evolution profiles. These products can be grouped according to the trends in their evolution profiles. Fragments with m/z values 79, 107 and 122 Da, show a broad peak with a maximum at 472°C and a shoulder at around 557°C. The evolution profiles of second group of products with m/z values 225, 197, 210 and 181 Da, show a peak at around 462°C and either a shoulder or a peak at around 557°C. The yield of products with m/z values 120 and 44 Da also show overlapping peaks with maxima at 462 and 557 °C, but, for these fragments the relative intensity of the high temperature is higher. The last group of products involves 91 and 92 Da fragments which show two overlapping peaks with maxima at 462 and 574°C.

In order to elucidate the structures of these products, collision induced dissociation, CID, experiments were acquired at different collision energies to provide fragmentation pathways to generate informative, structurally significant daughter ions. For most of the fragments evolved in the temperature range 400-500°C during the pyrolysis of neat polybenzoxazine, daughter spectra cannot be recorded even at low energies, due to the low abundances.

Taking into account the trends in the evolution profiles, it may be suggested that the polymer segments generated by attack of NCH_2 groups to phenol ring decomposes by elimination of aminopyridine at initial stages of pyrolysis (Scheme 3.14a). The radicals generated may combine to form unsaturated linkages as shown in Scheme 3.16. These units are expected to decompose at elevated temperatures at around 573 °C. On the other hand the evolution of fragments at around 518 °C are related to decomposition of units generated via attack of NCH_2 groups to pyridine rings (Scheme 3.14b).

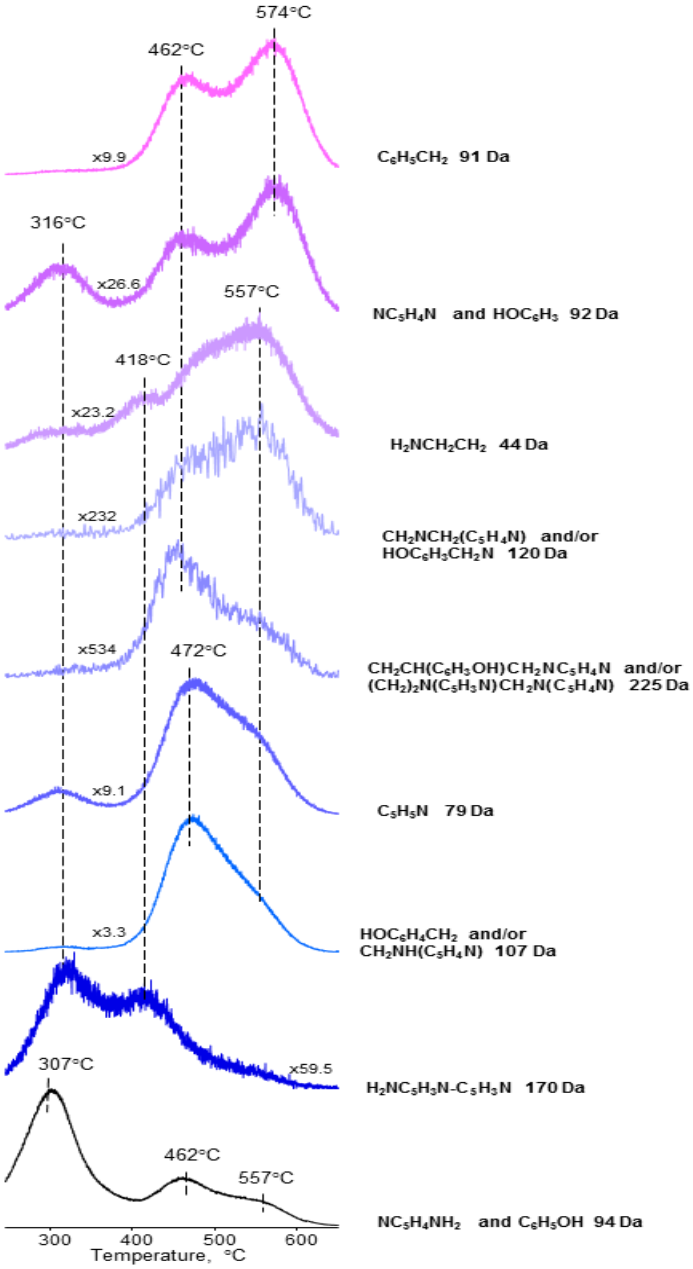

Figure 3.40 Single ion pyrograms of selected products recorded during the pyrolysis of PPh-2ap

Scheme 3.16 Loss of 2-aminopyridine during the pyrolysis of polybenzoxazine

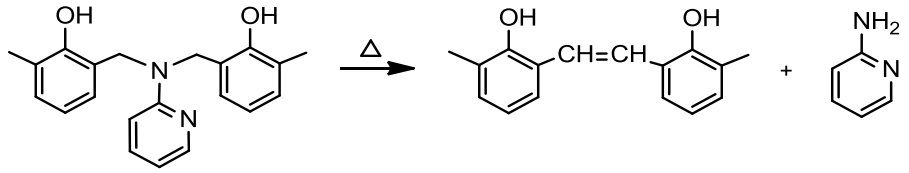

3.2. Metal functional polybenzoxazines

3.2.1. Benzoxazine based on aminopyridine, Ph-ap

3.2.1.1. Co^{2+}-functional PPh-ap

In Fig.3.41 the FTIR spectra of benzoxazine monomer, Ph-ap, and Co^{2+} functional benzoxazine monomer, Co^{2+}-Ph-ap are depicted. The intensities of the peaks due to pyridine stretching and bending modes at 1597, 1436 and 947 cm^{-1} are decreased relative to the absorption bands of phenyl ring in the FTIR spectra of Co^{2+} functional benzoxazines supporting the coordination of the metal ion to the electron-rich segment of the benzoxazine monomers, the nitrogen atom in the pyridine rings (Fig. 3.41b) i and ii). The decrease becomes more significant as the Co^{2+}/monomer mole ratio increases. Apparently, peak broadening as a consequence of coordination to metal ion is noted.

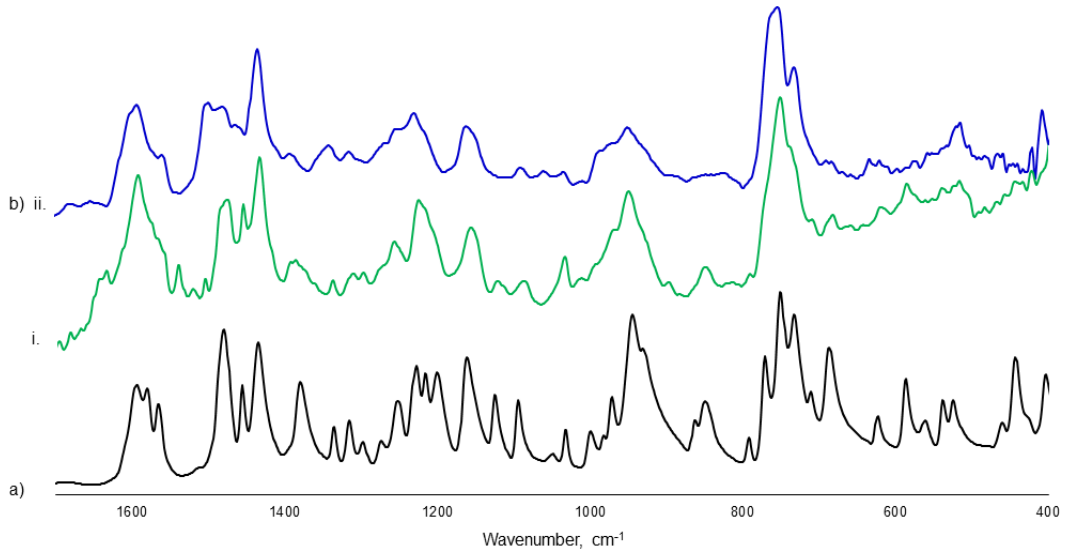

Figure 3.41 FTIR Spectra of a) benzoxazine monomer based on aminopyridine, PPh-ap and b) Co^{2+} functional polybenzoxazine based on aminopyridine, Co^{2+}-PPh-ap

Curing of Co^{2+} functional Benzoxazine Monomers

Preliminary curing of the neat and Co^{2+} functional monomers were achieved inside the mass spectrometer in order to gain better insight on the processes taking place. In Fig.3.42, total ion current, (TIC) curve, the variation of total ion yield as a function of time, and the mass spectrum at the maximum of the peak present in the TIC curve recorded during the curing of neat benzoxazine monomer is presented.

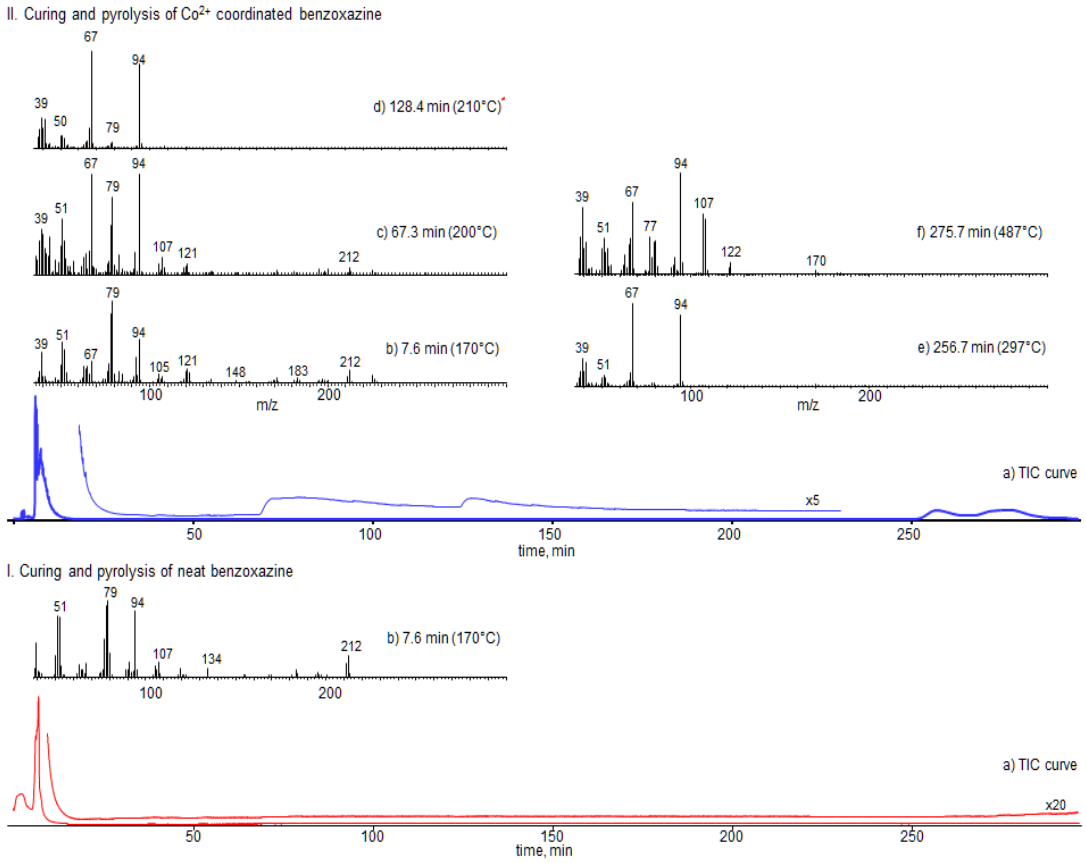

Figure 3.42 a) TIC curves and b) the mass spectra recorded during the curing and pyrolysis of I. neat and II. Co^{2+} functional benzoxazines.

Almost all the monomer was lost under the high vacuum conditions of the mass spectrometer, due to extensive evaporation at around 170°C. The extent of evaporation of the monomer was reduced noticeably during the curing of the Co^{2+} functional monomers suggesting that incorporation of metal ions successfully stabilize the monomer. As an example, the TIC curve for Co^{2+} functional benzoxazine prepared by using equal moles of Co^{2+} and monomer is given in Fig.3.42. Indeed, though diminished, the mass spectra recorded up to 200°C, reveal the evaporation of the monomer for this sample also. Furthermore, strong evidences for eliminations of pyridine and aminopyridine at around 200 and 210°C are detected in the mass spectra. It is worth nothing that, upon further heating the sample to 650°C after the curing cycle was completed, release of fragments indicating the degradation

of the polymer was detected. Thus, it may be concluded that polymerization of Co^{2+} functional benzoxazine was achieved even under the high vacuum conditions of the mass spectrometer.

Unfortunately, the FTIR spectrum of Co^{2+} functional polymer is not informative due to the significant broadening of the peaks as a result of metal ion coordination. However, SEM images of Co^{2+} functional polybenzoxazine confirm presence of composite particles as shown in Fig.3.43.

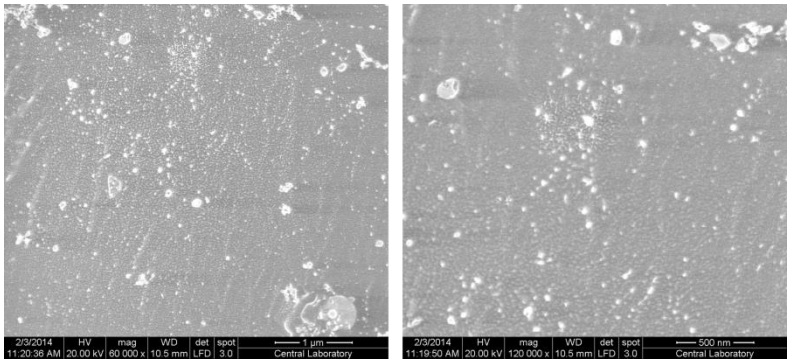

Figure 3.43 SEM images of Co^{2+} functional polybenzoxazine (Co^{2+}:M=1:1)

The TGA curve of Co^{2+}-functional PPh-ap shows almost identical trends with the neat PPh-ap (Fig.3.44). T_{max} is at 276°C and the % char yield at 600°C is 62.4, almost same with PPh-ap. However, as the sample contains 17.2% Co^{2+}, it is clear that % char yield is reduced upon coordination to metal ion.

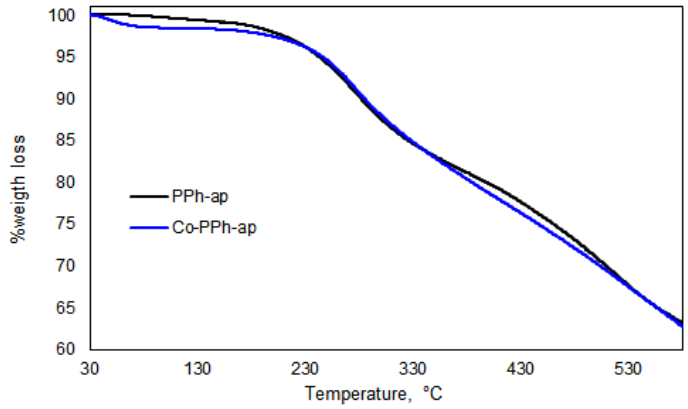

Figure 3.44 TGA curve for neat PPh-ap and Co^{2+}-functional PPh-ap

The TIC curves of Co^{2+} (Co^{2+}:M=1.0) coordinated polybenzoxazines are shown in Fig.3.45. Two peaks with maxima at around 306 and 525°C are present in the TIC curve of the metal ion coordinated sample. The trends in the TGA curves are similar, indicating three and two step-weight loses for neat and metal ion functional polymers respectively. The trends in TGA and TIC curves, and the very high char yield are in accordance with the expectations confirming the heterogeneous and cross-linked polymer structures.

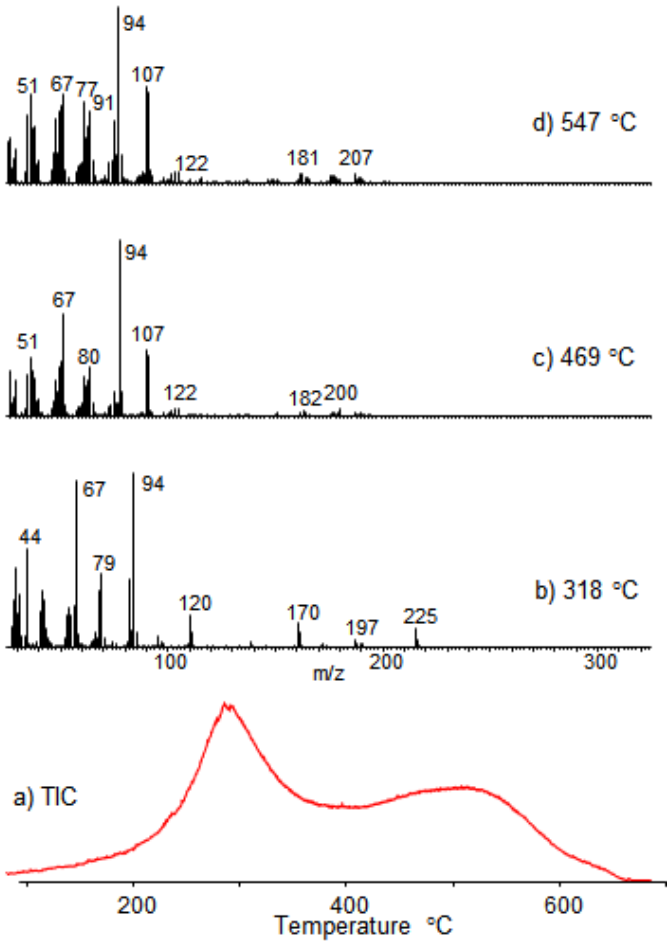

Figure 3.45 a)TIC curve and pyrolysis mass spectra at b)318, c) 469 and d) 547°C of Co^{2+} functional polybenzoxazines

The pyrolysis mass spectra recorded just above 300 °C of Co^{2+} functional polymer are more crowded and contain also high mass peaks. The high temperature pyrolysis mass spectra of metal ion functional polymer involve similar peaks with the neat polymer. Yet, noticeable differences in their relative intensities are recorded.

In Fig.3.46, the single ion pyrograms of dominant fragment ions of Co^{2+} functional PPh-ap grouped according to the trends in their evolution profiles are given. The corresponding ones recorded during the pyrolysis of neat polymer are also included for comparison.

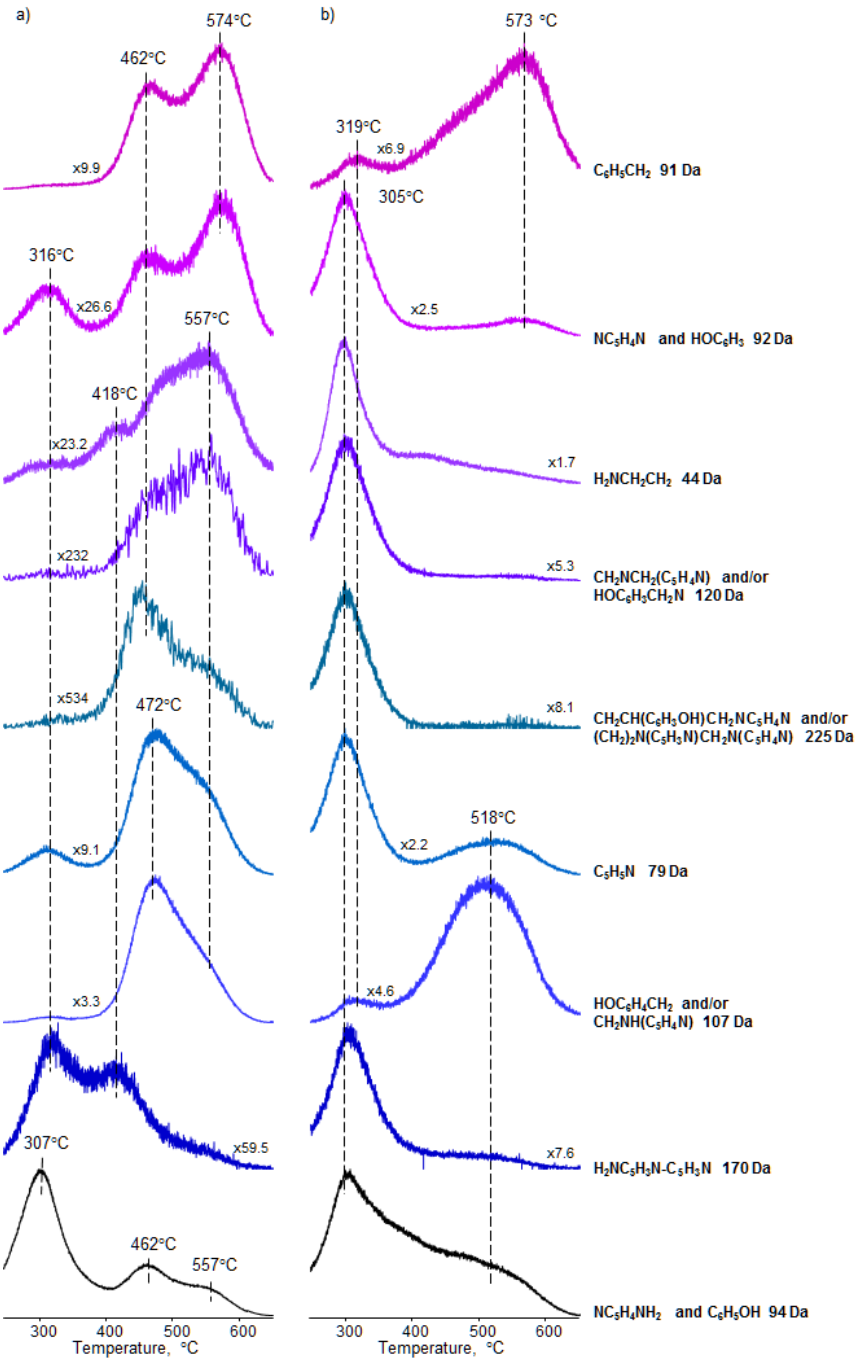

Figure 3.46 Single ion pyrograms of selected products recorded during the pyrolysis of a) neat and b)Co^{2+} functional polybenzoxazines

The peaks in the temperature range of 400-500°C are totally disappeared during the pyrolysis of the polymer coordinated to Co^{2+}. The products with m/z values 44, 79, 92, 120, 197 and 225 Da evolved almost exclusively at initial stages of pyrolysis, and their relative yields are increased drastically. In contrast, only limited amounts of products with m/z values 91, 107, 122, 107, 181 and 210 Da, are lost at initial stages. Their evolution profiles show a broad and intense peak above 500 °C and a weak peak at around 306°C. Among these products 44, 79 and 91 Da fragments can readily be assigned to $C_2H_4NH_2$, C_5H_4N and $C_6H_5CH_2$ respectively. On the other hand, for the rest of the products at least two different structures can be assigned.

Some of the fragments lost at initial stages of pyrolysis of Co^{2+} functional analogue, are quite abundant, contrary due the ones recorded during the pyrolysis of neat polymer. However, it may be thought that these fragments have the same structure with those evolved during the pyrolysis of neat polymer. Eventually, CID experiments were performed at the temperatures where precursor ions are generated with sufficient abundances, during the pyrolysis of either from the neat polymer or Co^{2+} coordinated analogue. In Fig.3.47, the daughter spectra of the precursor ion with m/z value 107 Da, generated at 470°C during the pyrolysis of the neat polymer, and those of the ions with m/z values 225, 170, 120, and 94 Da generated at 300 °C during the pyrolysis of Co^{2+} functional polybenzoxazine are given. The assignments done considering the pyrolysis mass spectra, the trends in the evolution profiles and CID spectra indicate that thermal degradation of aminopyridine based polybenzoxazine starts with extensive loss of aminopyridine. However, elimination of phenol ring in this region cannot be justified. Thus, it may be thought that upon loss of aminopyridine polymer chains with unsaturated linkages are generated as shown in Scheme 3.16. Thermal degradation of the unsaturated and/or cross-linked polymer backbone should produce various fragments involving H deficiency at relatively high temperatures. The products released at elevated temperatures such as C_7H_7 and HOC_6H_3 can be correlated with decomposition of the polymer chains generated upon loss of aminopyridine. Evolution of products that can be associated with decomposition of chains generated by attack of NCH_2 groups to phenol and pyridine rings (**P1** and **P2**)

are detected in the temperature range of 400-500°C. The slight variations in the peak maxima can be attributed to extent of crosslinking. In this region, the main products are $HOC_6H_4CH_2$ and C_5H_4N indicating degradation of the polymer backbone.

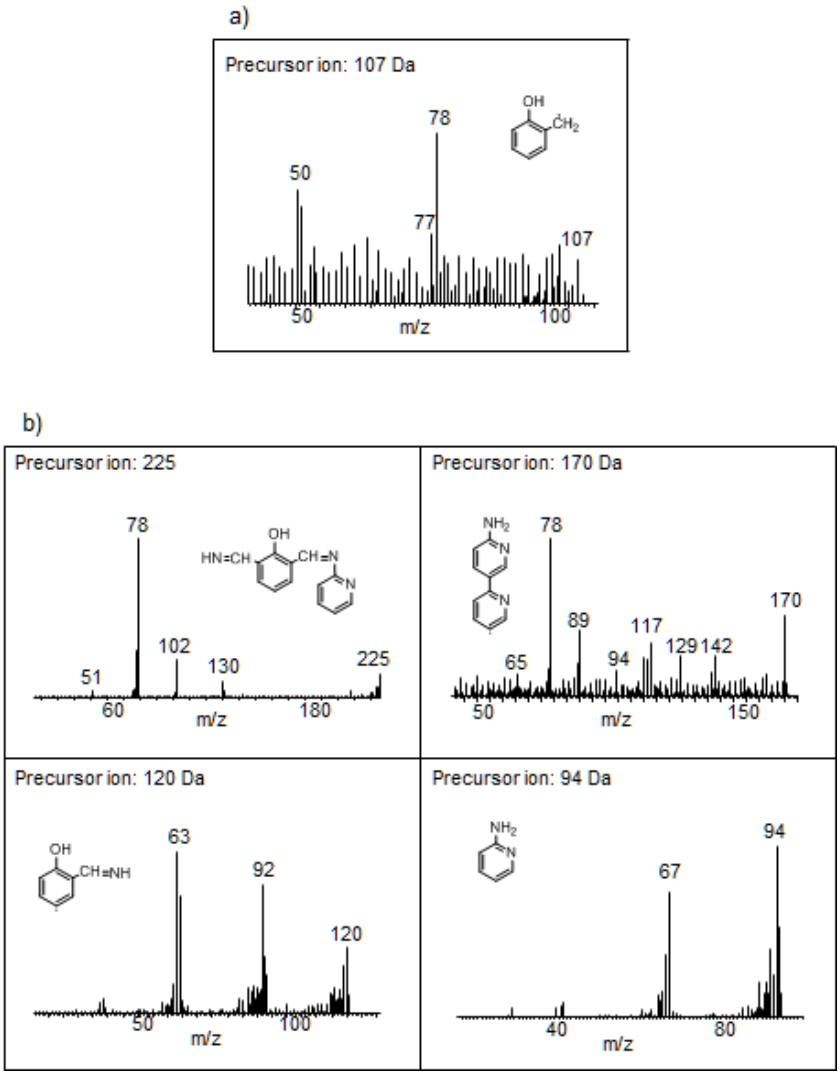

Figure 3.47 CID spectra of a) the precursor ion with m/z value 107 Da, generated at 470°C during the pyrolysis of the neat polymer and b) the precursor ions with m/z values 225, 170, 120, and 94 Da generated at 300 °C during the pyrolysis of Co^{2+} functional polybenzoxazines

It may be thought that upon coordination to metal ion, the side chains become bulkier and the reaction pathways involving loss of side chains become energetically

favorable. Eventually, pyridine ring and/or segments involving pyridine ring are lost at initial stages of pyrolysis and unsaturated units along the main chain can be formed (Scheme 3.17). On the other hand, it may further be thought that coordination of Co^{2+} to pyridine ring inhibits the attack of NCH_2 groups to pyridine ring due to steric hindrance. This in turn should decrease the extent of crosslinking.

Scheme 3.17 Loss of aminopyridine and pyridine during the pyrolysis of Co^{2+} functional polybenzoxazine

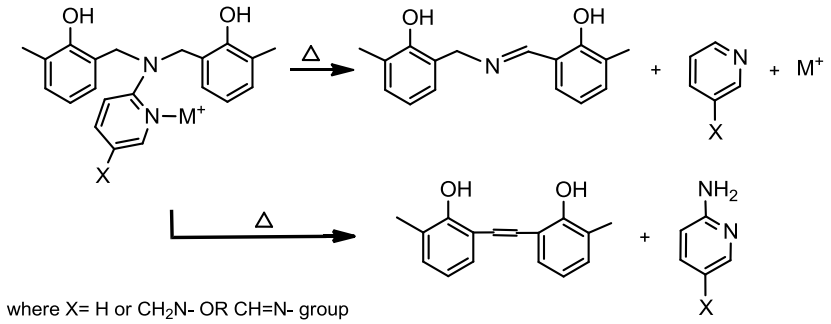

Single ion evolution profiles of pyridine, aminopyridine and monomer recorded during the curing of the neat and Co^{2+} functional benzoxazine monomers (Co^{2+}: monomer mole ratios were 0.5, 1.0 and 2.0) are given in Fig. 3.48. It is clear that the increase in the amount of Co^{2+} present in the sample reduces the relative yield of the monomer evolved and enhances that of the pyridine during the curing process. Actually, the decrease in the extent of monomer evaporation may be associated with the decrease in the amount of uncoordinated monomer left in the sample and the increase in the boiling point of the monomer upon coordination to Co^{2+}. On the other hand, it may be thought that as a consequence of coordination of Co^{2+} to nitrogen atom of the pyridine ring, the side chains being bulkier can be eliminated more readily.

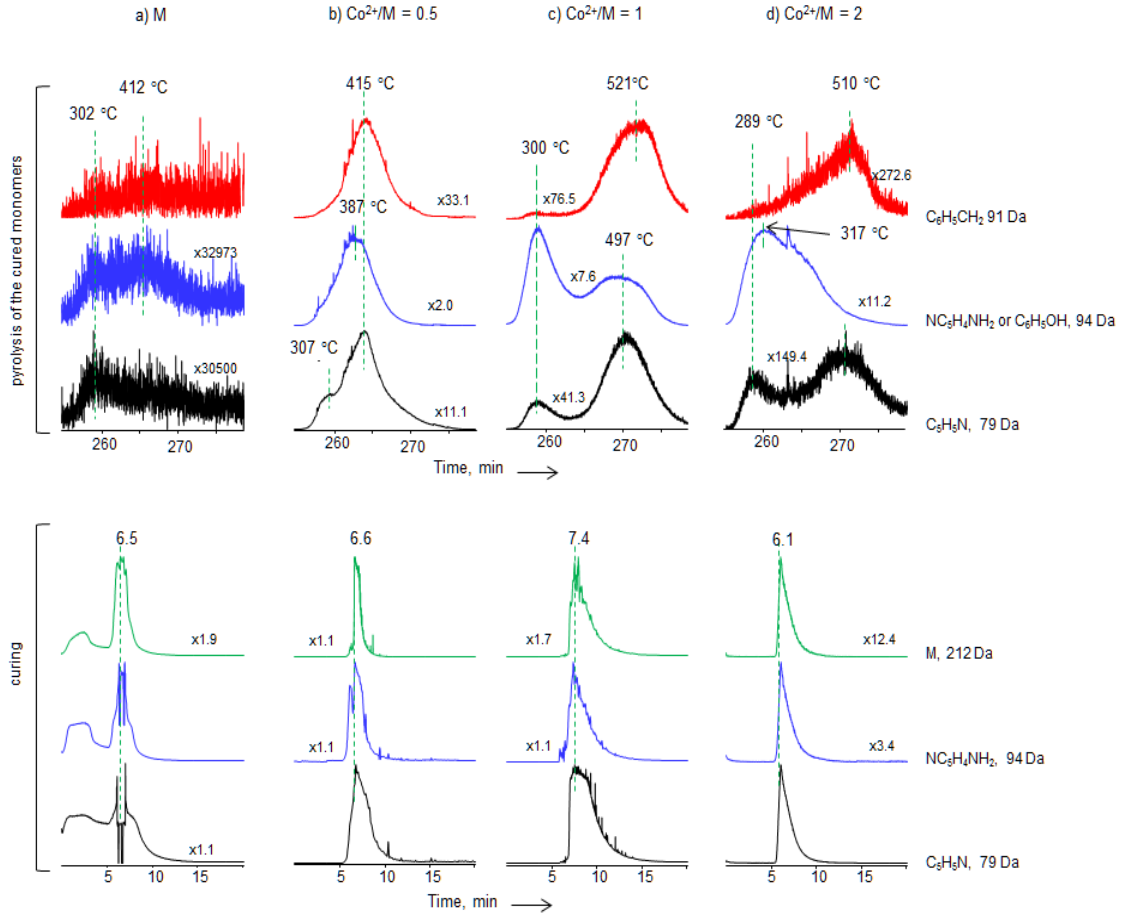

Figure 3.48 Single ion pyrograms of selected species evolved during the curing and pyrolysis of I. neat and II. Co^{2+} functional benzoxazine monomers

Further heating of the samples, after the curing cycles were completed, indicated decomposition of the polymers generated during the curing process. The polymer formed during the curing of the neat monomer was almost negligible. In contrast, for the Co^{2+} functional samples, the relative yields of degradation products were almost comparable to those of the evolved species during the curing process. The single ion pyrograms of the abundant degradation products show broad overlapping peaks with maxima at different temperatures suggesting either a multi-step thermal degradation process or presence of chains with different thermal stabilities and structures. When

the amount of metal ion used in the preparation was low, the degradation of the polymer generated was completed before the temperature was reached to 500 °C. As the amount of Co^{2+} was increased, the eliminations of pyridine and aminopyridine were shifted slightly to lower temperatures. On the other hand, for the sample prepared using equal amounts of Co^{2+} ion and monomer, the relative yields of fragments indicating unsaturated units, such as $C_6H_5CH_2$, were increased at relatively high temperature ranges, at around 521°C.

3.2.1.2. Cr functional PPh-ap

FT-IR spectra of neat PPh-ap and Cr functional PPh-ap are shown in Fig.3.49. Further broadening of the peaks may be attributed to the coordination of metal.

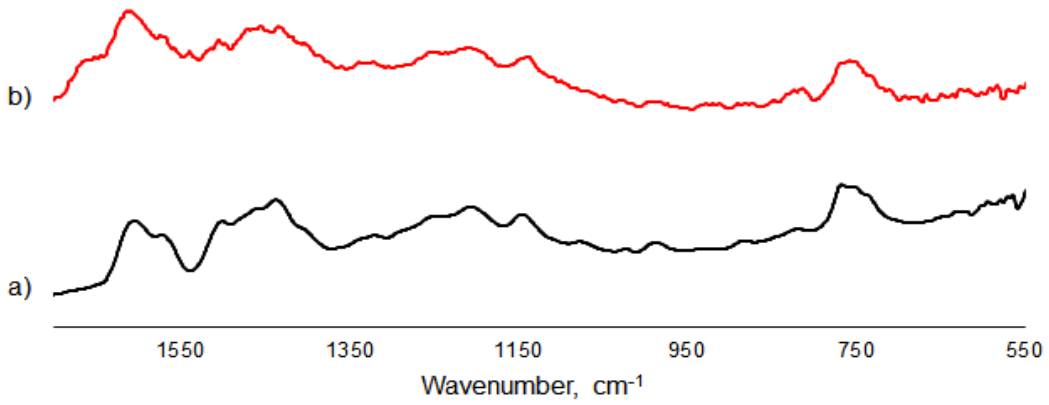

Figure 3.49 FTIR Spectra of a) polybenzoxazine based on aminobenzonitrile, PPh-ap and b) Cr functional polybenzoxazine based on aminobenzonitrile, Cr-PPh-ap

The TGA curve of Cr functional PPh-ap indicates faster weight loss at initial stages of heating. T_{max} is at 230 and 402 °C and the % char yield at 600°C is only 63.0. As, the sample contains about 12 %Cr metal, it may be thought that the char yield due to organic part is only about 51 %.

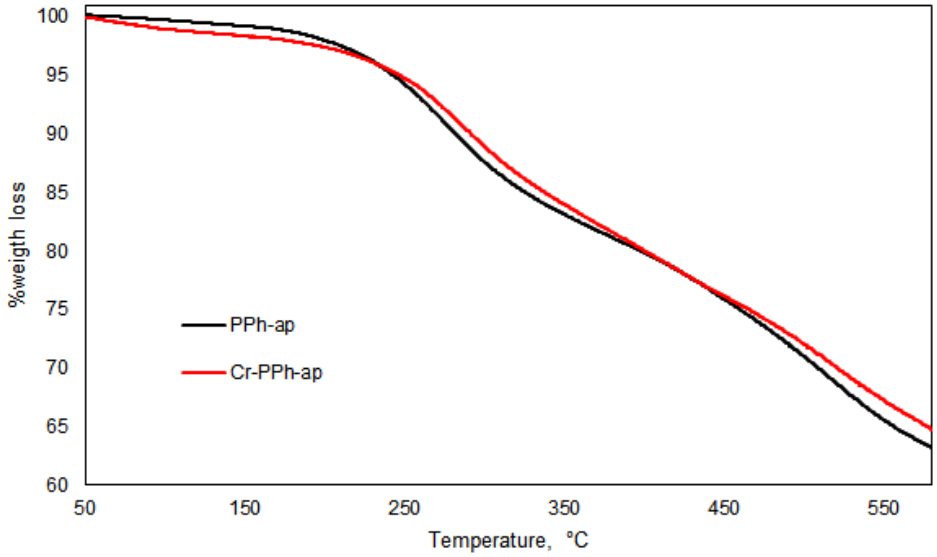

Figure 3.50 TGA curve for neat PPh-ap and Cr-functional PPh-ap

Preliminary curing of the Cr functional monomer was also achieved inside the mass spectrometer in order to gain better insight on the processes taking place. In Fig.3.51, total ion current, (TIC) curve, the variation of total ion yield as a function of time, and the mass spectrum at the maximum of the peak present in the TIC curve recorded during the curing of Cr functional benzoxazine monomer is presented.

Extensive loss of monomer took place again under the high vacuum conditions of the mass spectrometer, due to extensive evaporation at around 170°C. Again eliminations of pyridine and aminopyridine at around 170 and 200°C are detected in the mass spectra. Upon further heating the sample to 650°C after the curing cycle was completed, release of fragments indicating the degradation of the polymer was

detected. Thus, it may be concluded that polymerization of Cr functional benzoxazine was achieved even under the high vacuum conditions of the mass spectrometer.

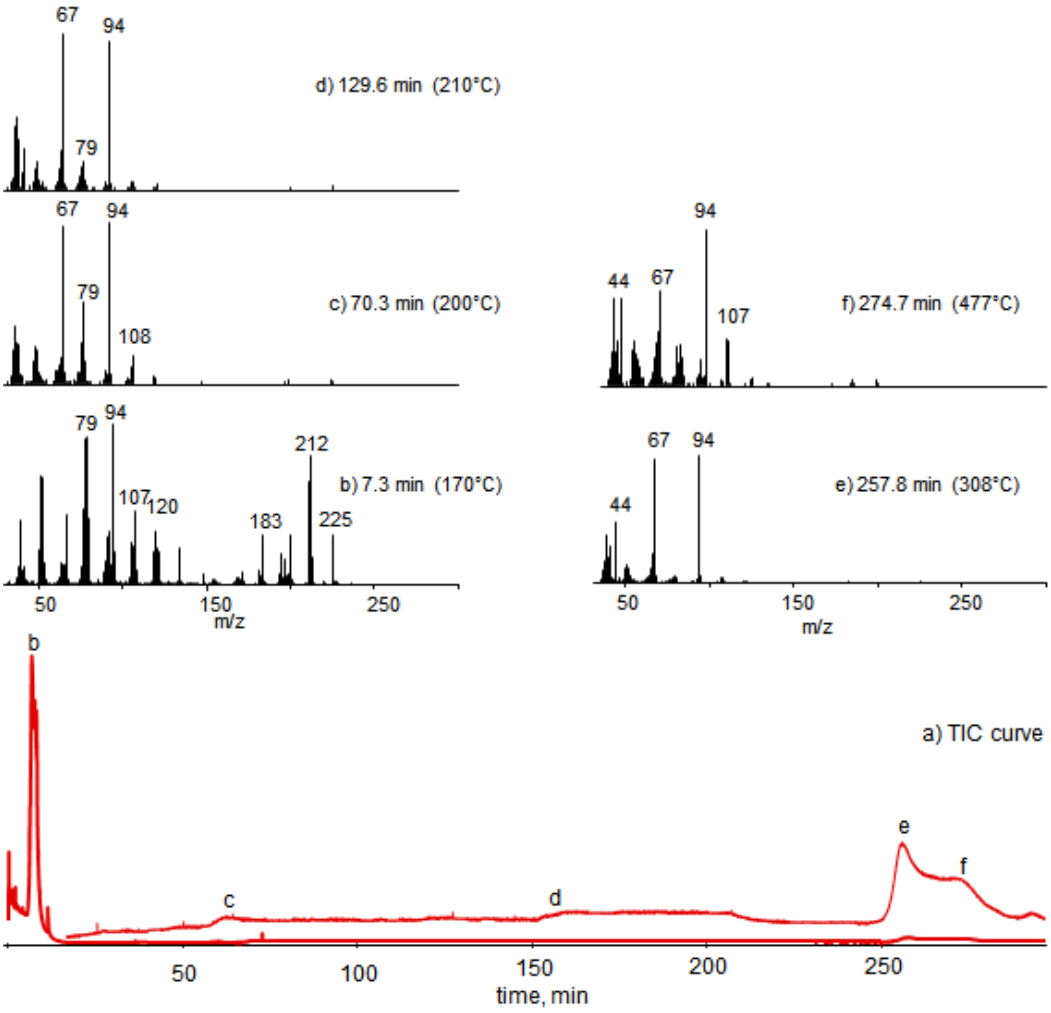

Figure 3.51 a) TIC curves and b) the mass spectra recorded during the curing and pyrolysis of Cr-functional benzoxazines

The TIC curves and mass spectra at the peak maxima recorded during the pyrolysis of Cr-functional polybenzoxazines are shown in Fig.3.52. Two peaks with maxima at around 312 and 489°C are present in the TIC curve of the metal ion coordinated sample. The low temperature mass spectrum shows the evolution of aminopyridine.

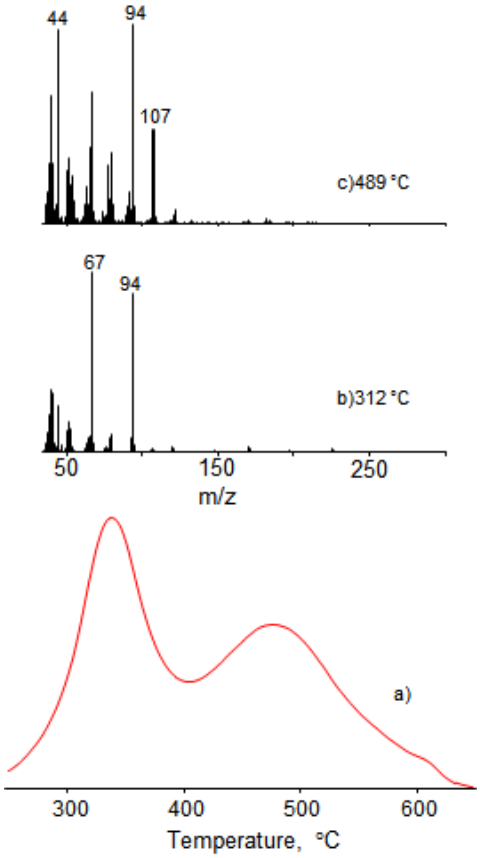

Figure 3.52 a)TIC curve and pyrolysis mass spectra at b)312 and c)489°C of Cr-functional polybenzoxazines

Single ion evolution profiles of diagnostic products selected also for neat polymer are shown in Fig.3.53. The corresponding ones recorded during the pyrolysis of neat polymer are also included for comparison.

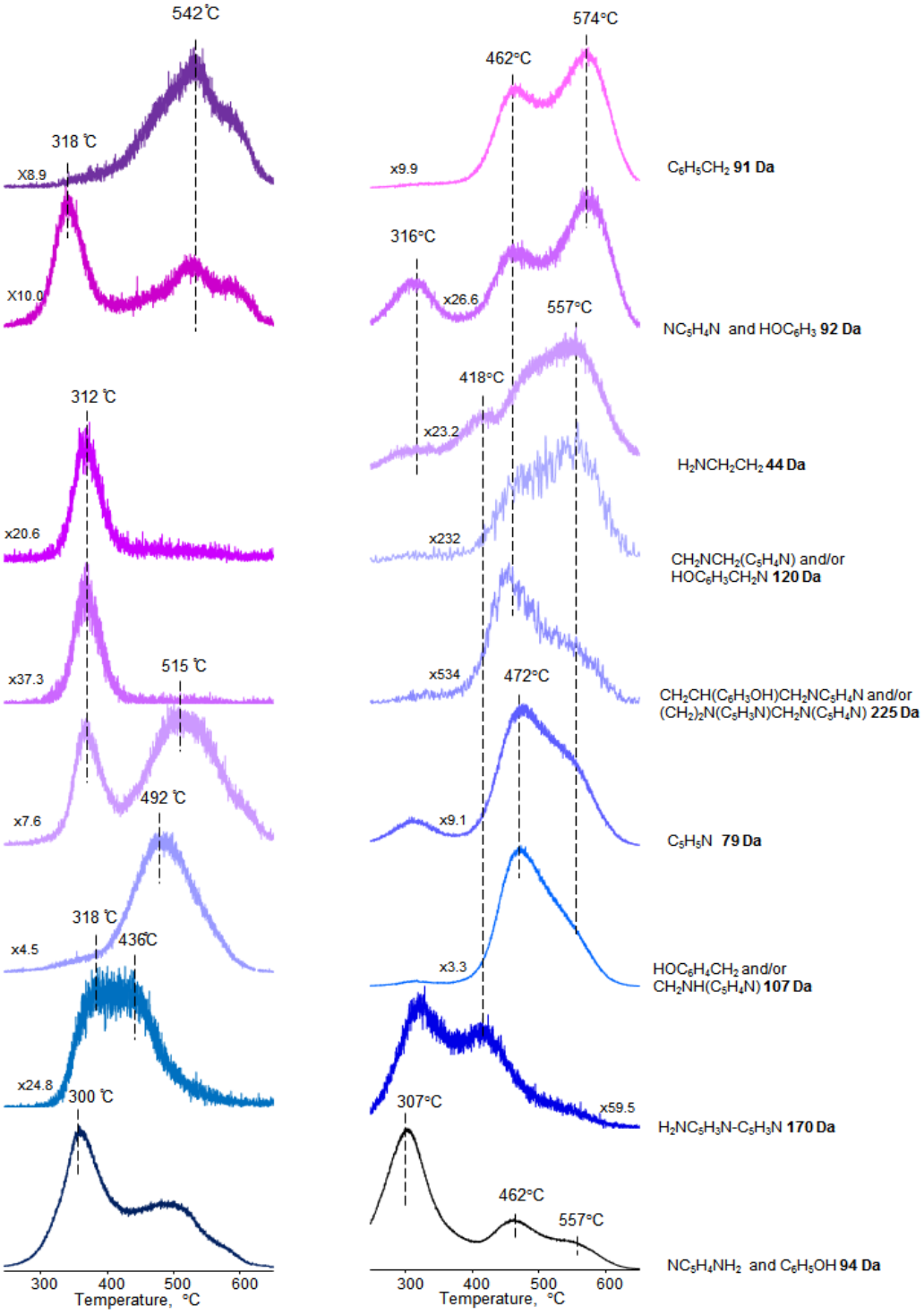

Figure 3.53 Single ion evolution profiles of selected products detected during the pyrolysis of a)Cr-PPh-ap and b) PPh-ap

The peaks in the temperature range of 400-500°C are almost disappeared during the pyrolysis of the polymer coordinated to Cr metal. The products with m/z values 92, 120 and 225 Da evolved almost exclusively at initial stages of pyrolysis, and their relative yields are increased drastically. The low temperature evolution of 79 Da is increased in intensity and high temperature evolution shifted to higher values significantly. In contrast, only limited amounts of products with m/z values 91 and 107 Da, are lost at initial stages. The evolution of 91 Da at elevated temperatures due to the decomposition of unsaturated chains are shifted to lower temperatures, indicating a lower thermal stability for Cr-functional PPh-ap.

3.2.1.3. Cr^{3+} functional PPh-ap

FT-IR spectra of neat PPh-ap and Cr^{3+} functional PPh-ap are shown in Fig3.54. Further broadening of the peaks may be attributed to the coordination of metal.

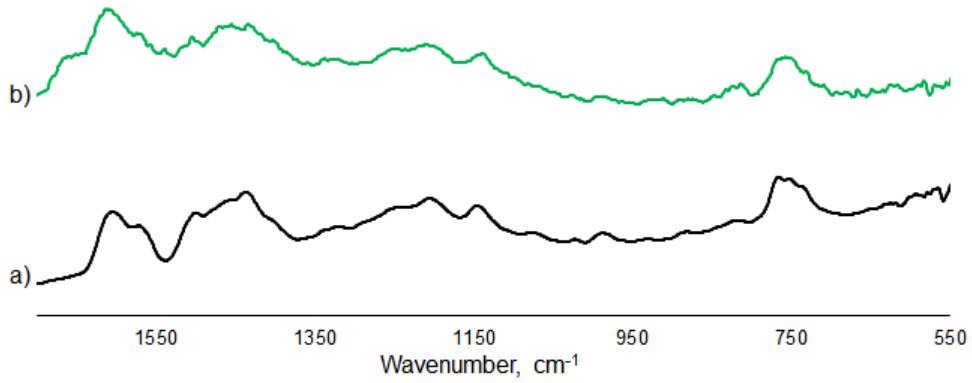

Figure 3.54 FTIR Spectra of a) polybenzoxazine based on aminobenzonitrile, PPh-ap and b) Cr^{3+} functional polybenzoxazine based on aminobenzonitrile, Cr^{3+}-PPh-ap

The TGA curve of Cr^{3+} functional PPh-ap indicates significant weight loss at initial stages of heating (Fig.3.55). T_{max} is at 251.5°C and the % char yield at 600°C is decreased from 63.2 to 58.1. As the sample contains 10.9% Cr^{3+}, it is clear that % char yield is reduced almost three-folds upon coordination to metal ion. Thus, the decrease in % char yield is greatest for Cr^{3+} functional polymer.

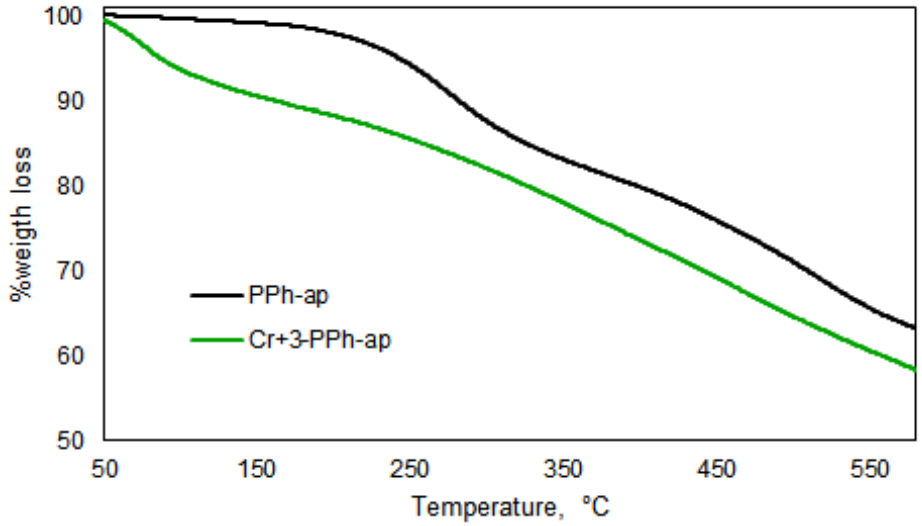

Figure 3.55 TGA curve for neat PPh-ap and Cr^{3+}-functional PPh-ap

In Fig.3.56, total ion current, (TIC) curve, the variation of total ion yield as a function of time, and the mass spectrum at the maximum of the peak present in the TIC curve recorded during the curing of Cr functional benzoxazine monomer inside the mass spectrometer are presented. Again loss of monomer is recorded under the high vacuum conditions of the mass spectrometer. Nevertheless, when the heating process was continued after the curing program was completed, evolution of diagnostic thermal degradation products of the polymer was detected confirming the polymerization even under the high vacuum conditions of the mass spectrometer.

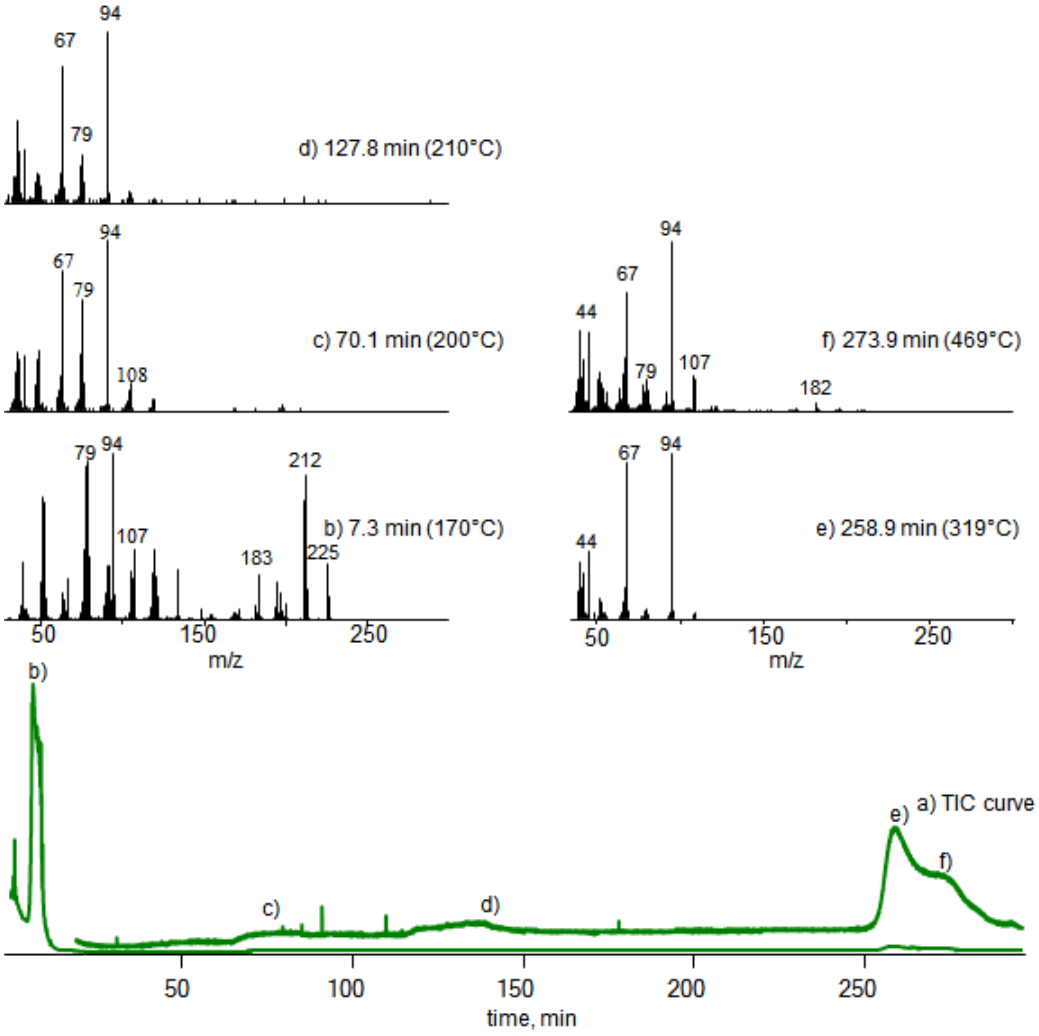

Figure 3.56 a) TIC curves and b) the mass spectra recorded during the curing and pyrolysis Cr^{3+}-functional benzoxazines

The TIC curves and mass spectra at the peak maxima recorded during the pyrolysis of Cr-functional polybenzoxazines are shown in Fig.3.57. Two peaks with maxima at around 312 and 489°C are present in the TIC curve of the metal ion coordinated sample. Extensive evolution of HCl (36 Da) is recorded in all temperatures in the mass spectra.

The TIC curves and mass spectra at the peak maxima recorded during the pyrolysis of Cr-functional polybenzoxazines are shown in Fig. 3.57. Two peaks with maxima at around 392 and 502 °C are present in the TIC curve of the metal ion coordinated sample. The low temperature mass spectrum shows the evolution of aminopyridine. But the base peak is at 36 Da that can directly be attributed to evolution of HCl. The significantly high temperature indicates generation of HCl during the pyrolysis process.

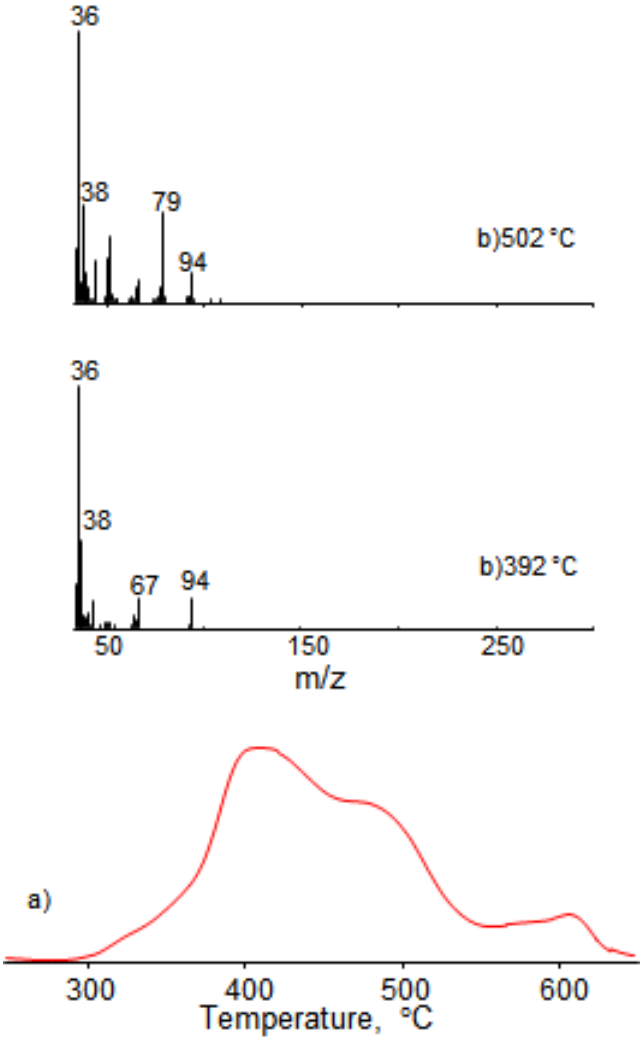

Figure 3.57 . a) TIC curve and mass spectra at b) 392 °C and c) 502 °C for Cr^{3+}-PPh-ap

The single ion evolution profiles of characteristic products are depicted in Fig.3.58.

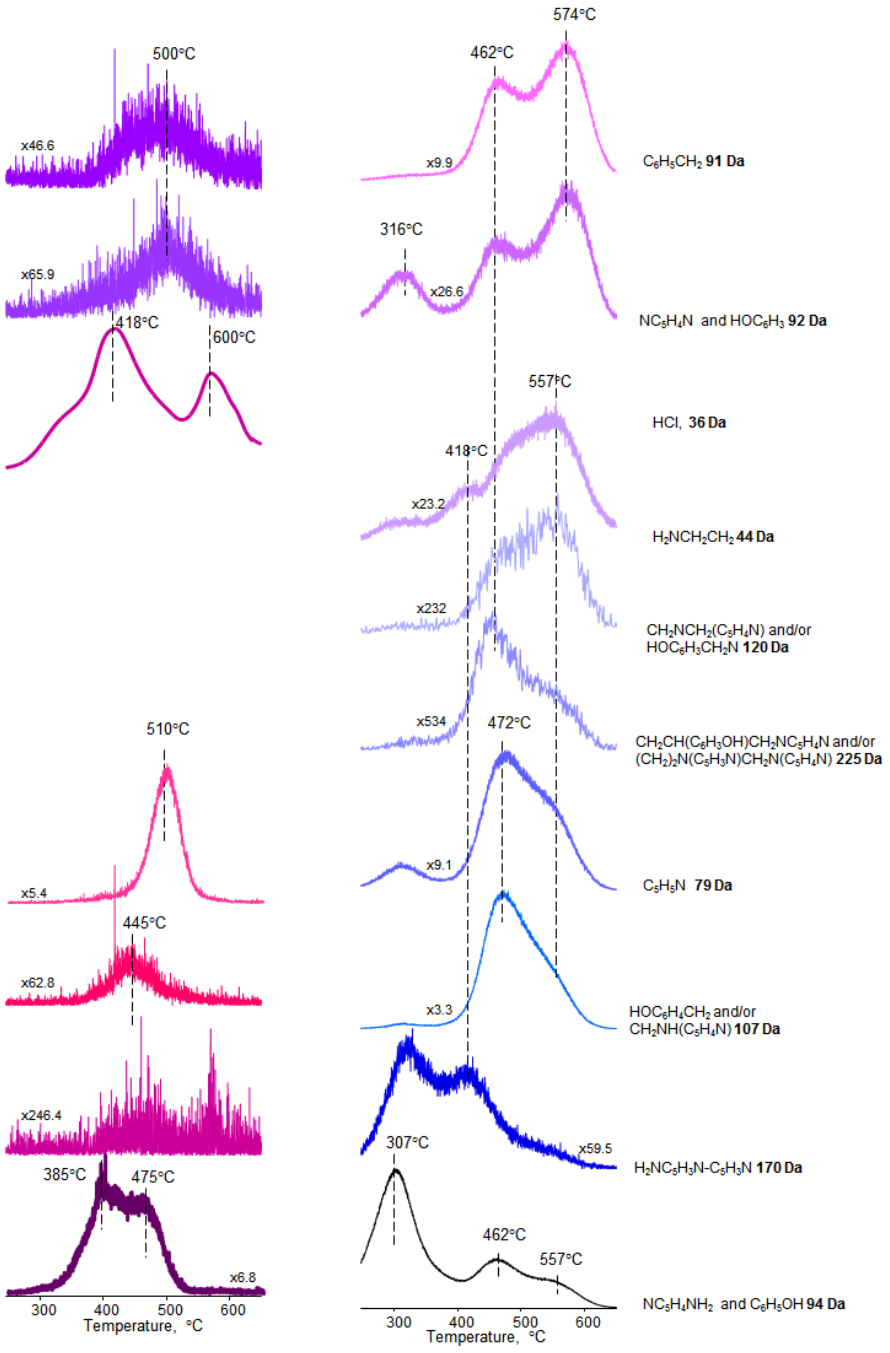

Figure 3.58 Single ion evolution profiles of selected products detected during the pyrolysis of a)Cr^{3+}-PPh-ap and b) PPh-ap

Contrary to what were observed for Co^{2+} and Cr functional analogues, low temperature evolutions, mainly aminopyridine is not detected for this sample. The initial degradation temperature at 307 °C is shifted to 385 °C but the decomposition of polymer is completed at around 500 °C and the evolution of the high mass fragments are disappeared and/or decreased drastically. It can be thought that the incorporation of Cr^{3+} inhibits the loss of aminopyridine during the pyrolysis.

Extensive loss of HCl is recorded during the pyrolysis of Cr^{3+}-functional PPh-ap at around 410 and 600 °C. Although, products associated with produced by coupling of radicals formed are not detected (Scheme 2b and Scheme 4), elimination of HCl at around 600 °C, indicates chains with relatively high stabilities. It may be thought that the chloride present in the medium reacts with the unsaturated linkages formed during the curing process. The segments also involving crosslinking decomposes at significantly elevated temperatures at around 600 °C by eliminating HCl.

To compare the effect of metal type, all the metal functional benzoxazine monomers were cured inside the mass spectrometer. Single ion evolution profiles of pyridine, aminopyridine and monomer recorded during the curing of the neat and metal functional benzoxazine monomers (metal: Co^{2+}, Cr and Cr^{+3}) are given in Fig.3.59.

Actually elimination of aminopyridine and pyridine are detected at initial stages of pyrolysis when the pyrolysis of the samples achieved following the curing process inside the mass spectrometer. In Fig.3.59, single ion evolution profiles of some diagnostic products detected during the pyrolysis of the samples cured in the mass spectrometer are shown.

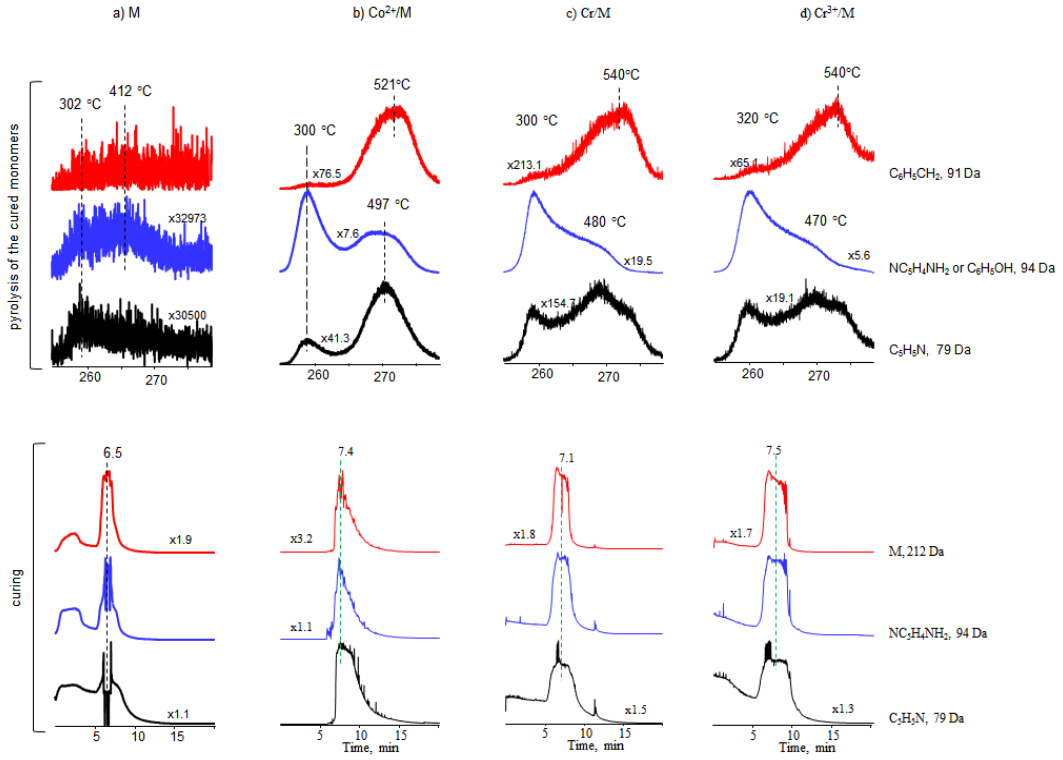

Figure 3.59 Single ion pyrograms of selected species evolved during the curing and pyrolysis of a) neat. b) Co^{2+}. c) Cr. d) Cr^{3+} functional benzoxazine monomers

The degradation of polymer generated is completed before the temperature is reached to 550℃ for all the samples. Cr and Cr^{+3} functional polybenzoxazines show almost the same thermal stability. The evolution of Co^{2+} functional polybenzoxazines is completed at slightly lower temperature regions. The relative yields of the fragment related to unsaturated units, such as $C_6H_5CH_2$ for Co^{2+} functional polybenzoxazine are highest and the evolution of unreacted monomer left in the sample at initial stages of curing is lowest for Co^{2+}-functional polybenzoxazine among the other metal and metal ion functional polybenzoxazines. It can be assumed that Co^{2+} ion is more effectively coordinated to the N atom of the pyridine ring, promoting the loss of pyridine and aminopyridine and so the formation of unsaturated polymer chains.

3.2.2. Benzoxazine based on aminobenzonitrile, Ph-abn

3.2.2.1. Co^{2+}-functional PPh-abn

FT-IR spectra of neat PPh-abn and Co^{2+} functional PPh-abn are shown in Fig.3.60. Further broadening of the peaks and disappearance of the nitrile peak at around 2200 cm^{-1} may be attributed to the coordination of metal.

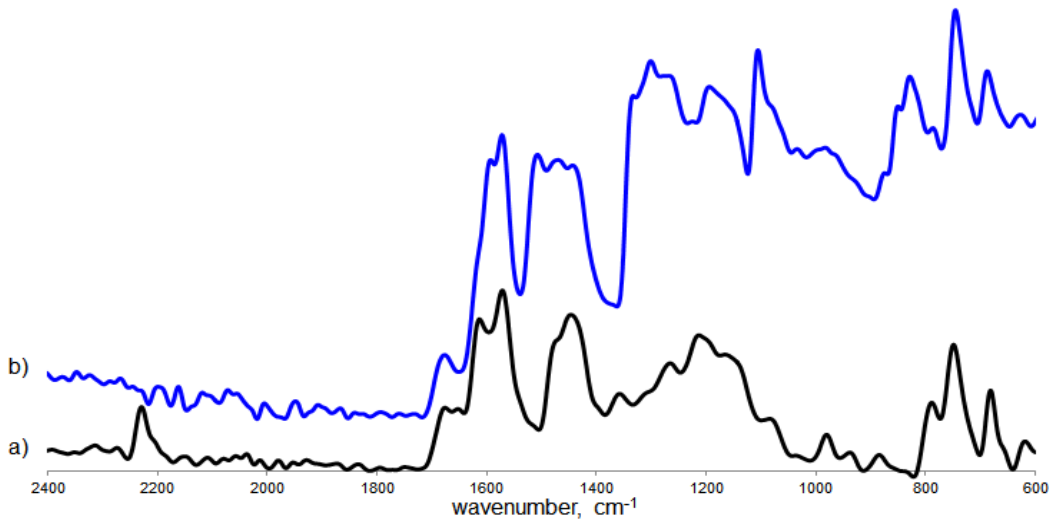

Figure 3.60 FTIR Spectra of a) polybenzoxazine based on aminobenzonitrile, PPh-abn and b) Co^{2+} functional polybenzoxazine based on aminobenzonitrile, Co^{2+}-PPh-abn

The TGA curve of Co^{2+} functional PPh-abn indicates significant weight loss. T_{max} is at 309°C and the % chat yield at 600°C is only 47.6. As the sample contains 16.1% Co^{2+}, it is clear that % char yield is reduced almost three-folds upon coordination to metal ion.

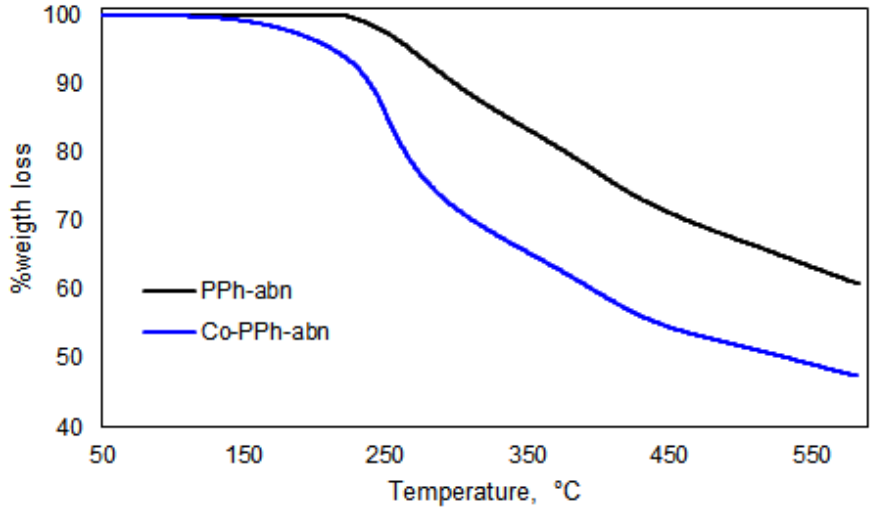

Figure 3.61 TGA curve for neat PPh-abn and Co^{2+}-functional PPh-abn

The TIC curve and mass spectrum at the peak maxima recorded during the pyrolysis of Co^{2+}-functional PPh-abn are given in Fig.3.62. A single broad peak with a maximum at around 350°C is detected in the TIC curve.

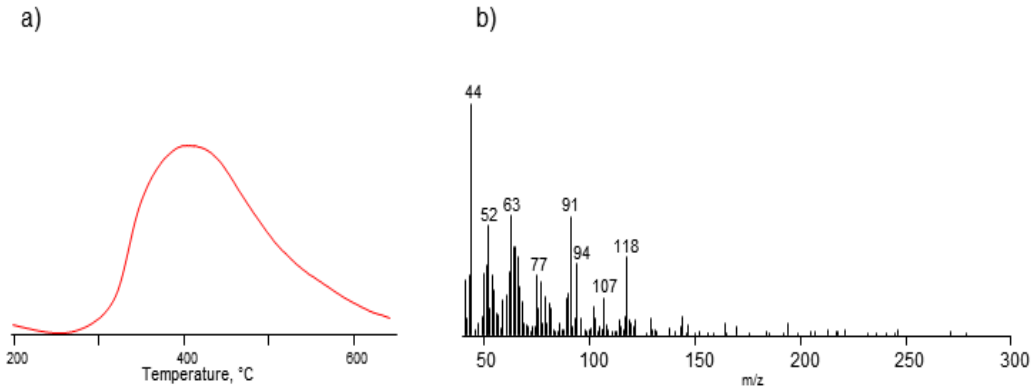

Figure 3.62 a) TIC curve and b) the mass spectrum at 407 °C recorded during the pyrolysis of Co^{2+} functional polybenzoxazines, Co^{2+}-PPh-abn

The single ion evolution profiles of some selected products of neat PPh-abn and Co^{2+} functional-PPh-abn are shown in Fig.3.63. The base peak in the pyrolysis mass spectra of Co^{2+} functional polybenzoxazine recorded at around at around 350°C, is at 44 Da indicating elimination of $CH_2CH_2NH_2$. In addition, extensive loss of HCl at around 467 °C is confirmed by the presence of peaks at 36 ($H^{35}Cl$) and 38 Da ($H^{37}Cl$) with intensity ratios about 3:1.

The evolution of aminobenzonitrile at around 295 °C is shifted to 345 °C upon coordination of metal ion to the nitrile group. Again the evolution of HCN is increased as coordination to metal ion weakens Ar-CN bond. At the same time the relative yield of aniline (93 Da) evolution is increased about four-folds as in the case of Cr-functional analogue.

The relative yields of the products attributed to substituted aminobenzonitrile such as 130 and 146 Da are decreased significantly. In addition, the evolution fragments with m/z values 179 and 195 Da, associated with decomposition of unsaturated polymer chains at elevated temperatures are almost disappeared. These fragments may be also due to units generated via attack of NCH_2 groups to benzonitrile rings, $C_6H_4CH_2NHC_6H_4CH_2$ (195 Da) and $C_6H_4CH{=}NC_6H_4$ (179 Da). Thus, it may be proposed that polymerization via attack of NCH_2 groups to benzonitrile rings are inhibited upon coordination to metal which in turn causes decrease in the extent of crosslinking.

The evolution of the fragments that were observed mainly at elevated temperatures for neat polybenzoxazine was almost disappeared after the evolution of HCl starts at 460 °C.

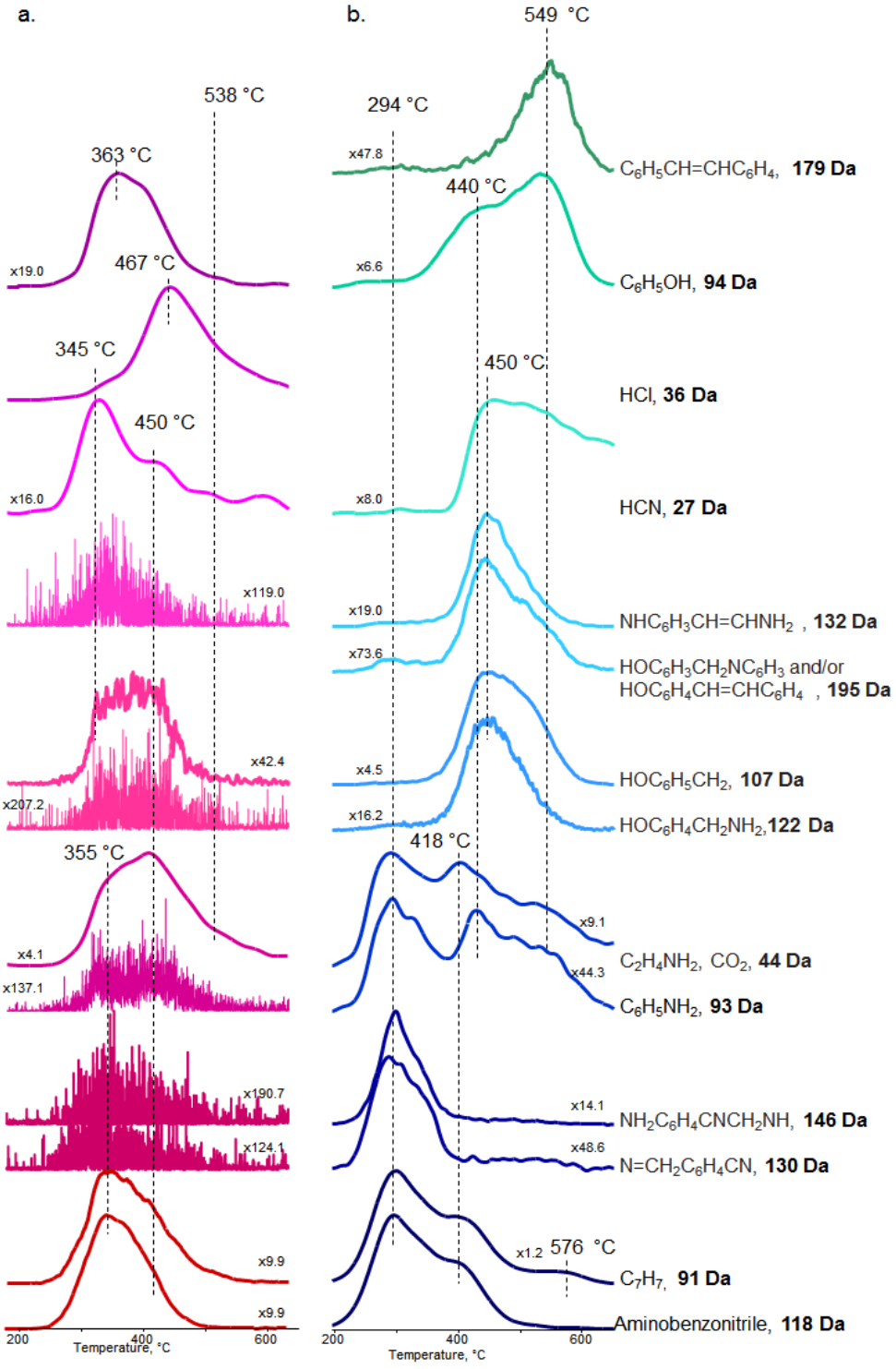

Figure 3.63 Single ion evolution profiles of selected products detected during the pyrolysis of a) Co^{2+}-PPh-abn and b) PPh-abn.

The normalized ion yields at the maxima of the peaks present in the single ion evolution profiles of the some selected fragments detected during the pyrolysis of the polybenzoxazines based on aminobenzonitrile are collected in Table 3.7 for a better comparison.

Table 3.7 Normalized ion yields at the maxima of the peaks present in the single ion evolution profiles the some selected fragments

Fragment	**Co-PPh-abn**		**PPh-abn**	
	350°C	467 °C	294 °C	450 °C
HCN, 27 Da	126	35		400
HCl, 36 Da	157	1000		
$CH_2CH_2NH_2$, 44 Da	244	199	160	
$CH_2C_6H_5$, 91 Da	169	35	777	
$H_2NC_6H_5$, 93 Da	16	1	20	
HOC_6H_5, 94 Da	78	35		399
$HOC_6H_5CH_2$,107 Da	33	13		611
$H_2NC_6H_4CN$, 118 Da	175	20	1000	
$HOC_6H_4CH_2NH$, 122 Da	10	7		156
$CH_2NC_6H_4CN$, 130 Da			12	
$H_2N(C_6H_3CN)CH_3$,$NHC_6H_3CH=CHNH_2$,132Da	14	4		151
$NH_2C_6H_4(CN)CH_2NH$, 146 Da	0.2		47	
$C_6H_5CH=CHC_6H_4$, $C_6H_4CH=NC_6H_4$, 179 Da	2			28
$HOC_6H_4CH=CHC_6H_4$,$C_6H_4CH_2NHC_6H_4CH_2$, 195Da	1			19

It is clear that the yields of unsaturated fragments are reduced drastically. During the pyrolysis of Co-PPh-abn, the base peak is at 36 Da which due to the evolution of HCl. It may be thought that the anions of the $CoCl_2$. It may be thought that under the curing conditions, the chlorides present in the medium react with the unsaturated segments generated upon loss of aniline groups that decompose by elimination of HCl.

In general, the relative yield of all the fragments were decreased compared to neat polybenzoxazine. It can be thought that the presence of HCl during curing and pyrolysis cause the decomposition of polymer chains

3.2.2.2. Cr functional PPh-abn

FT-IR spectra of neat PPh-abn and Cr functional PPh-abn are shown in Fig.3.64. Further broadening of the peaks and decrease in the intensity of the nitrile peak at around 2200 cm^{-1} may be attributed to the coordination of metal.

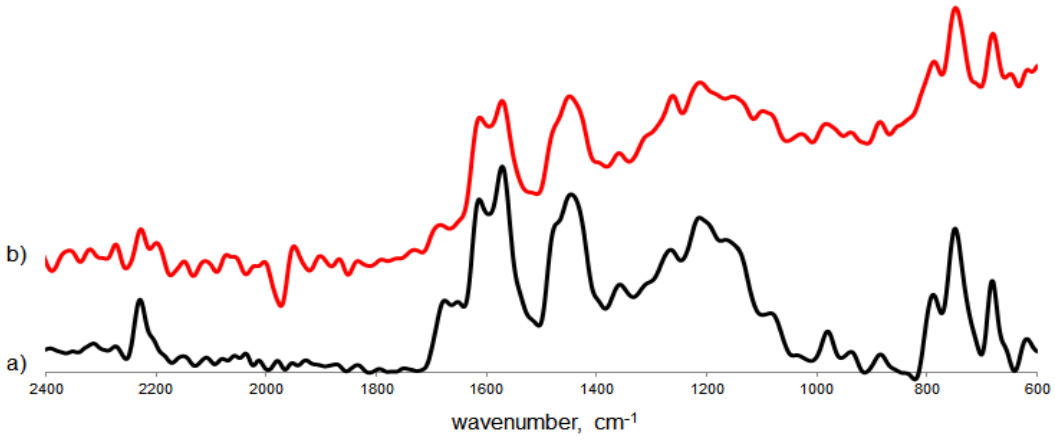

Figure 3.64 FTIR Spectra of a) polybenzoxazine based on aminobenzonitrile, PPh-abn and b) Cr functional polybenzoxazine based on aminobenzonitrile, Cr-PPh-abn

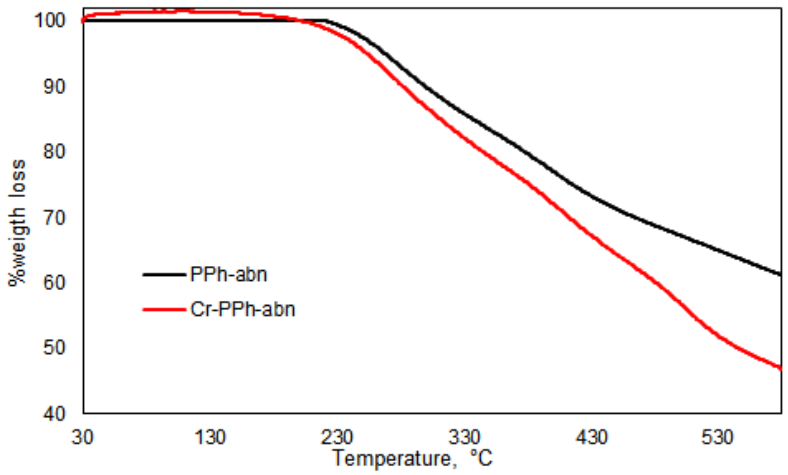

Figure 3.65 TGA curve for neat PPh-abn and Cr-functional PPh-abn

TGA analyses indicated that upon coordination to Cr atom, thermal stability of the polybenzoxazine produced decreased significantly. Maximum %weight loss is observed at around 272°C, significantly lower than the corresponding value detected for uncoordinated analogue. Furthermore, char yield is also decreased to 46.5%. Actually, Cr metal should also be present in the char. As the metal/monomer mole ratio was selected as 1, the polymer sample involves at least 11.4 % Cr metal. Thus, it can be concluded that the organic char yield is reduced more than 50 %.

The TIC curve and the pyrolysis mass spectra recorded at the maximum of the peaks present in the TIC curve recorded during the pyrolysis of Cr functional PPh-abn are given in Fig.3.66.

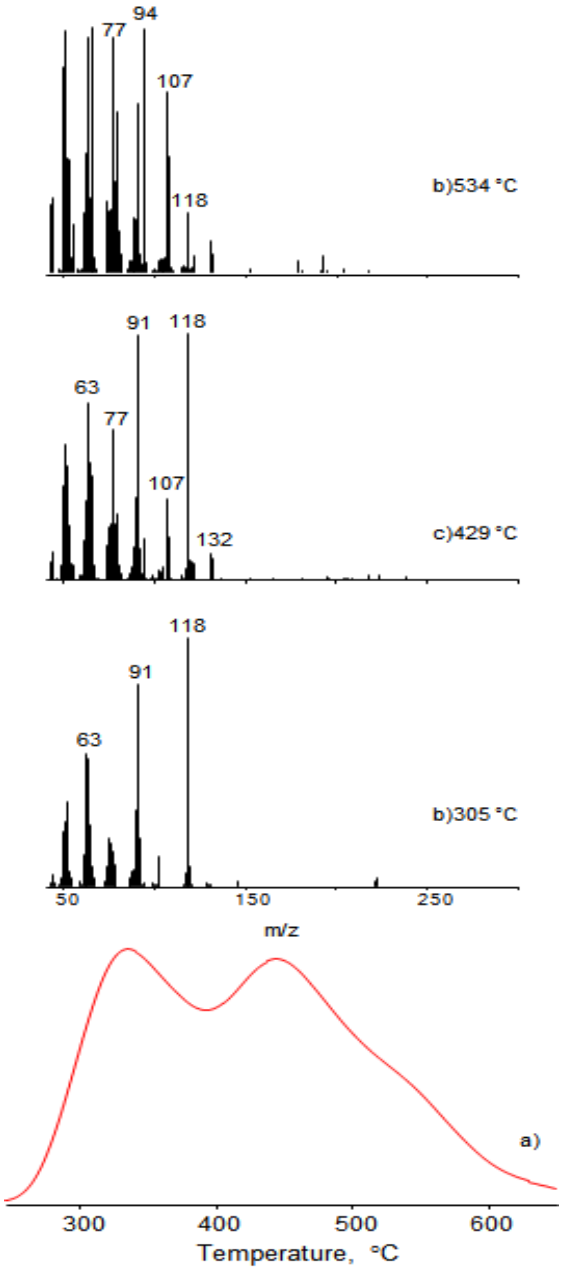

Figure 3.66. The TIC curve and the pyrolysis mass spectra recorded at the maximum of the peaks present in the TIC curve recorded during the pyrolysis of Cr functional PPh-abn.

The single ion evolution profiles of some selected products of neat PPh-abn and Cr functional-PPh-abn are shown in Fig.3.67. The thermal stability of the polymer chains is not affected significantly upon coordination to metal but the relative yields of the

products are changed. The major change occurs in the evolution of HCN. It may be thought that the coordination of metal to the nitrile group can promote the cleavage of Ar-CN bond. The evolution of HCN in a narrower temperature region and more than two-fold increase in its relative yield is in accordance to expectations. On the other hand, the increase in the relative yield of $NH_2C_6H_5$ (93 Da), being almost eight-folds, is more than the expected. It may be thought that when the nitrile group coordinates to metal, the interaction between the nitrile group and aniline ring is weakened. Thus, it may be suggested that aniline generation is promoted as a consequence of coordination of nitrile group to Cr metal. In contrast, the relative yields of the products attributed to substituted aminobenzonitrile such as $CH_2NC_6H_4CN$ (130 Da) and $NH_2C_6H_3(CN)CH_2NH$ (146 Da) are decreased significantly.

The fragments reaching maximum yield at around 450 °C such as 132 that can be generated after loss of HCN are increased in intensity due to the promoted HCN loss. In addition, the evolution of fragments with m/z values 179 and 195 Da, associated with decomposition of unsaturated polymer chains at elevated temperatures are also diminished. These fragments may also be due to units generated via attack of NCH_2 groups to benzonitrile rings, $C_6H_4CH_2NHC_6H_4CH_2$ (195 Da) and $C_6H_4CH{=}NC_6H_4$ (179 Da). Thus, it may be suggested that polymerization via attack of NCH_2 groups to benzonitrile rings are inhibited upon coordination to metal which in turn causes decrease in the extent of crosslinking. The increase in the relative yield of aniline supports this proposal.

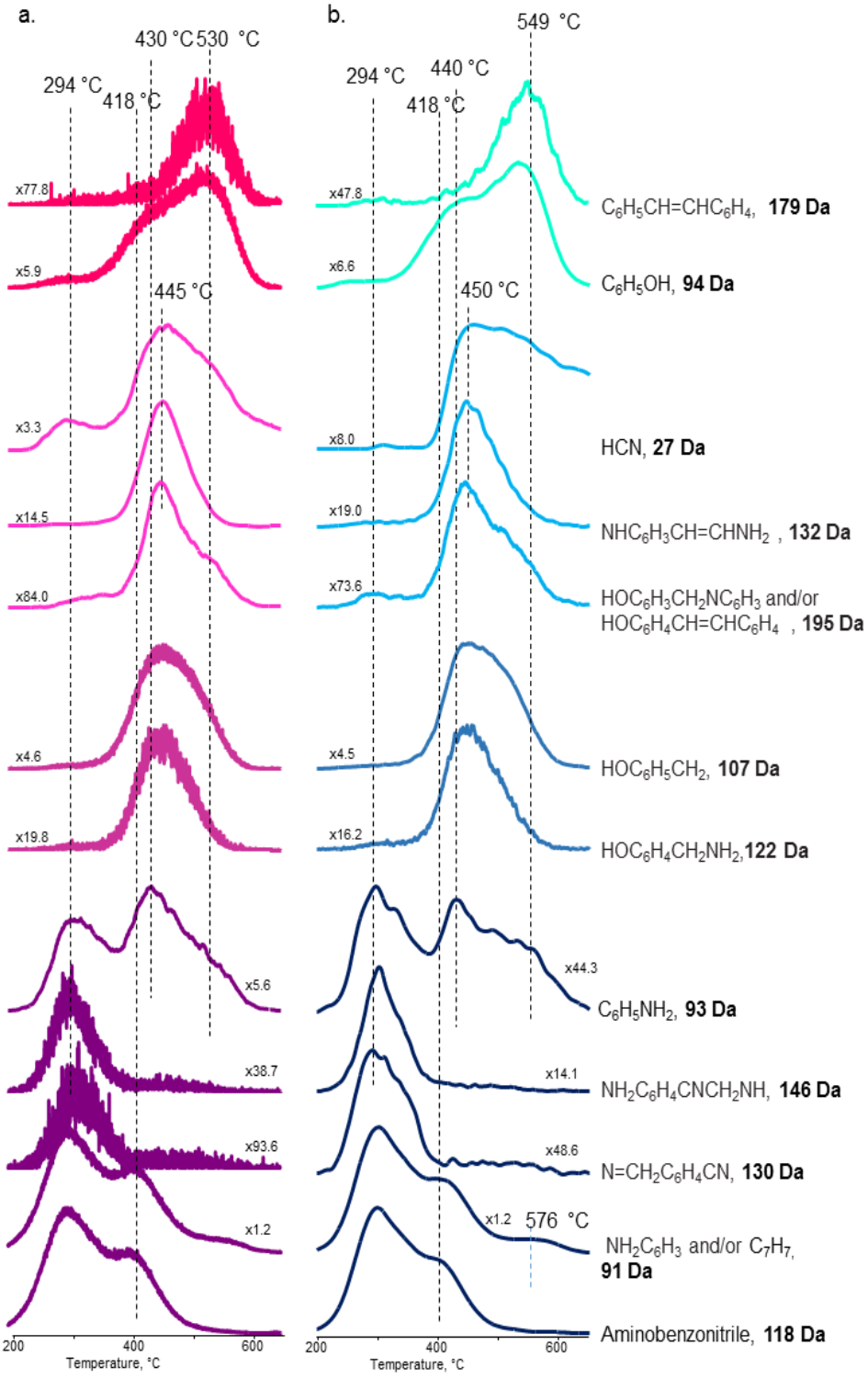

Figure 3.67 Single ion evolution profiles of selected products detected during the pyrolysis of a) Cr-PPh-abn and b) PPh-abn.

3.2.3. Benzoxazine based on 4-nitroaniline, Ph-na

3.2.3.1. Co^{2+} functional PPh-na

FT-IR spectra of neat PPh-na and Co^{2+}-functional PPh-na are shown in Fig.3.68. Further broadening of the peaks is again associated with the coordination of metal ion. The band at around 1750 cm^{-1} attributed to C=O stretching due to the oxidation of methylene groups by the NO_2 radicals to the carboxylic acid is again disappeared as in case of Cr functional polymer.

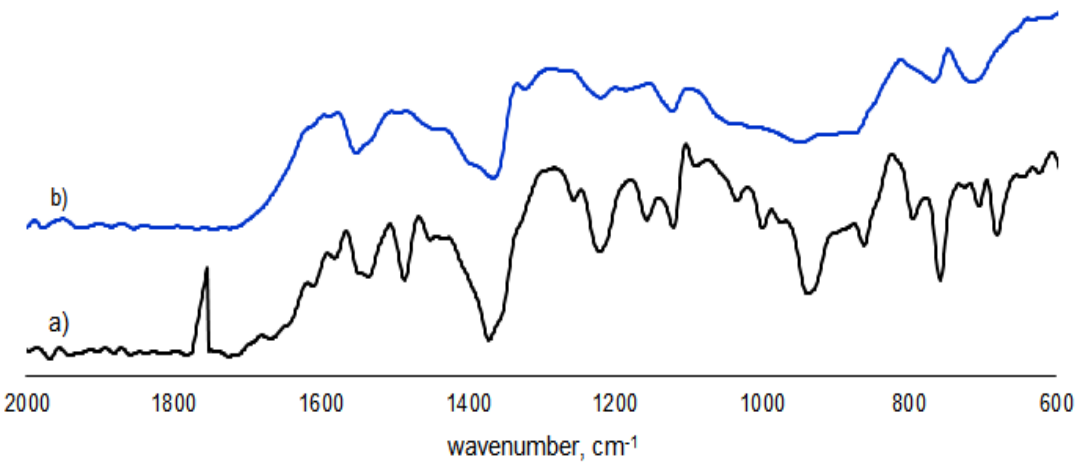

Figure 3.68 FT-IR spectrum of a)PPh-na and b)Co^{2+}-PPh-na

The thermal characteristic of the Co^{2+}-PPh-na was also studied and TGA curve for neat PPh-na and Co^{2+}-PPh-na are given below. The T_{max} is recorded at 297 °C for Co^{2+}-PPh-na and the char yield is 55.6% at 600 °C. Taking into account, the presence of about 15.3 % by mass Co^{2+} in the sample, the organic char yield may be regarded as almost 40 %.

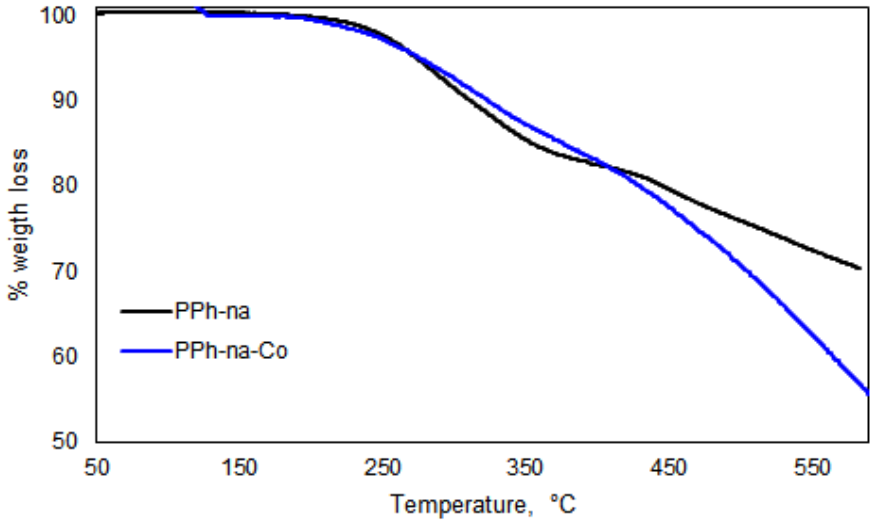

Figure 3.69 TGA curve for neat PPh-na and Co^{2+}-functional PPh-na

TIC curve and the mass spectra at the peak maxima are given in the Fig.3.70. Two distinct peaks at 294 and 467 °C are present in the TIC curve. The base peak is 36 Da (HCl) for both mass spectra. The mass spectra recorded at low temperature regions consists of diagnostic peaks for the nitroaniline. The relative yields of the fragments due to the decomposition of nitroaniline and HCl are comparable in this temperature region. However, only limited amount of fragments due to the decomposition of polymer chains are detected in the high temperature mass spectra.

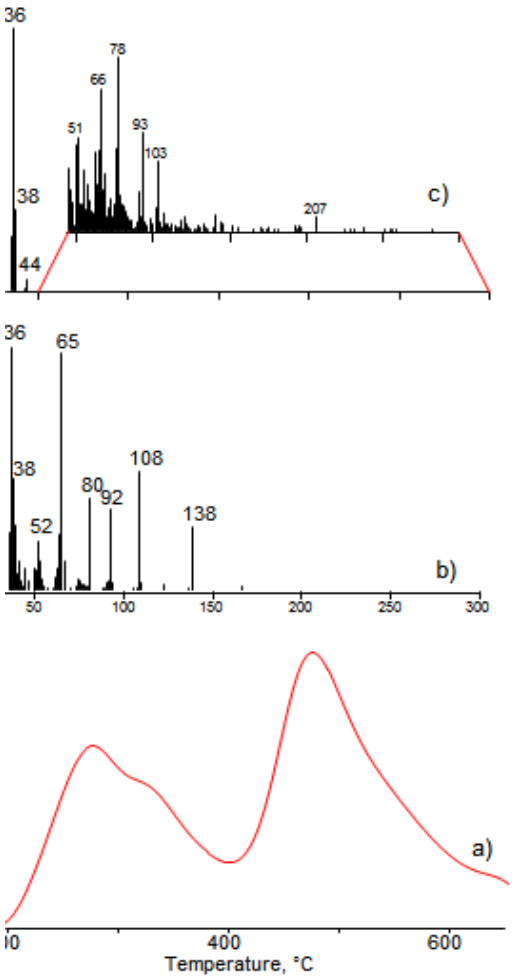

Figure 3.70 a) TIC curve and mass spectra at b) 294 °C and c) 474 °C for Co^{2+}-PPh-na

The single ion evolution profiles some selected products of neat PPh-na and Co^{2+}-PPh-na are shown in Fig.3.71. The initial degradation temperature is shifted to lower temperature for the metal ion coordinated polybenzoxazines and the high temperature peaks are disappeared for Co^{2+}-functional PPh-na, indicating a lower stability. The relative yields of nitroaniline and characteristic products of nitroaniline such as 130 and 108 Da are increased. The coordination of metal ion to the nitro group diminished the formation of thermally stable polymer chains as the relative yields of 91, 78 and 94 Da which can be generated at high temperatures from decomposition unsaturated and crosslinked polymer chains, were decreased significantly, which is in accordance

with the decrease in the char yield from 70 to 40 % upon coordination to Co^{2+}. The normalized ion yields at the maxima of the peaks present in the single ion evolution profiles of some selected products detected during the pyrolysis of Co^{2+}-PPh-na and PPh-na for a better comparison.

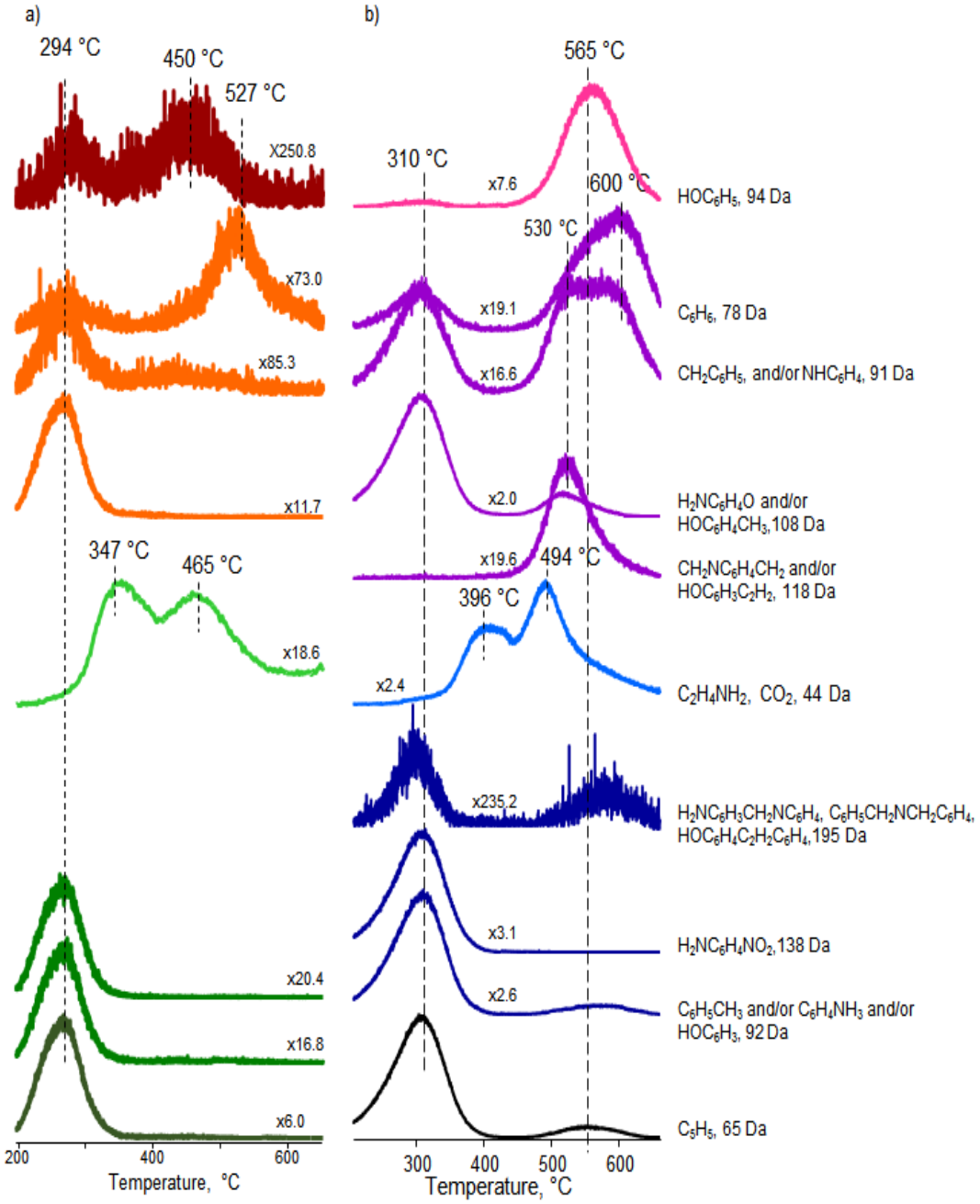

Figure 3.71 Single ion evolution profiles of selected products detected during the pyrolysis of a)Co^{2+}-PPh-na and b) PPh-na

Table 3.8 Normalized ion yields at the maxima of the peaks present in the single ion evolution profiles of some selected products detected during the pyrolysis of Co^{2+}-PPh-na and PPh-na.

Fragment	Co^{2+}-PPh-na		Ph-na			
	273 °C	474 °C	313 °C	522 °C	560 °C	593 °C
HCl, 36 Da	152	1000				
$C_2H_4NH_2$, 44Da	12	50.9	13	909	560	412
C_5H_5, 65 Da	151	2	1000		336	
C_6H_6 , 78 Da		2.7	1		161	194
$CH_2C_6H_5$, 91 Da			20	195	206	213
$CH_2C_6H_5$, 92 Da	58		142		116	
HOC_6H_5, 94 Da		2.2	2		475	
$HOC_6H_4CH_3$. $NH_2C_6H_4O$, 108 Da	85		191	339	168	73
$HOC_6H_3C_2H_2$, $CH_2NC_6H_4CH_2$, 118 Da				194	105	33
$NH_2C_6H_4NO_2$, 138 Da	42		127		2	2

3.2.3.2. Cr functional PPh-na

FT-IR spectra of neat PPh-na and Cr functional PPh-na are shown in Fig.3.72. Further broadening of the peaks may be attributed to the coordination of metal. The characteristic CO stretching peak at around 1750 cm^{-1} due the oxidation of methylene groups by the NO_2 radicals to the carboxylic acid is disappeared.

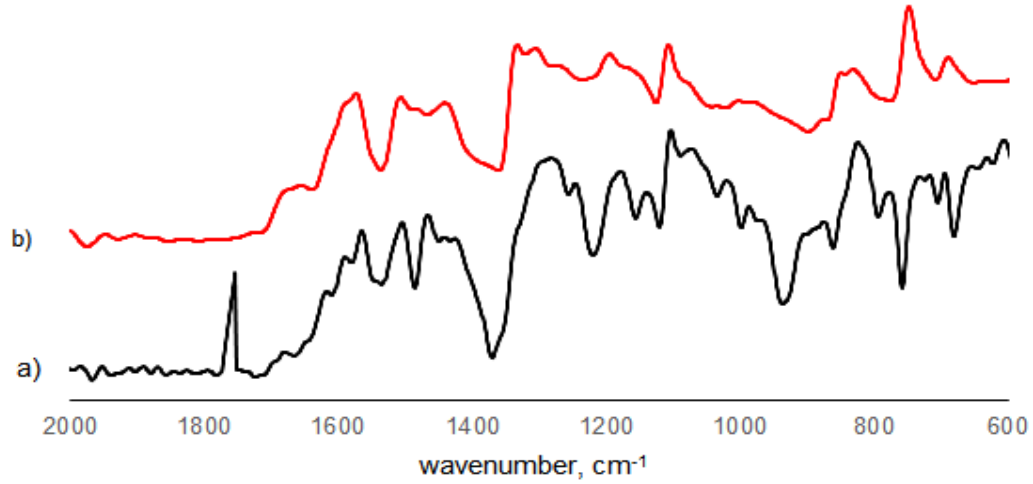

Figure 3.72 FT-IR spectrum of a)PPh-na and b) Cr-functional PPh-na

The thermal characteristic of the Cr-PPh-na was also studied and TGA curve for neat PPh-na and Cr-PPh-na are given below. The instant weight loss for Cr-PPh-na can be assumed as the evolution of HCl at low temperatures. The T_{max} is seen at 279 °C for Cr-PPh-na and the char yield is %51.7 at 600 °C. Actually, the sample heated involves 11.9 % Cr by mass. Thus, the organic char yield is less than 40%, noticeably lower than what was observed for the neat polymer.

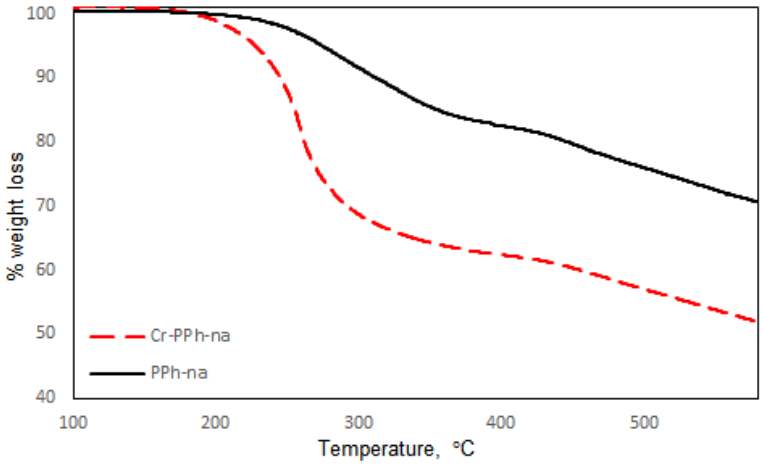

Figure 3.73 TGA curve for neat PPh-na and Cr-functional PPh-na

TIC curve and the mass spectra at the peak maxima are given in the Fig.3.74. Two distinct peaks at 337 and 497 °C are present in the TIC curve.

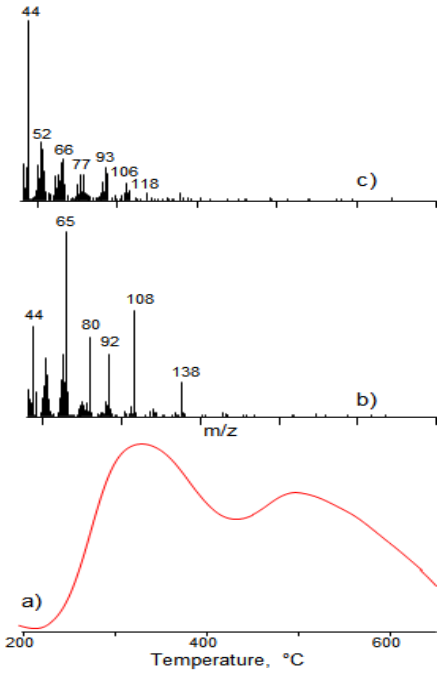

Figure 3.74 a) TIC curve and mass spectra at b) 337 °C and c) 492 °C for Cr-PPh-na

The single ion evolution profiles some selected products of neat PPh-na and Cr-PPh-na are shown in Fig.3.75. The initial thermal degradation shifts slightly to higher temperatures for the Cr coordinated polybenzoxazine. The relative yields of diagnostic products are increased, indicating a decrease in extent of crosslinking. The relative yields of fragments with m/z values 91, 78 and 94 Da generated at high temperatures due to decomposition of unsaturated and crosslinked polymer chains, are decreased significantly, in accordance with the decrease in the char yield from 70 to about 40 % for Cr-PPh-na at 600 °C. Thus, it can be concluded that the coordination of Cr metal to nitro groups inhibits the formation of thermally stable polymer linkages.

Table 3.9 Normalized ion yields at the maxima of the peaks present in the single ion evolution profiles of some selected products detected during the pyrolysis of Cr-PPh-na and PPh-na.

	Cr-PPh-na		**Ph-na**			
	337 °C	492 °C	313 °C	522 °C	560 °C	593 °C
$C_2H_4NH_2$, 44Da	485	652	13	909	560	412
C_5H_5 , 65 Da	1000	100	1000		336	
C_6H_6 , 78 Da	62	10			161	194
$CH_2C_6H_5$, 91 Da	105	79	20	195	206	213
$CH_2C_6H_5$, 92 Da	350	35	142		116	
HOC_6H_5, 94 Da	30	106			475	
$HOC_6H_4CH_3$. $NH_2C_6H_4O$, 108 Da	620	28	191	339	169	73
$HOC_6H_3C_2H_2$, $CH_2NC_6H_4CH_2$, 118 Da	2	57		194	105	33
$NH_2C_6H_4NO_2$, 138 Da	15	6	126			

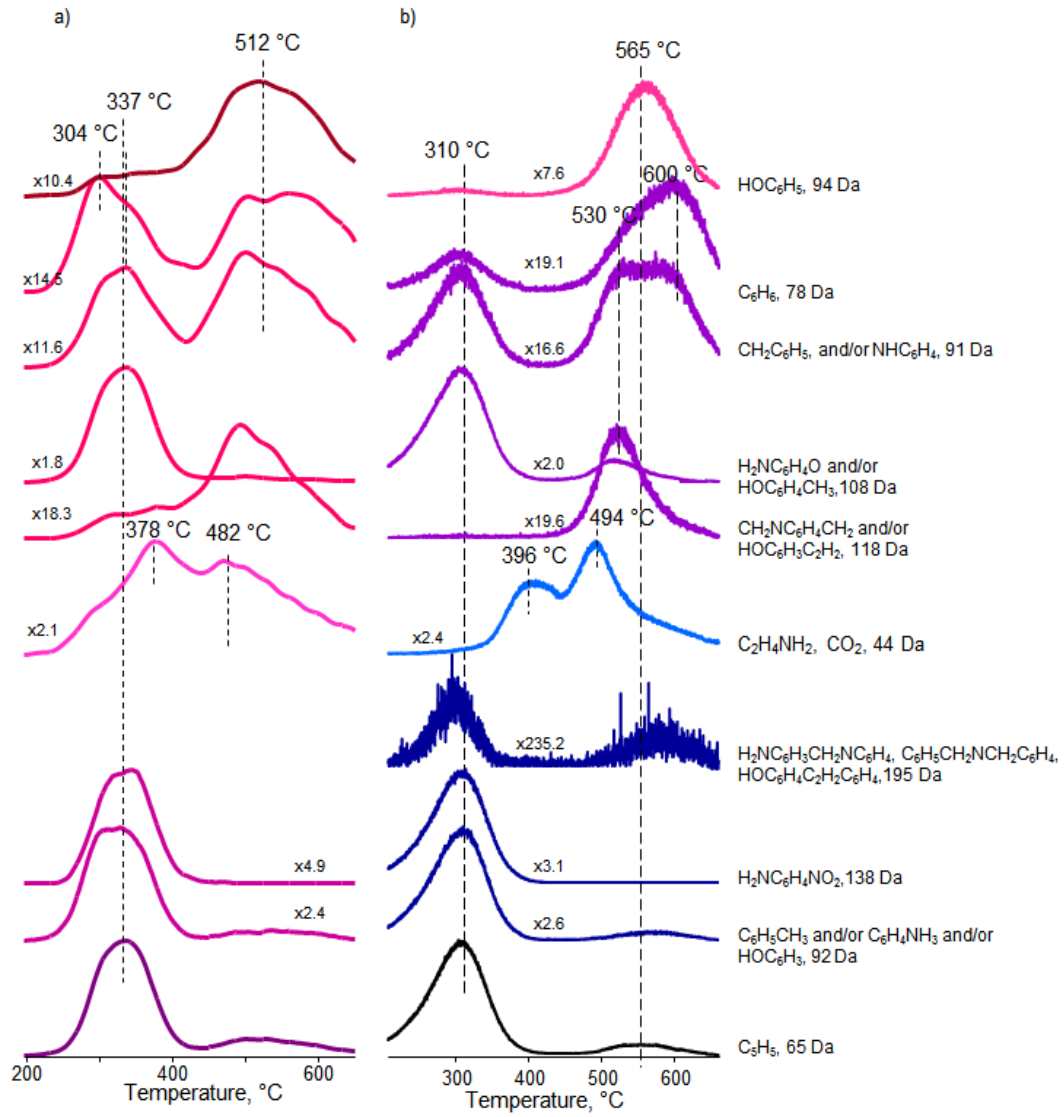

Figure 3.75 Single ion evolution profiles of selected products detected during the pyrolysis of a)Cr-PPh-na and b) PPh-na

CHAPTER 4

CONCLUSIONS

In the first part of this work, benzoxazines based on phenol and aniline or aniline derivatives namely aminopyridine, aminobenzonitrile and nitroaniline are synthesized and polymerized by curing the monomers systematically. In the second part of the work metal or metal ions are incorporated to benzoxazine monomers based on aminopyridine, aminobenzonitrile and nitroaniline. The structural and thermal characteristics of the polybenzoxazines and metal or metal ion functional polybenzoxazines are analyzed via FTIR, NMR, DSC, TGA and DP-MS techniques. The effects of curing program used and incorporation of metal and/or metal ion on structural and thermal characteristics of the polybenzoxazines are investigated.

It has been determined that the structure and thermal characteristics of the polymers depend not only on the aromatic amine used but also on the curing program applied.

In terms of the structure of the polymers:

- In general, the benzoxazines based on aniline or aniline derivatives are polymerized via ring opening of oxazine ring followed by attack of NCH_2 groups to mainly para positions of phenol and aniline ring. In addition coupling of the dimers generated upon ring opening process takes place to a certain extend. As a consequence of elimination of aniline or aniline derivatives taking place during the curing process to a certain extent, unsaturated linkages are generated. The char yield and presence of chains that can only decompose at elevated temperatures mainly depend on extent of crosslinking and unsaturated linkages.

- The position of substituents on aniline ring affects the attack of NCH_2 groups to aniline rings, and coupling of the dimers generated upon ring opening process. As a consequence the extent of crosslinking decreases.

- Curing at elevated temperatures promotes the evolution of aniline or its derivatives during the polymerization process. Eventually, the polymerization mainly proceeds via coupling of the radicals generated.

In terms of thermal characteristics of the polymers:

- Thermal stability of the polymer chains generated depends on the structure but not on the aromatic amine used.

- The polymer chains generated via attack of NCH_2 groups to phenol rings decomposes in two steps; loss of aromatic amine being the first step at early stages of pyrolysis at around 300°C and the decomposition of the unsaturated chains produced by coupling of the radicals formed in the first step at around 500°C.

- The chains generated via attack of NCH_2 groups to aniline rings decompose at around 400 °C by random chain cleavages without the elimination of aromatic amines. In general, these segments involving crosslinking degrade at elevated temperatures and cause increase in char yield.

Coordination of metal and/or metal ion to pyridine in case of aminopyridine based benzoxazine, to CN groups in case of aminobenzonitrile and finally to NO_2 groups in case of nitroaniline cause drastic changes in structural and thermal characteristics of the polybenzoxazines produced. The interactions depend on type of the metal or metal ion used, the functional group acting as ligand and mole ratio of the metal or metal ion and the monomer. Considering also the complex polymerization and thermal degradation processes of polybenzoxazines to understand the effect of each variable on structural and thermal characteristics of polybenzoxazines is almost impossible. Thus, only general trends are stated.

The effects of incorporation of metal and/or metal ion on structural and thermal characteristics of the polybenzoxazines:

- The most effective coordination of metal or metal ion was seen for benzoxazine based on aminopyridine, having a lone pair on the N atom that can coordinate to metal or metal ion easily.

- For the aniline derivatives, aminobenzonitrile and nitroaniline, the polymerization of metal functional benzoxazine monomer is achieved only to a limited extent.

- The coordination of metal or metal ion to the aromatic ring of the benzoxazine monomer promotes the evolution of amine or substituted amine groups which in turn causes an increase in the formation of unsaturated linkages but a decrease in the extent of crosslinking. The thermal stability is decreased due to the low degree of crosslinking, upon coordination to the metal or metal ion.

REFERENCES

[1] Ning X, Ishida H. Phenolic Materials via Ring- Opening Polymerization of Benzoxazines : Effect of Molecular Structure on Mechanical and Dynamic Mechanical Properties. J Polym Sci Part B Polym Phys 1994;32:921–27.

[2] Gârea S, Lovu H, Nicolescu A, Deleanu C. A new strategy for polybenzoxazine–montmorillonite nanocomposites synthesis. Polym Test 2009;28:338–47.

[3] Gârea S-A, Lovu H, Nicolescu A, Deleanu C. Thermal polymerization of benzoxazine monomers followed by GPC, FTIR and DETA. Polym Test 2007;26:162–71.

[4] Brunovska Z, Lyon R, Ishida H. Thermal properties of phthalonitrile functional polybenzoxazines. Thermochim Acta 2000;357-358:195–203.

[5] Brunovska Z, Ishida H. Thermal Study on the Copolymers of Phthalonitrile and Phenylnitrile-Functional Benzoxazines. J App Polym Sci 1999;73:2937–49.

[6] Low HY, Ishida H. Improved thermal stability of polybenzoxazines by transition metals. Polym Degrad Stab 2006;91:805–15.

[7] Low HY, Ishida H. Mechanistic Study on the Thermal Decomposition of Polybenzoxazines : Effects of Aliphatic Amines J Polym Sci Part B Polym Phys1998;36:1935–46.

[8] Hemvichian K, Kim HD, Ishida H. Identification of volatile products and determination of thermal degradation mechanisms of polybenzoxazine model oligomers by GC–MS. Polym Degrad Stab 2005;87:213–24.

[9] Hemvichian K, Laobuthee A, Chirachanchai S, Ishida H. Thermal decomposition processes in polybenzoxazine model dimers investigated by TGA–FTIR and GC–MS. Polym Degrad Stab 2002;76:1–15.

[10] Hemvichian K, Ishida H. Thermal decomposition processes in aromatic amine-based polybenzoxazines investigated by TGA and GC–MS. Polymer 2002;43:4391–402.

[11] Holly W, Cope C. Condensation Products of aldehydes and ketones with o-aminobenzyl alcohol and 0-hydroxybenzylamine. Amines 1944;66:1875-79.

[12] Wang Y-X, Ishida H. Development of low-viscosity benzoxazine resins and their polymers. J Appl Polym Sci 2002;86:2953–66.

[13] Galia M. Synthesis and Characterization of Benzoxazine-Based Phenolic Resins : Crosslinking Study. J App Polym Sci 200;90:470-81.

[14] Ning X, Ishida H. Phenolic Materials via Ring-Opening Polymerization: Synthesis and Characterization J Polym Sci Part A Polym Chem 1994;32:1121–9.

[15] Allen DJ, Ishida H. Polymerization of linear aliphatic diamine-based benzoxazine resins under inert and oxidative environments. Polymer 2007;48:6763–72.

[16] Allen DJ, Ishida H. Effect of phenol substitution on the network structure and properties of linear aliphatic diamine-based benzoxazines. Polymer 2009;50:613–26. doi:10.1016/j.polymer.2008.11.007.

[17] Low HY, Ishida H. An Investigation of the Thermal and Thermo-Oxidative Degradation of Polybenzoxazines with a Reactive Functional Group. J Polym Sci Part B Polym Phys 1998;37:647–59.

[18] Qi H, Ren H, Pan G, Zhuang Y, Huang F, Du L. Synthesis and characteristic of polybenzoxazine with phenylnitrile functional group. Polym Adv Technol 2009;20:268–72.

[19] Agag T, Takeichi T. Synthesis and Characterization of Novel Benzoxazine Monomers Containing Allyl Groups and Their High Performance Thermosets. Macromolecules 2003;36:6010–7.

[20] Agag T, Takeichi T. Novel Benzoxazine Monomers Containing p -Phenyl Propargyl Ether : Polymerization of Monomers and Properties of Polybenzoxazines 2001:7257–63.

[21] Baqar M, Agag T, Ishida H, Qutubuddin S. Methylol-functional benzoxazines as precursors for high-performance thermoset polymers: Unique simultaneous addition and condensation polymerization behavior. J Polym Sci Part A Polym Chem 2012;50:2275–85.

[22] Ishida H, Ohba S. Synthesis and characterization of maleimide and norbornene functionalized benzoxazines. Polymer 2005;46:5588–95.

[23] Kiskan B, Demirel a. L, Kamer O, Yagci Y. Synthesis and characterization of nanomagnetite thermosets based on benzoxazines. J Polym Sci Part A Polym Chem 2008;46:6780–8.

[24] Kumar KSS, Nair CPR, Ninan KN. Effect of fiber length and composition on mechanical properties of carbon fiber-reinforced polybenzoxazine. Polym Adv Technol 2008;19:895–904.

[25] Agag T, Takeichi T. Polybenzoxazine – montmorillonite hybrid nanocomposites : synthesis and characterization. Polymer 2000;41:7083–90.

[26] Xu R, Zhang P, Wang J, Yu D. Handbook of Benzoxazine Resins: Polybenzoxazine-CNT Nanocomposites, 2011;1/31: 541–54

[27] Huang J-M, Kuo S-W, Huang H-J, Wang Y-X, Chen Y-T. Preparation of VB-a/POSS hybrid monomer and its polymerization of polybenzoxazine/POSS hybrid nanocomposites. J Appl Polym Sci 2008;111:628-34.

[28] Lee Y-J, Kuo S-W, Huang C-F, Chang F-C. Synthesis and characterization of polybenzoxazine networks nanocomposites containing multifunctional polyhedral oligomeric silsesquioxane (POSS). Polymer 2006;47:4378–86.

[29] Lee a, Lichtenhan J. Viscoelastic Responses of Polyhedral Oligosilsesquioxane Reinforced Epoxy Systems. Macromolecules 1998;31:4970–4.

[30] Demir KD, Kiskan B, Aydogan B, Yagci Y. Thermally curable main-chain benzoxazine prepolymers via polycondensation route. React Funct Polym 2013;73:346–59.

[31] Lichtenhan JD, Otonari YA, Cam MJ. Linear Hybrid Polymer Building Blocks:Methacrylate Functionalized Polyhedral Oligomeric Silsesquioxane Monomers and Polymers. Macromolecules 1995;28:8435–7.

[32] Sellinger A, Laine RM. Silsesquioxane as Synthetic Platforms. Thermally Curable and Photocurable Inorganic / Organic Hybrids. Macromolecules 1996;29:2327–30.

[33] Lee Y, Kuo S, Su Y, Chen J, Tu C, Chang F. Syntheses, thermal properties, and phase morphologies of novel benzoxazines functionalized with polyhedral oligomeric silsesquioxane(POSS) nanocomposites. Polymer 2004;45: 6321-31.

[34] Lee Y-J, Kuo S-W, Huang C-F, Chang F-C. Synthesis and characterization of polybenzoxazine networks nanocomposites containing multifunctional polyhedral oligomeric silsesquioxane (POSS). Polymer 2006;47:4378–86.

[35] Lu A-H, Salabas EL, Schüth F. Magnetic nanoparticles: synthesis, protection, functionalization, and application. Angew Chem Int Ed Engl 2007;46:1222–44.

[36] Ishida H, Sanders DP. Improved thermal and mechanical properties of polybenzoxazines based on alkyl-substituted aromatic amines. J Polym Sci Part B Polym Phys 2000;38:3289–301.

[37] Laobuthee A, Ishida H, Chirachanchai S. Metal Ion Guest Responsive Benzoxazine Dimers and Inclusion Phenomena of Cyclic Derivatives. J Inc Pheno and Mac Chem 2003;47:179–85.

[38] Wang Y, Ishida H. Synthesis and Properties of New Thermoplastic Polymers from Substituted 3,4-Dihydro-2H-1,3-Benzoxazines. Macromolecules 2000;33:2839–47.

[39] Burke WJ. 3,4-Dihydro-1,3-2H-benzoxazines. Reactions of p-Substituted Phenols with N,N-Dimethylolamines. J Am Chem Soc. 1949;71 (2):609–12.

[40] Dunkers JOY, Ishida H. Reaction of Benzoxazine-Based Phenolic Resins with Strong and Weak Carboxylic Acids and Phenols as Catalysts. J Polym Sci Part a: Polym Chem 1999;37:1913–21.

[41] Liu C, Shen D, Sebastián RM, Marquet J, Schönfeld R. Catalyst effects on the ring-opening polymerization of 1,3-benzoxazine and on the polymer structure. Polymer 2013;54:2873-8

[42] Bagherifam S, Uyar T, Ishida H, Hacaloglu J. The use of pyrolysis mass spectrometry to investigate polymerization and degradation processes of methyl amine-based benzoxazine. Polym Test 2010;29:520–6.

[43] Fam SB, Uyar T, Ishida H, Hacaloglu J. Investigation of polymerization of benzoxazines and thermal degradation characteristics of polybenzoxazines via direct pyrolysis mass spectrometry. Polym Int 2012;61:1532–41.

[44] Ishida H, Allen D. Physical and Mechanical Characterization of Near-Zero Shrinkage Poly benzoxazines. J Polym Sci Part B Polym Phys 1996;34:1019–30.

[45] Ishida H, Allen DJ. Gelation behavior of near-zero shrinkage polybenzoxazines. J Appl Polym Sci 2001;79:406–17.

[46] Chernykh A, Liu J, Ishida H. Synthesis and properties of a new crosslinkable polymer containing benzoxazine moiety in the main chain. Polymer 2006;47:7664–9.

[47] Liu Y, Zhao S, Zhang H, Wang M, Run M. Synthesis, polymerization, and thermal properties of benzoxazine based on p-aminobenzonitrile. Thermochim Acta 2012;549:42–8.

[48] Kim HJIN, Brunovska Z, Ishida H. Dynamic Mechanical Analysis on Highly Thermally Stable Polybenzoxazines with an Acetylene Functional Group 1998:857–62.

[49] Chernykh A, Agag T, Ishida H. Novel benzoxazine monomer containing diacetylene linkage: An approach to benzoxazine thermosets with low polymerization temperature without added initiators or catalysts. Polymer 2009;50:3153–7.

[50] Wang C-F, Su Y-C, Kuo S-W, Huang C-F, Sheen Y-C, Chang F-C. Low-surface-free-energy materials based on polybenzoxazines. Angew Chem Int Ed Engl 2006;45:2248–51.

[51] Takeichi T, Saito Y, Agag T, Muto H, Kawauchi T. High-performance polymer alloys of polybenzoxazine and bismaleimide. Polymer 2008;49:1173–9.

[52] Chaisuwan T, Ishida H. Highly Processible Maleimide and Nitrile Functionalized Benzoxazines for Advanced Composites Applications. J App Polym Sci 2010;117:2559-65.

[53] Hwang H-J, Lin C-Y, Wang C-S. Flame retardancy and dielectric properties of dicyclopentadiene-based benzoxazine cured with a phosphorus-containing phenolic resin. J Appl Polym Sci 2008;110:2413–23.

[54] Hardrict SN, Riffle JS, Mcgrath JE. Novel Novolac-Phthalonitrile and Siloxane-Phthalonitrile Resins cured with low melting Novolac Oligomers for Flame Retardant Structural Thermosets, Master's Thesis Dissertation, Virginia Polytechnic Institute and State University, Virginia, United States, 2003

[55] Ishida H, Low HY. A Study on the Volumetric Expansion of Benzoxazine-Based Phenolic Resin. Macromolecules 1997;30:1099-106.

[56] Huang J, Du W, Zhang J, Huang F, Du L. Study on the copolymers of silicon-containing arylacetylene resin and acetylene-functional benzoxazine. Polym Bull 2008;62:127–38.

[57] Kim HJ, Brunovska Z, Ishida H. Molecular characterization of the polymerization of acetylene-functional benzoxazine resins. Polymer 1999;40:1815–22.

[58] Andreu R, Reina J, Ronda JC. Studies on the thermal polymerization of substituted benzoxazine monomers: Electronic effects. J Polym Sci Part A Polym Chem 2008;46:3353–66.

[59] Huang JM, Yang SJ. Studying the miscibility and thermal behavior of polybenzoxazine/poly(e-caprolactone) blends using DSC, DMA and solid state 13C NMR spectroscopy. Polymer 2005;46:8068–78.

[60] Ishida H, Moran C. Synthesis and characterization of structurally uniform model oligomers of polybenzoxazine. Macromolecules 1998;31:2409–18.

[61] Russel V, Koenig JL, Low HY, Ishida H. Study of the characterization and curing of a phenyl benzoxazine using 15N solid-state nuclear magnetic resonance spectroscopy. J Appl Polym Sci 1998;70:1401–11.

[62] Liu Y, Zhao S, Zhang H, Wang M, Run M. Synthesis, polymerization, and thermal properties of benzoxazine based on p-aminobenzonitrile. Thermochimica Acta 2012;549:42– 8

[63] Dunkers J, Ishida H. Vibrational assignments of 3-alkyl-2,4-dihydro- 1,3-benzoxazines. Spectrochim Acta 1995;51:1061-74.

[64] Dunkers J, Ishida H. Vibrational assignments of N,N-bis(3,5-dimethyl- 2-hydroxybenzyl)methylamine in the fingerprint region. Spectrochim Acta 1995; 51:855–67.

[65] Varsanyi G. Vibrational Spectra of Benzene Derivatives. Academic Press New York 1969.

[66] Hemvician K, Ishida H. Thermal decomposition processes in aromatic amine-based polybenzoxazines investigated by TGA and GCMS. Polymer 2002;43:4391–402.

[67] Hemvician K, Laobuthee A, Chirachanchai S, Ishida H. Thermal decomposition processes in polybenzoxazine model dimers investigated by TGA-FTIR and TGA-GC-MS. Polym Degrad Stab 2002;76:1–15.

[68] Hemvichian K, Kim HD, Ishida H. Identification of volatile products and determination of thermal degradation mechanisms of polybenzoxazine model oligomers by GC-MS. Polym Degrad Stab 2005;87:213–24.

[69] Bagherifam S, Kiskan B, Aydogan B, Yagci Y, Hacaloglu J. Thermal degradation of polysiloxane and polyetherester containing benzoxazine moieties in the main chain. J Anal Appl Pyroly 2011;90:155–63.

[70] Uyar Y, Koyuncu Z, Ishida H, Hacaloglu J. Polymerisation and degradation of an aromatic amine-based naphthoxazine. Polym Degrad Stab 2008;93:2096-103.

[71] Uyar T, Toppare L, Hacaloglu J. Thermal and structural characterization of polypyrrole by direct-insertion probe pyrolysis mass spectrometry. Synth Met 2001;119:307-8.

[72] Gozet T, Hacaloglu J. Direct pyrolysis of freshed and aged $PF6^-$doped polythiophenes. Polym Int 2004;53(12):2162-68.

[73] Ning X, Ishida H. Phenolic materials via ring-opening polymerization: synthesis and characterization of bisphenol-A based benzoxazines and their polymers. J Polym Sci Polym Chem Ed 1994;32:1121-29.

CURRICULUM VITAE

Name : ORHAN LEKESİZ Tugba

Place of birth : Ankara

Date of birth : 23.01.1984

Sex : Female

Marital Status : Married

Education

Undergraduate : June 2007, METU Chemistry Department

Ms : July 2009, METU Chemistry Department

Ph D. : to be completed in September 2014, METU Chemistry Department

Scientific Experience

Research Ass. : 09.2009 – present, METU, Chemistry Department

Erasmus Exchange Program: 02.2007-08.2007 Eindhoven University of Technology, Netherlands

Scientific Interests

- Synthesis and characterization of benzoxazine monomers and polymers
- Incorporation and coordination of metal particles to polymers and the effect of metal coordination on thermal degradation
- Sustainable Polymers: Preparation of nanocomposites and fibers of biodegradable polymers, polymer blends and copolymers and investigation of thermal degradation mechanisms

- Polymerization and thermal degradation mechanisms of polymers.
- Synthesis of metal nanocomposites, structural and thermal characterization

Academic Awards and Fellows

TUBITAK Project Fellowship	Organometallic polymers and nanostructured metallic composites: Synthesis, structural and thermal characterization, 2007
TUBITAK Project Fellowship	Polybenzoxazines: Polymerization and thermal degradation mechanisms, 2009
TUBITAK Project Fellowship	Thermal and mechanical characterization of Poly(lactic acid) and Poly(lactic acid)/Poly(ethylene glycol) nanocomposites and nanocomposites fibers, 2014

TUBITAK: The Scientific and Technological Research Council of Turkey

Publications

1. **Tugba Orhan Lekesiz** and Jale Hacaloglu, Effects of curing on structural and thermal characteristisc of polybenzoxazines based on p-nitroaniline, submitted to Polymer 2014

2. **Tugba Orhan Lekesiz** and Jale Hacaloglu, Effect of curing process on polymerization and thermal degradation of benzoxazine based on phenol and aniline, submitted to Polymer Degradation and Stability 2014

3. **Tugba Orhan Lekesiz**, Ceyhan Kayran, Jale Hacaloglu, Preparation and Characterization of poly(2-vinylpyridine) copolymers coordinated to Cr nanoparticles *submitted to* **Journal of Analytical and Applied Pyrolysis**

4. **Tugba Orhan Lekesiz**, Jale Hacaloglu Synthesis and Characterization of Metal Functional Polybenzoxazines,. ***Polymer ,*** Volume 55, August 2014, 3533-3542

5. **Tugba Orhan Lekesiz**, Kadir Kaleli, Tamer Uyar, Ceyhan Kayran, Jale Hacaloglu. Preparation and characterization of polystyrene-b-poly(2-vinylpyridine) coordinated to metal or metal ion nanoparticles **Journal of Analytical and Applied Pyrolysis**, Volume 106, March 2014, Pages 81-85

6. **Tugba Orhan**, Jale Hacaloglu, Thermal degradation of poly(2-vinylpyridine) copolymers **Polymer Degradation and Stability**, Volume 98, Issue 1, January 2013, Pages 356-360.

7. **Tugba Orhan,** Nihat Ali Isitman, Jale Hacaloglu, Cevdet Kaynak. Thermal degradation of organophosphorus flame-retardant poly(methyl methacrylate) nanocomposites containing nanoclay and carbon nanotubes. **Polymer Degradation and Stability**, Volume 97, Issue 3, March 2012, Pages 273-280

8. **Tugba Orhan**, Sahin Ates, Jale Hacaloglu, Yusuf Yagci, Thermal degradation characteristics of polysulfones with benzoxazine end groups **Journal of Analytical and Applied Pyrolysis**, Volume 94, March 2012, Pages 146-152

9. **Tugba Orhan,** Nihat Ali Isitman, Jale Hacaloglu, Cevdet Kaynak Thermal degradation mechanisms of aluminium phosphinate, melamine polyphosphate and zinc borate in poly(methyl methacrylate. **Polymer Degradation and Stability**, Volume 96, Issue 10, October 2011, Pages 1780-1787

Manuscripts in Preparation

10. **Tugba Orhan Lekesiz** and Jale Hacaloglu, Polymerization and Characterization of aminobenzonitrile based benzoxazine, to be submitted to Reactive and Functional Polymers 2014

11. **Tugba Orhan Lekesiz** and Jale Hacaloglu, Phenol and Bisphenol-A and Aminopyridine based benzoxazines; Effects of metal type coordinated to monomer on thermal degradation to be submitted to Polymer Degradation and Stability 2014

12. **Tugba Orhan Lekesiz** and Jale Hacaloglu, Effects of substituent on aniline ring on metal coordination to benzoxazines 2014 to be submitted to Reactive and Functional Polymers

13. Esra Ozdemir, **Tugba Orhan Lekesiz**, Teoman Tincer, Jale Hacaloglu, Polylactide/montmorillonite composites to be submitted to Composites Part B. Engineering

International Conferences Attended

1. **Tugba Orhan Lekesiz,** Esra Ozdemir, Teoman Tincer, Jale Hacaloglu Preparation and Characterization Of Polylactide/Montmorillonite Composites **ICCE2014** Malta

2. **Tugba Orhan Lekesiz** Berrin Özkan, Jale Hacaloğlu, Copolymers of Polylactide via Direct Pyrolysis Mass Spectrometry **ISPAC 2014** 27th International Symposium on Polymer Analysis and Characterization Switzerland, June 16-18, 2014

3. **Tugba Orhan Lekesiz**, Jale Hacaloğlu, Direct Pyrolysis Mass Spectrometry Analyses of Polybenzoxazines. **PDDG Conference 2013** Polymer Degradation and Stability 1-4 Eylül 2013 Paris, Fransa

4. Berrin Özkan, Esra Özdemir, **Tugba Orhan Lekesiz**, Jale Hacaloğlu, , Direct Pyrolysis Mass Spectrometry Analyses of Polylactide **PDDG Conference 2013** Polymer Degradation and Stability 1-4 Eylül 2013 Paris, Fransa

5. **Tugba Orhan Lekesiz**, Jale Hacaloğlu,, Synthesis and Characterızation of Metal Functional Polybenzoxazines **APME2013** IUPAC 10th International Conference on Advanced Polymers via Macromolecular Engineering18-22 Ağustos 2013 Durham, İngiltere

6. Berrin Özkan, Esra Özdemir, **Tugba Orhan Lekesiz**, Jale Hacaloğlu, Polylactide and Poly(ethylene glycol) Blends and Copolymers **APME2013** IUPAC 10th International Conference on Advanced Polymers via Macromolecular Engineering18-22 Ağustos 2013 Durham, İngiltere

7. **Tuğba Orhan**, Shahla Bagheri Fam, Ceyhan Kayran, Jale Hacaloglu Effect of Metal Nano-particles on Thermal Degradation of Polybenzoxazines via Pyrolysis Mass Spectrometry **Baekeland 2009**,2nd International Symposium on Thermosets November 22-25, Antalya, TURKEY, 2009.

National Conferences Attended

1. **Tuğba Orhan**, Kadir Kaleli, Ceyhan Kayran, Jale Hacaloğlu Nano Yapılı Metalik Kompozitler: Yapısal ve Isıl Karakterizasyonu 24. Ulusal Kimya Kongresi Zonguldak Turkey 2010

REFERENCES

1. Prof. Dr. Jale Hacaloglu

Department of Chemistry, METU, jale@metu.edu.tr

2. Prof. Dr. Yusuf Yağcı

Faculty of Science and Letters, Department of Chemistry, ITU, yusuf@itu.edu.tr